The Measurement of Convective Mass Transfer Coefficients by Holographic Interferometry

by

Americo Luis Larez, B.Sc., M.Sc.

Thesis submitted for the Degree of
Doctor of Philosophy

University of Edinburgh
August, 1982

And a man should not abandon his work, even if he cannot achieve it in full perfection; because in all work there may be imperfection, even as in all fire there is smoke.

Bhagavad Gita 18-48

Dedication

To my family, who endured the long harsh winters.

Acknowledgement

The author is deeply indebted to his supervisor, Dr. Norman Macleod for his help and useful advice throughout the course of this research. Thanks are also due to Dr. D.H. Glass for his supervision during the first year of this work.

The author is also indebted to Mr. E. Lucey for his help in relation to photographic matters; to Mr. D. Ketchin and the workshop staff; to Mr. A. McEwan for his help in the preparation of the photographic material.

Finally, thanks are due to FONINVES and the Universidad de Oriente for their financial support throughout the course of this research.

Table of Contents

Summary

This work has been concerned with the experimental determination of local mass transfer coefficients for a system in which mass is transferred from a swollen polymer to an air stream.

The technique used was that of double-exposure holographic interferometry by which fringes were recorded, these registering the shrinkage of the swollen polymer coating as a consequence of the mass transfer process. Total internal reflection made it possible to see and to photograph the fringes by means of a still camera.

In order to calculate the local mass transfer coefficient from the fringes recorded in the holographic plates and later reconstructed and photographed, it was necessary to know the absolute fringe order. To achieve this, we used a new method, based on the fact of the proportionality between the absolute fringe order and the times involved in a given run.

For each set of runs carried out under given flow conditions, this proportionality allowed the construction of a master curve utilising all the data from runs of different duration; from this and the other curves for the flow conditions in question, information was extracted to set up a series of equations, from which by trial the values of the absolute fringe orders were ascertained.

For the experimental work, three ducts of aspect ratios 1:1, 2:1 and 3:1 were chosen. Duct 1:1 however, was soon discarded because for optical reasons the narrowness of this duct made it impossible to get good fringes with it.

A glass plate coated with polymer and swollen with isobutyl benzoate, constituted the inner fourth wall of the ducts, this swollen coating being the transferring surface. The external part of this wall (glass plate) had a prism glued to it, to allow the recording of

the fringe production by means of total internal reflection process.

Using this technique it was hoped to investigate a number of rectangular duct convective transfer problems of practical interest, notably the streamwise and spanwise variation of transfer coefficients in turbulent flow, the influence of a fluid calming section on the phenomena and the effect of symmetric and asymmetric transfer from the duct walls.

For the symmetric transfer experiments, the ducts had two opposite, parallel, transferring surfaces: the already mentioned coated glass plate and a brass plate coated with polymer and held in position by means of screws.

Developing of the holographic plates was done insitu. During the experimental work several practical problems arose, the most serious being that of vibrations transmitted through the antivibratories pads on which the original table rested. This problem was solved by the design of a pneumatic support for the top of the table. Tests, made by means of an interferometer, showed that the table was now vibration free.

The results obtained in this research are on the whole consistent with, and more informative than, previous results from other authors. The extent of the comparison is, however, limited, because the references used for comparison purposes were the results of heat transfer experiments, some in pipes, some in rectangular ducts.

However, the general character of the results shows that the trial and error method used for the calculation of the absolute order of the fringes, and hence for obtaining local mass transfer coefficients, is a useful one. Certain, occasional inconsistencies or anomalies in the results indicate that some factor or factors affecting the reliability of the method have not yet been fully identified or controlled.

CHAPTER 1

Mass Transfer

1.1 Convective Mass Transfer Coefficients

Mass transfer can occur in several ways, but in this literature survey we are concerned with forced convective mass transfer between a fluid and a solid surface, and particularly where that surface forms the inner wall of a duct or rectangular section.

Mass transfer correlations in ducts have been obtained for many flow situations. Gilliland and Sherwood (1934) studied the vapourization of nine different liquids into air, from the inner wall of a cylindrical tube for various flows, and found the correlation:

$$\frac{Kd}{D}\frac{P_{BM}}{P} = 0.023\ Re^{0.83}\ Sc^{0.44}$$

to be reliable over the range $2000 < Re < 3500$, $0.6 < Sc < 2.5$ and $0.1 < P > 3$ atm. But because the Schmidt number varied only between these limits, the exponent 0.44 was put in question. Later, Linton and Sherwood (1950) made water to flow through pipes made by casting molten benzoic acid in pipe form. Similar experiments were conducted using other materials, such as cinnamic acid, and β-naphtol. The data was correlated by the relation:

$$Sh = \frac{Kd}{D} = 0.023\ Re^{0.83}\ Sc^{0.33}$$

for $2000 < Re < 70\ 000$; $1000 < Sc < 2200$. This expression gives the correct value of the exponent for the Schmidt number.

Beek and Mutzel (1975) give a usable relation on the basis of the analysis for heat transfer between a wall and turbulent flow in a pipe. This relation reads:

$$Sh = 0.027\ Re^{0.8}\ Sc^{0.33}$$

valid for $2000 < Re < 100\,000$ and $Sc > 0.7$. Vivian and Peaceman (1956) correlated the liquid side convective mass transfer coefficient for a falling liquid film in a wetted-wall column and found the following correlation:

$$\frac{K_L Z}{D} = 0.433\ Sc^{0.5}\ \left(\frac{\rho^2 g z^2}{\mu^2}\right)\ Re_L^{0.4}$$

In their data, 44% of the points lie within 57% of the line given by

$$K_L\ \sqrt{H/D} = 7.13\ \Gamma^{0.4}$$

and 78% lie within 10% of this line. The above correlation was deduced by dimensional analysis and their experimental data.

The coefficients given by it were found to be 10 to 20% lower than expected from theory and it is believed that this was due to ripples along the liquid surface or to disturbances at the two ends of the wetted-wall column. These discrepancies led to the suggestion that a resistance to the mass transfer exists at the gas-liquid interface. Investigations, however, by Scriven and Pigford (1958), Raimondi and Toor (1959) and Chiang and Toor (1959) have determined that the interfacial resistance is negligible in normal mass transfer operations.

1.2 The Analogy between Mass and Heat Transfer

There is a definite analogy between mass and heat transfer. When the equations of continuity, motion and energy are made non-dimensional, it is found that for negligible viscous heating and no chemical reactions, the non-dimensional equation of energy and continuity read:

$$Re\ Pr\ \frac{DT^*}{Dt^*} = \nabla^{*2}\ T^*$$

and

$$\mathrm{Re\ Sc}\ \frac{DC_A^*}{Dt^*} = \nabla^{*2}\ C_A^*$$

(continuity of species A), respectively.

These relations, for a turbulent boundary layer in a long duct where entrance effects are not present, signify that $C_A^*\ (X^*, Y^*, Z^*, t^*, Re, Sc) = T^*\ (X^*, Y^*, Z^*, t^*, Re, Pr)$, which means that the concentrations profile when the Prandtl number (Pr) is replaced by the Schmidt number (Sc) and vice versa, when the boundary conditions on the non-dimensional temperature difference and the non-dimensional concentration difference are the same.

These non-dimensional differences are functions of Nusselt number (Nu) for temperature and the Sherwood number (Sh) for concentration. Then in the analogy Sh replaces Nu and vice versa, giving:

$$Sh\ (Re, Sc) = Nu\ (Re, Pr)$$

for a long duct where entrance effects are negligible. This relationship can be obtained by dimensional analysis methods, such as the Buckingham Pi method, applying them to the given heat or mass transfer process.

From dimensional analysis we find that $Sh = Sh\ (Re, Sc)$ but the form of the relation between those quantities is found empirically. The relationship between these non-dimensional quantities is generally assumed to be expressible as products of their powers. Graphical procedures are applied to the data to obtain values of the exponents for each number and the value of the coefficient from log-log plots.

The values of the different exponents and the coefficient thus found depend upon the quality of the existing data for convective mass transfer in long tubes in such as to allow it to fit equally well the expressions $Sh \propto Re^{0.83}\ Sc^{0.33}$ and $Sh \propto Re^{0.8}\ Sc^{0.33}$.

The value of the constant also has been variously reported. Dittus and Boelter (1930) studied turbulent heat transfer in pipes and found the constant to be 0.023, McAdams (1954) obtained a constant value of 0.021 for such heat transfer situations and Beek and Mutzel report a value of 0.027. However, the value of 0.023 is considered by Knudsen and Katz (1958) to be more satisfactory to correlate most of the available data.

In relation to the value of the exponent of the Reynolds number it has been reported as 0.83 for experiments in wetted-wall columns, with the problems pointed out before, and 0.8 which is the value more widely used and which we adopted, the complete expression being:

$$Sh = 0.023\ Re^{0.8}\ Sc^{0.33}$$

For forced convective heat transfer in a pipe, McAdams (1954) found using the same methods, the following correlation:

$$Nu = 0.023\ Re^{0.8}\ Pr^{0.33}$$

These two correlations show the similarity between the two processes in a striking way.

The Chilton-Colburn (1934) analogy extends this similarity from the particular case of duct flow to more general flow situations, allowing the calculation of mass transfer coefficients from knowledge of heat transfer coefficients and vice versa for all sorts of systems. This analogy states that the mass transfer factor jD is equal to the heat transfer factor jH for all dynamically similar situations, i.e.

$$jH = jD \quad \text{or} \quad \frac{Sh}{Re\ Sc^{0.33}} = \frac{Nu}{Re\ Pr^{0.33}} \qquad \begin{matrix} 0.6 < Sc < 2500 \\ 0.6 < Pr < 100 \end{matrix}$$

This empirical analogy has proven sound and useful for flow through packed beds, transverse flow over cylinders and flow in pipes at high Reynolds numbers and this wide applicability seems to confirm

the correctness of the exponent 0.33 on the Schmidt number in the equation for the Sherwood number for the particular case of turbulent flow in long ducts.

1.3 Momentum Boundary Layer

When a fluid enters a conduit a boundary layer, or stratum of fluid whose motion is significantly affected by wall friction, begins forming at the entrance.

This momentum boundary layer appears as the result of the condition of no-slip at the wall. Viscous fluids are retarded by the friction between the fluid and the walls of the conduit and the formation of a momentum boundary layer or region of appreciably curved velocity profile, which grows progressively thicker downstream is due to the inward diffusion of this viscous effect. As more fluid is retarded at the walls, the fluid near the centre of the conduit accelerates, so that continuity is preserved. The pressure gradient across the boundary layer is negligible because the streamlines there are nearly parallel; in other words the pressure in the boundary layer is the same as the pressure in the flow outside. As a consequence, the stream pressure gradient can be computed from the outer flow.

In turbulent flow, we can distinguish three layers which form the totality of the momentum boundary layer: a) The viscous sub-layer which is a very thin layer close to the wall, inside which the flow is to a great extent streamline or predominantly controlled by molecular viscosity b) The buffer layer which lies between the laminar sub-layer and the turbulent layer. In this buffer zone the flow is equally affected by molecular and eddy viscosity c) The turbulent layer in which the flow is totally turbulent, so that eddy viscous effects predominate.

Transport of momentum, heat and mass transfer occurs through the respective momentum, heat and mass transfer boundary layers and these

boundary layers are generally of different thicknesses. Each of these transport phenomena is affected mainly by molecular diffusion in the viscous sub-layer. In the buffer zone transport occurs through the dual mechanism of molecular diffusion and eddy transfer, which are of comparable magnitude.

In the turbulent portion of the boundary layer transport occurs predominantly by means of eddy transfer. The fluctuation in the velocity and in the direction of the flow gives rise to eddies inside the fluid, which are responsible for the transfer of momentum within the turbulent region of the fluid generating shear stresses additional to those caused by molecular viscosity. In the turbulent layer eddy motion is large compared with the molecular diffusion and because the effects of eddy diffusion are generally far greater than those of the molecular diffusion, the main resistance to transfer will lie in the regions where molecular diffusion alone is occurring.

The turbulent heat and mass transfer coefficients are much higher at high Reynolds numbers because the thickness of the viscous sub-layer is almost inversely proportional to the Reynolds number.

1.4 Entrance Lengths

The momentum boundary layer so formed, continues to grow to the point where it reaches the axis of the conduit, after which the flow is fully developed, in the sense that its character ceases to change with distance downstream. The distance from the entrance to where this occurs is called the hydrodynamic or momentum entrance length.

For laminar flow, various equations for this length have been developed from first principles, among them the one given by Langhaar (1942) who made an analysis for laminar flow in pipes and found that the expression

$$\frac{L_{hy}}{d} = 0.0575\ Re$$

gives the length (Lh_y) needed for the centre-line velocity to reach 99 per cent of its fully developed value. Friedmann et al (1968) tabulated values of the entrance length for uniform entrance profile which are in good agreement with experimental values. Their results are best approximated by Chung (1973) as:

$$\frac{Lhy}{d} = \frac{0.60}{0.035\ Re + 1} + 0.056\ Re$$

For turbulent flow, there is not a theoretical equation which can predict the distance for the turbulent velocity profile to develop fully. Latzko (1921) using the 1/7th power law for the velocity distribution in the boundary layer got the relation:

$$\frac{Lhy}{d} = 0.693\ Re^{0.25}$$

This relation, however, gives shorter inlet lengths than any found in practice.

For Reynolds numbers greater than 10 000, Schiller and Kirsten (1929) observed that entrance lengths greater than 50 tube diameters were generally necessary for the formation of a fully developed turbulent velocity profile. These workers used a rounded entrance to the pipes.

Nikuradse (1932) found, for disturbed entry conditions at a Reynolds number of 900 000, a distance of 40 diameters, and Deissler (1950) working with rounded entrance to the pipes, found that a distance of more than 50 diameters is needed for the velocity profile to become fully developed.

For rectangular ducts the hydrodynamic entrance length has been investigated by several workers, for laminar flow. Shah and London (1978) present a table of different values of this parameter in terms of $L^+hy = Lhy/Re\ dh$ and they recommend as the more accurate ones,

those of Wiginton and Dalton (1970). These authors get for a 1:1 duct a value of L^+hy of 0.09 and for a 2:1 duct a value of L^+hy of 0.085, or

$$\frac{Lhy}{dh} = 0.09 \text{ Re} \quad \text{and} \quad \frac{Lhy}{dh} = 0.085 \text{ Re},$$

respectively. Persen (1972) finds, assuming that Spalding's "Law of the wall" (1961) holds, the hydrodynamic length as a function of the Reynolds number, for turbulent flow in a rectangular duct. His results are plotted in semi-logarithmic form as L/h vs Re, where L is the hydrodynamic entrance length and h is half the depth of the duct. The plot is a straight line and it shows that for Re = 10^4 (lowest Reynolds number) L/h = 40 and for Re = 10^6 (highest Reynolds number) L/h = 65.

The entrance length for fully developed velocity profile differs considerably from that for the velocity gradient at the wall, the latter being smaller. Two conditions exist in the entrance region which cause the friction factor to be greater than in fully developed flow. First, the extremely large wall velocity gradient and hence the very large viscous shear stress, right at the entrance. This gradient decreases downstream becoming constant before the velocity profile becomes constant.

The second factor, is that the velocity of the fluid outside the boundary layer increases as a consequence of the retardation of the fluid inside the boundary layer, at the wall. This acceleration of the outer flow produces an additional drag force whose effect is incorporated in the friction factor. Langhaar (1942) in his laminar flow studies mentioned above show the friction factor to be highest in the vicinity of the entrance and then to decrease smoothly to the fully developed flow value.

Deissler (1953) analysed the friction factor for turbulent flow

in the entrance region of pipes and found that the distance required for the factor friction to reach its developed value is considerably less than the hydrodynamic entrance length, as is true for laminar flow also. Assuming the boundary layer to begin at the tube entrance, Deissler found that at a distance of 10 diameters, the friction factor had reached its fully developed value for Reynolds numbers between 10^4 and 10^5.

For laminar flow in rectangular ducts Curr et al (1972) and Carlson and Hornbeck (1973) found values of the friction factor in the hydrodynamic region. They presented the results as plots of fappe Re vs x^+, where fapp is the apparent Fanning friction factor which takes into account both the skin friction and the change of momentum due to the change in the shape of the velocity profile, in the hydrodynamic entrance region, and it is based on the total pressure drop from x = 0 to x = x, x^+ is the axial co-ordinate for the hydrodynamic entrance region, given by:

$$x^+ = x/Re\ dh$$

Persen (1972) shows a graph of the friction factor, for the entrance of a rectangular channel in turbulent flow, versus x/h (distance from the entrance length/half depth of the duct). From this plot, it can be seen that at approximately x/h = 10 the friction factor starts levelling off. The Reynolds numbers varied from 10^3 to 10^6.

1.5 Concentration Boundary Layer

Mass transfer will take place if a concentration gradient exists within a fluid flowing over a surface. The whole resistance to transfer can be regarded as lying within a boundary layer in the vicinity of the surface. This layer is called the concentration boundary layer.

Laminar Flow

An extension of the exact solution developed by Blasius (1908) for the skin friction for an unbounded laminar flow parallel to a flat surface, applied to convective mass transfer in a similar situation, leads to an equation which Hartnett and Eckert (1957) solved and presented graphically. Their solution was restricted to Schmidt numbers equal to one. The relationship between the different non-dimensional quantities is: $Sh\ x = 0.332\ Re\ x^{\frac{1}{2}}$.

By using the relation $\delta m/\delta c = Sc^{1/3}$, which is the ratio of the thickness of the momentum to the concentration boundary layer, a new equation was deduced for $Sc \neq 1$. It reads:

$$Shx = 0.032\ Rex^{0.5}\ Sc^{0.33}$$

Integration of this equation over the length of the plate gives the average Sherwood number which is related to the local one by $Sh_L = 2\ Shx$. These two equations have been verified experimentally by Christian and Kezios (1959).

For laminar, fully developed flow in a pipe, by analogy with the corresponding equation for heat transfer: $Sh = 4.1$. The boundary condition which leads to this equation is constant temperature at the wall, or constant concentration in the case of mass transfer.

Turbulent Flow

For turbulent flow on a flat plate an approximate solution for the mass transfer coefficient can be found using the Reynolds analogy. For equimolecular counterdiffusion or when the concentration gradients are small, if the Reynolds number is so high that the resistance of the viscous sublayer is very small, the following equations given by Coulson and Richardson (1964) apply:

$$Kx/u = 0.03\ Rex^{-0.2}\ (Sc = 1).$$

The average mass transfer coefficient over the whole length of the plate is:

$$K_L/u = 0.037\ Re_L^{-0.2} (Sc = 1)$$

When, however, the resistance of the viscous sublayer is taken into account, we have for a flat plate:

$$Sh\ Re^{-1}\ Sc^{-1} = 0.03\ Rex^{-0.2} \Big/ \left[1 + 2.1\ Rex^{-0.1}\right] (Sc = 1)$$

For turbulent flow in pipes, from the Taylor-Prandtl relation for equimolecular counterdiffusion or low concentration gradient, we have:

$$Sh\ Re^{-1}\ Sc^{-1} = \frac{0.032\ Rex^{-0.2}}{1 + 2.1\ Rex^{-0.1}\ (Sc - 1)}$$

1.6 Flow in Channels

For fully developed laminar flow in channels, the velocity profile provided by the solution of the equation

$$\frac{\partial^2 u}{\partial y^2} + \frac{\partial^2 u}{\partial z^2} = c_1,$$

with the boundary condition u = 0 at the walls, is in good agreement with the experimental results of Holmes and Vermenlen (1968) and Muckrink et al (1973). The constant c_1 is equal to

$$\frac{g_c}{\mu}\ \frac{dp}{dx}$$

Shah and London (1971, solved for the friction factor the relationship

$$f\ Re = \frac{8\ c_1\ a^2}{U\ max\ [1 + (a/b)]^2}$$

(a and b are half width and half depth of the channel, respectively).

Their results agree with those of Ruthfus et al (1964) who presented the friction factor as a function of the aspect ratio. Hartnett et al (1962) give the critical Reynolds number for several aspect ratios taking into account the nature of the entrance (smooth or abrupt).

The same authors studied the influence of the aspect ratio on the friction factor for fully developed turbulent flow following the method of Deissler (1955) and Deissler and Taylor (1956). Their results showed that for turbulent regime this influence is not as great as predicted. The Deissler-Taylor method will give an accurate prediction of the velocity field for aspect ratio larger than 5:1. For smaller aspect-ratio channels, the predicted velocity field is not

totally correct with the deviations of 12% for square ducts, as the biggest deviations. Another important finding of their research was that for Reynolds numbers between 6000 and 50 000, the circular tube correlation correctly represents the friction factor coefficients for any and all aspect ratios.

There is however a type of flow which arises in turbulent channel flow and which was not considered by Hartnett et al. This important type of flow is secondary flow.

Secondary Flow

Secondary flow occurs when a fluid is flowing along a curved duct. The velocity of the fluid approaching the bend is zero along all portions of the boundary because little or no centrifugal pressure gradient exists in these regions. However, just inside this boundary the velocity is finite and the unbalanced centrifugal force of this portion of the fluid produces a secondary flow outward along the plane of the bend and inward around the boundary, as indicated in the figure below.

Fig. 1.1 Variation in Head vs r/D

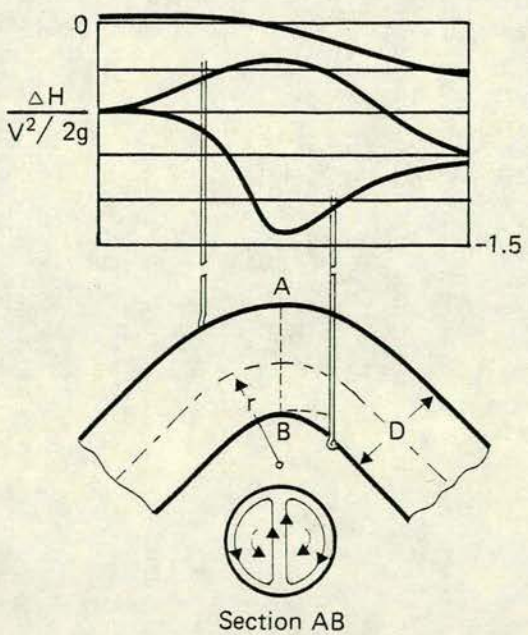

Section AB

As a result, the fluid leaving the bend moves in a double spiral which diminishes in intensity gradually as the fluid goes downstream and dies out at some 50 to 75 pipe diameters from the bend, in the case of a circular bend. The effect of this induced circulation is threefold, in addition to the energy lost in normal boundary resistance, further energy is taken from the primary flow to produce the secondary movement. The velocity distribution at the bend is completely modified, because the spiral motion transposes the region of maximum velocity towards the outside of the bend. Finally, as long as this movement persists, conditions of established uniform motion will not prevail.

This type of secondary flow occurs whatever may be the section of the duct, and it is called secondary flow of the first kind. Secondary flow of this type has the effect in the bends of rivers of removing material from the outer side and filling it up on the inner side of the bend.

Secondary flow of the second kind

This type of flow occurs in straight non-circular ducts at turbulent regimes only. That this type of flow does not occur in non-circular ducts at laminar regimes has been proved analytically by Moissis (1957) and Maslen (1958), and experimentally by Owan (1959).

Nikuradse (1926) determined the experimental contours of constant velocity in rectangular and triangular ducts. Subsequent flow visualization studies by Nikuradse (1936) confirmed the existence of secondary flow in the form of stream-wise helical vortices in the corner region.

The shape of the countors was explained by Prandtl (1926) assuming the existence of a transverse mean flow superimposed upon

the axial mean flow and reaching into the corners of the channel and then returning towards the centre. The secondary flow continuously transports momentum towards the corner along the bisectrix of the angle, generating high velocities there, and then up in both directions.

Gessner and Jones (1965) studied secondary flow in steady, incompressible, fully-developed turbulent air flow in both rectangular and square channels. They found from their experiments that: a) For the range of Reynolds numbers considered (50 000, 150 000 and 300 000), secondary-flow velocities decrease in relation to the mean stream velocity with increasing Reynolds number. This, the authors suggest, may be explained by increased turbulent mixing at high Reynolds numbers, which tends to reduce gradients in the flow. b) In planes normal to the axial-flow direction, opposing forces are exerted by the Reynolds stresses and static-pressure gradients. Small differences in magnitude of these forces cause secondary flow i.e. these small differences of magnitude are the actual driving mechanism of secondary flow. Also the findings of these authors show that the assumption of no Reynolds shear stresses on planes normal to isotachs (lines of constant axial mean-flow velocity), used by Deisler and Taylor (1959) in their theoretical investigation of turbulent channel flow, is invalid.

Gessner (1973) examining conclusion b) says that this conclusion is not definite because the terms indicative of momentum transfer by secondary flow was two orders of magnitude less than the static pressure and Reynolds stress terms in the equation, and in this work (1973) he found that a transverse flow is initiated and directed towards the corner as the direct result of turbulent shear stress gradients normal to the bisector, so that these transverse gradients components of Reynolds shear stresses are responsible for the generation of secondary flow in turbulent flow along a corner.

Launder and Ying (1972) worked with square-sectioned ducts with smooth and equally roughened surfaces. They found that when the secondary velocities are normalised by the friction velocity, i.e. when each velocity is divided by the friction velocity, the resultant profiles are the same for both surfaces. This result means that the secondary velocity in a fully developed flow through a duct of square section is independent of whether the duct is rough or smooth, provided that the velocity is normalised with the average friction velocity.

The importance of taking into account the effects of secondary flow on the transport of momentum, heat and mass is obvious from the above considerations. Ibragimor et al (1971) took into account secondary flow for their calculations of heat transfer in a square duct at turbulent regime, and they found that their calculations give a much more faithful agreement with the experimental data than in the case where secondary flow was not considered.

Launder and Ying (1973) although considering important the results of Ibragimor et al (1971) believe that they cannot be generalised to other geometries and they present numerical predictions of the hydrodynamic and heat transfer characteristics of fully developed flow in square ducts; although because no explicit mention is made of the shape of cross-section, in the model of flow, they present, they believe it can have applicability to other geometries.

The results show agreement with the work of Launder and Ying (1972) in relation to the secondary flow profiles in the plane of the channel for flow in a smooth and rough walled duct. Also, they are in good agreement with the experimental data presented by Brundrett and Baines (1967) in relation to contours of turbulence energy and the predictions confirm Brundrett and Baines overall conclusion that the energy contours are much more distorted by the secondary flow than are those of axial velocity.

Brundrett and Burroughs (1967) obtained local wall heat-transfer rates in a vertical aluminium square duct for turbulent air flow. They compared the distribution of wall shear stress by Leutheusser (1961) with the distribution of local wall heat-transfer data and found that the whole data fall on a single curve over the range of Reynolds and Nusselt numbers to an accuracy of ± 2 per cent. They interpret this assuming that the mixing properties of the secondary currents have a similar effect on heat transfer as for momentum transfer. Since fluid from the centre of square duct is brought into closest proximity to a wall at points, partway between the corners and the mid point of the wall, where the wall shear stresses are largest, this movement must produce the largest wall temperature gradients and hence the largest wall heat-transfer rates at these points. Hence, the distribution for wall shear stress and wall heat transfer must be similar.

A further conclusion is that the mixing action of the secondary flow currents can be likened to the mixing action of two dimensional turbulent flows such as occur in pipes and on flat plates. These works illustrate very well the importance of secondary flow and its implications in the determination of the transport coefficients.

CHAPTER 2

Holography

Holography is an interference method of registering optical appearances, in which the reflected or refracted light waves from an object are recorded in the form of an interference pattern produced by combination with an unmodulated beam. The record itself is called a hologram.

The hologram stores information about the wave front of the light modified by the object by recording both its amplitude and its phase.

2.1 The making of a hologram

To make a hologram it is necessary to have a source of coherent light, i.e. light which remains permanently in phase with itself. Without coherence, the interference pattern referred to above cannot be observed, because in normal incoherent light the phase, and hence the interference field, varies at random with the time more rapidly than the time of response of the detector. Consequently, without coherence there cannot be stable interference and without such time-invariant interference there cannot be detectable information which is required to be encoded in the interference pattern of a successful hologram.

The laser provides such a coherent light due to the physical process by which it emits radiation. For the purpose of generating the interference field, the beam of the laser light is split in two. The object beam, directed towards the object, by which it is modulated en route to the detector, and the reference beam, which passes directly to the detector and acts as the unmodulated coherent background (Fig. 2.1.) When these two beams intersect on the detector (usually a photographic plate), they create a complex interference pattern in which

Fig. 2.1 a) Holographic Recording

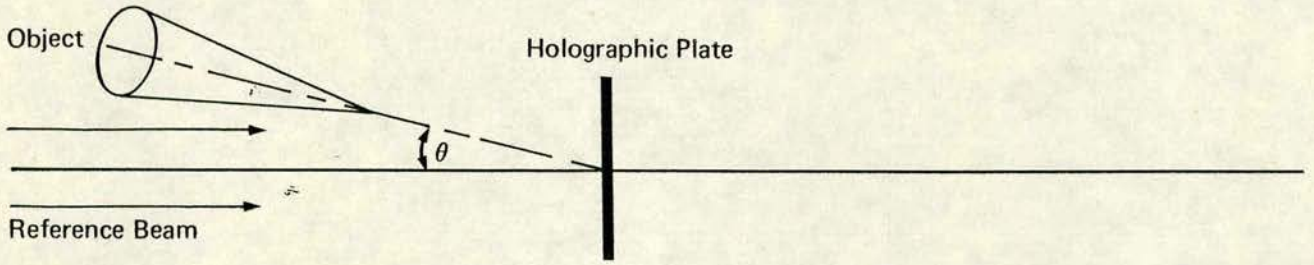

b) Holographic Reconstruction

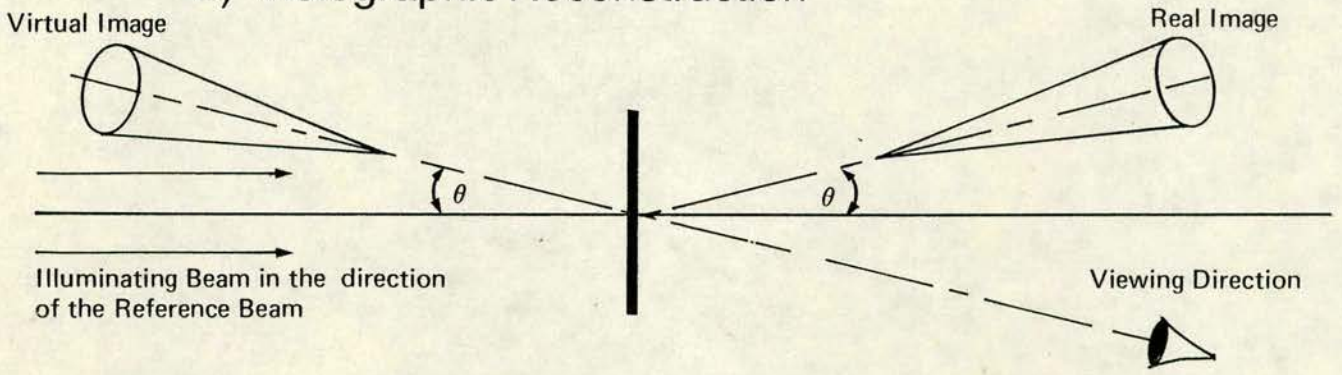

intensity and phase information about the wave front modified by the object is encoded on terms of patterns of exposure of the silver halide grains or other elements of the recording medium.

Three characteristics of the optical system require attention in order to make a hologram, namely, the optical path difference, the intensity ratio between reference and object beams and the angle between beams.

The optical path length difference between object and reference beam must be less than the coherence length of the laser, i.e. the distance over which the beam remains in phase with itself, in order to have interference at all. This distance is normally of the order of half the length of the laser tube, i.e. ten or twenty centimeters, but in practice the path lengths must differ by substantially less than this for sharp holograms to be obtained.

The intensity ratio between reference and object beams is important because of its effect on the quality of the fringes. Elementary theory suggests that this ratio should be unity. In normal practice, however, the intensity of the reference beam is several times that of the object beam for best results. Because if the chosen ratio is unity the result will be overmodulation because the depth of modulation of the fringes is at a maximum, this will have a distorting effect on the fidelity of the image.

The angle between the beams governs the fringe spacing, i.e. their coarseness or fineness, as can be seen from the equation:

$$d = \frac{\lambda}{2 \sin \Theta/2}$$

derived in Appendix (A) where d, is the fringe spacing, λ, the laser wave length and $\Theta/2$ the angle between beams. The reciprocal of the fringe spacing gives the fringe spatial frequency in lines/unit length,

and must be matched by the resolution of the film. The fine resolution required in practice was a drawback at the beginning of holography when films were not able to resolve the fringe structure.

After all these conditions are met and the hologram is taken, the next step is to develop it in a suitable developer and to fix it as with any other photograph. After the photographic process is finished and the hologram is dry, the reference beam is made to illuminate the plate. The image of the object is then reconstructed by diffraction, the developed hologram acting as a diffraction grating. The reconstruction can be seen either as a virtual image occupying the object space, on looking through the hologram, or as a real but pseudoscopic image on the far side of the hologram from the original position of the object.

The process of reconstruction of the object, from the interference pattern on the plate, occurs when the reference beam alone illuminates the plate, the object beam being blocked.

CHAPTER 3

Holographic Interferometry

Holographic interferometry like classical interferometry is used to make measurements of great accuracy, both techniques being able to detect minute changes or movements of surfaces under study. These changes or movements are detected as pattern of fringes.

However, conventional interferometry is limited to highly polished surfaces and relatively simple shapes, while holographic interferometry can be applied to arbitrarily shaped three dimensional objects, largely independent of surface condition. Also, by holographic methods an object can be examined from different perspectives, due to the unique property of parallax of the holographic image. This was not possible to achieve with classical non-coherent methods. But the greatest difference between holographic and classical interferometry is that holographic interferometry allows the object to be compared with itself at a later time, so that it can be tested before and after it is subject to any kind of deforming process.

Among the several types of arrangements for holographic interferometric measurement and which are relevant to this work, we have the following.

3.1 Real-Time Interferometry

This entails taking a hologram of an undisturbed object, which is then developed insitu or developed elsewhere but later placed exactly on the original place.

The virtual, reconstructed image of the initial state of the object is then superimposed on the object itself. Any small changes in the position of the surface of the object occurring since the initial recording, will be seen as a set of fringes, due to the mismatch between

the present configuration of the object and its initial image consequent on the relative displacement and/or rotation between the two. Any permanent irregularities or optical imperfections in the surface of the object will not affect the interference pattern, since both sets of interfering waves will be distorted by the same extent by them, due to the fact that the reconstructed wave is created by the object itself in its initial state.

In practice, what it is done is to make two waves existing at different times to interfere, and interference is possible because the light scattered by the object is coherent with the light from the virtual image. So, by means of real-time interferometry we can follow the changes in form or position of the object at the moment when they are happening. These are, however, two complicating factors to take into account in this type of technique. The first is the swelling and subsequent shrinking of the emulsion during developing, which leads to an initial residual fringe pattern. This pattern has to be subtracted from the observed pattern to obtain accurate data from the changes in the object.

The second factor is stresses frozen in the emulsion which are released during processing and which provoke movements in the emulsion. These movements are sources of irregularities in the fringe pattern. To eliminate the first problem Duffy (1970) recommends that one should not fix the emulsion and for the second, Butters and Leendertz (1969) recommend soaking the plate in water and then allowing it to dry, speeding up the process of drying by the use of methylated spirits.

3.2 Double-Exposure Interferometry

In this technique, two holograms of the same object, in two different states, are consecutively taken on the same plate. This creates a 'frozen' record of the fringes due to changes in the object

between exposures. This method avoids the effects of emulsion instability which, as noted above, is a drawback of real-time interferometry, because each hologram will be affected identically in the single stage of chemical processing.

CHAPTER 4

Practical Procedures

4.1 Description of Equipment and Materials

1. Lasers

The two lasers used, the spectra Physics 124A and the Scientifica Cook were continuous-wave Helium-Neon lasers, emitting at 633 nm, with a power output of 15 mW and a coherent length of 30 cms.

2. Channels

The metal carcass of each rectangular channel was made of brass and their specifications are as follows:

Aspect Ratio	Width(cm)	Depth(cm)	Length(cm)	Hydraulic Diameter(cm)
1:1	0.95	0.95	15	0.95
2:1	1.91	0.95	15	1.27
3:1	2.86	0.95	15	1.43

There were two 3:1 and two 2:1 ducts for the asymmetric and symmetric transfer runs. (Figures 4.1, 4.2). The 3:1 channels because of their bigger width had two outlets, to insure a uniform flow near the exit. Furthermore, the channels for symmetric transfer had a detachable wall, made of brass. One side of this wall had the polymer cast on it. This side was one of the internal walls, so that when the channel was assembled, with the carcass clamped to the polymer-coated glass plate and prism, two internal walls covered by polymer were facing one another.

3. Calming Section

Two calming sections made of dural, were each of the same cross-section and aspect ratios as the channels 2:1 and 3:1. Their specifications were:

Fig. 4.1 : Channel for Asymmetric Mass Transfer

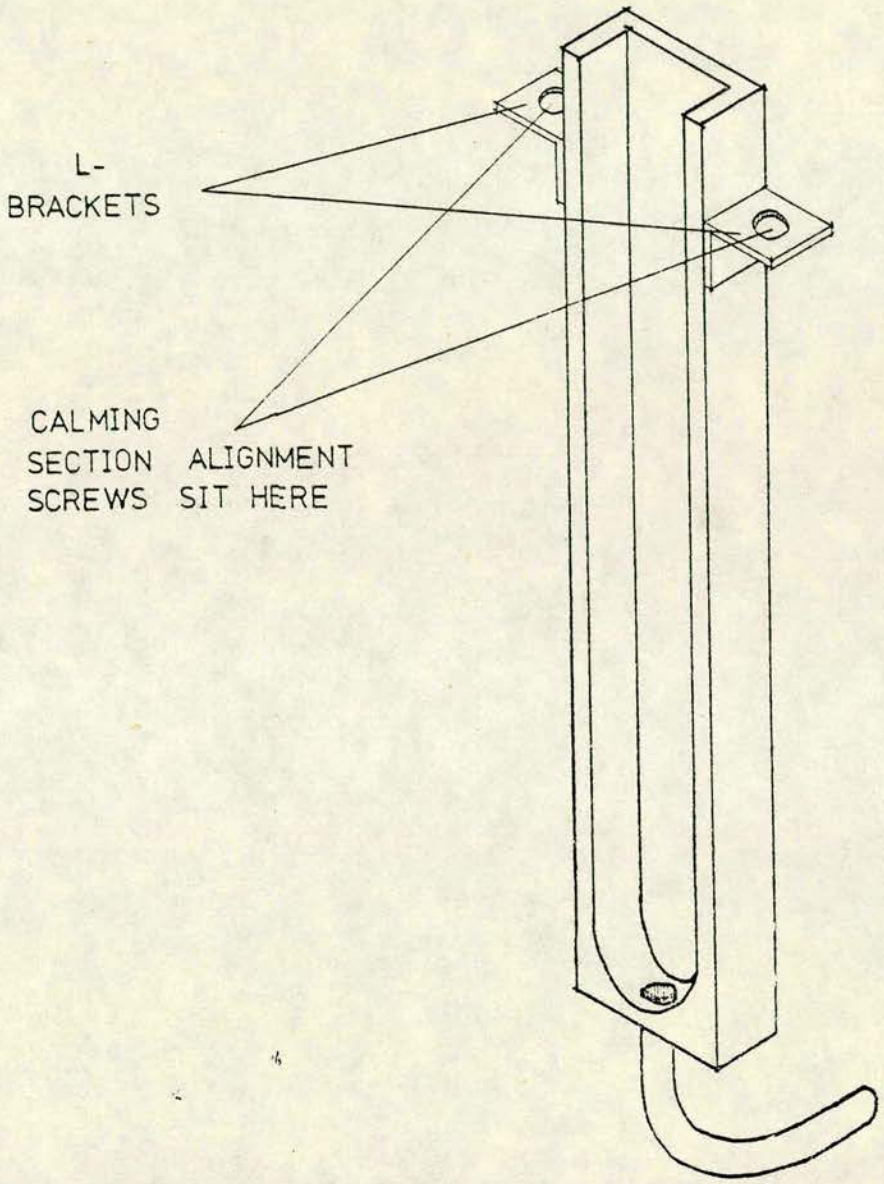

Aspect Ratio	Width(cm)	Depth(cm)	Length(cm)	Hydraulic Diameter(cm)
2:1	1.91	0.95	30.5	1.27
3:1	2.86	0.95	35.6	1.43

Each calming section was secured to the top of the channel by means of screwed studs, having plain portions engaging holes in locating lugs. (Figure 4.3). By these means internal discontinuities at the junction of calming and test sections were avoided.

4. Optical Table

The work top of the optical table consists of a slab of steel-mesh-reinforced concrete and has the top cemented. Its dimensions are 2.56 m x 1.22 m x 9 cms. This slab rests on inflated car (Mini) tyre inner tubes, supported by a plate framed of wooden boards on a frame of steel channel bolted to the brickwork (Fig. 4.4).

5. Interferometer

The interferometer was made to check the stability of the optical table. The system consisted of: (a) the laser, as the source of light, (b) the beam expander, (c) collimator, (d) lens, (e) beam splitter, (f) adjustable mirrors and (g) screen (Figure 4.5).

The light after being focused by the lens on the splitter, went to two adjustable mirrors. By moving the mirrors (fine adjustment) it was possible to make the two beams to coincide on the screen. When they were so coincident they produce an interference pattern. The stillness or motion of these fringes was examined to ascertain the degree of stability of the optical system.

6. Supporting Mass Transfer Coating

This consisted of an ordinary window glass (crown glass) of dimensions: 19 cm x 14 cm x 0.5 cm. The plate is an essential part of

Fig. 4.2 : Channel for Symmetrical Mass Transfer

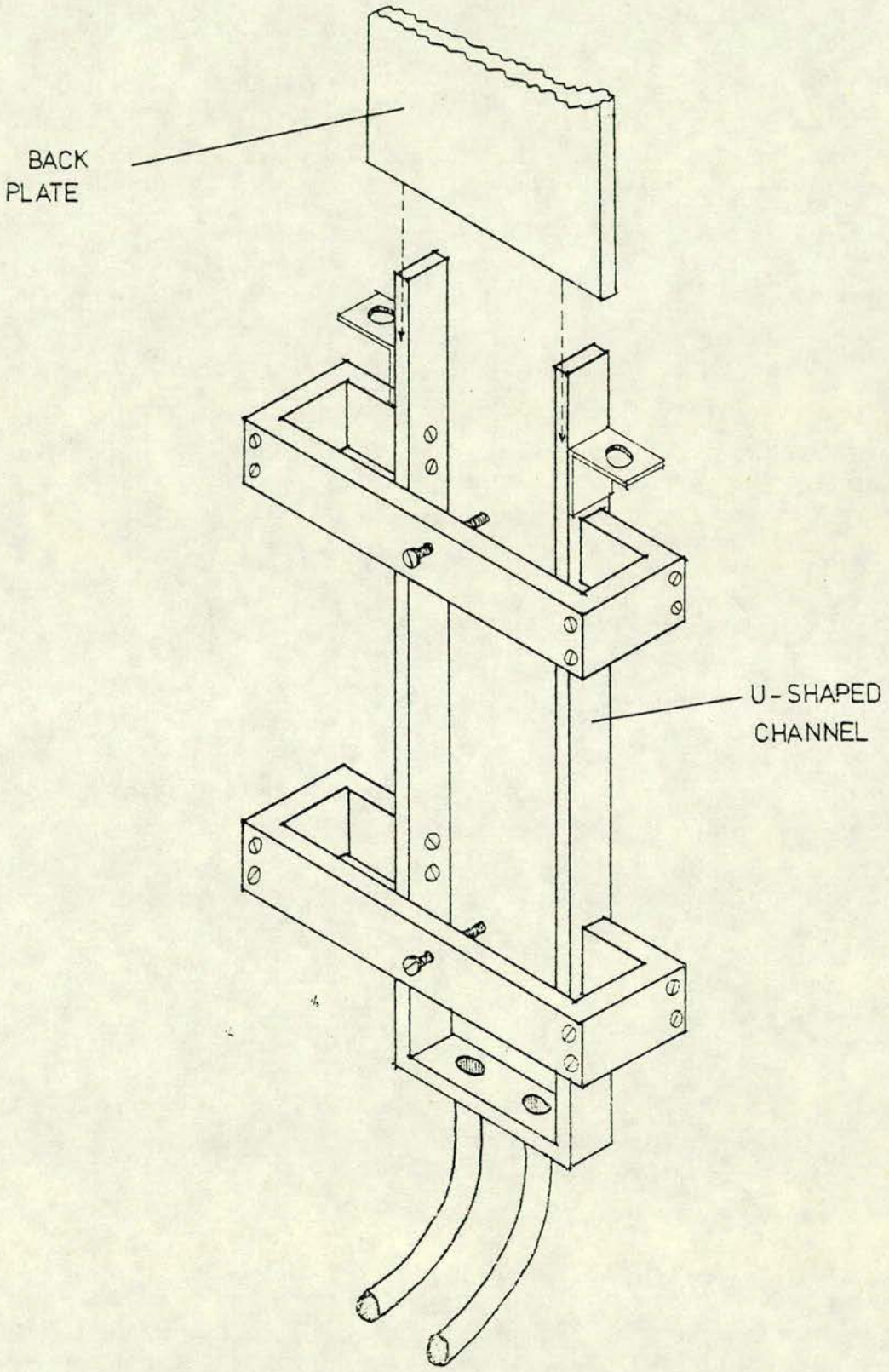

the set-up because it forms one of the walls of the channel. One side of this wall (glass plate) had a 45^{o} prism glued to it. The other side, is one of the internal walls of the channel and had the polymer cast on it.

7. Air Circuit

The air circuit was designed to allow inflation or any one of the tyre tubes, or even the removal of some of them without affecting the others. If the need arises, the top of the table can be made to rest on wooden blocks.

8. Optical Circuits

Several arrangements were made but they can be reduced to three: a) Laser on steel angle extension to the table b) Laser on table cross-wise and c) Laser on table lengthwise.

The final arrangement to be used was that of b), (Figure 4.6).

The optical circuits consisted basically of:

a) Laser (already described), b) beam expanders, c) pin holes, d) mirrors, e) beam splitter, f) magnifying glass and g) cylindrical lenses.

b) Beam Expanders

Their function is to expand the narrow beam from the laser by the use of a telescopic system which consists of a microscope objective.

c) Pin Holes

When the light goes through the objective of the beam expander, the focus of this objective is not a true point but a diffraction circle with a disk of 7 mm in diameter. This diffraction pattern is combined with others caused by dust and dirt on the lens.

A pinhole of a suitable diameter will eliminate all these diffraction patterns which are outside of the central disk,

Fig. 4.3 : The Calming Section

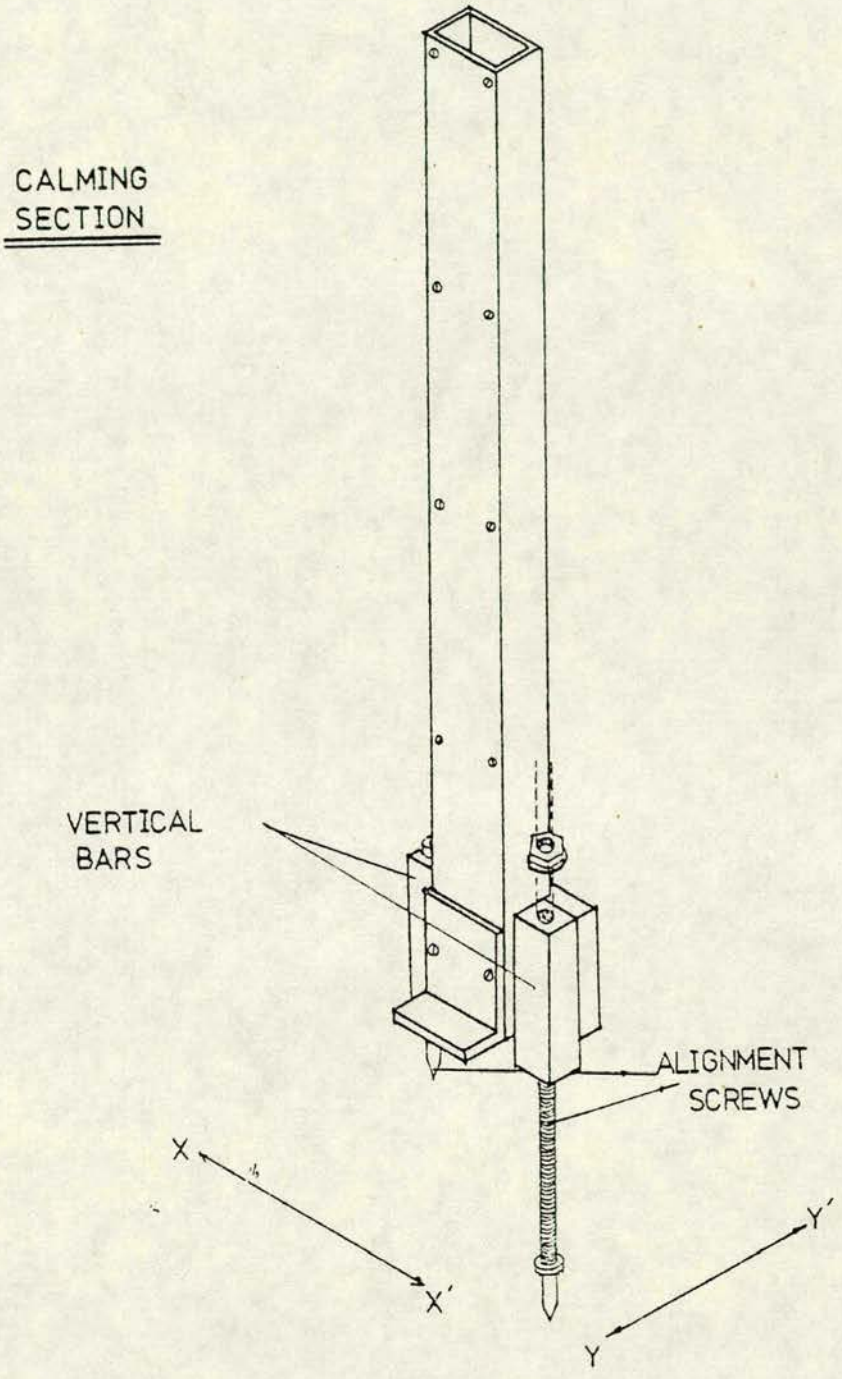

producing as a result a clean beam. In this way, the pin-hole acts as a spatial filter. The pin holes used in this work were manufactured by a process of photo-etching a copper alloy film. They had a diameter of 20 μm.

d) Mirrors

Were used for steering the reference beam from the beam splitter, directing it to fall on the photographic plate at a suitable angle.

e) Beam Splitter

Splits the beam from the laser into a reference and object beam. This is done by a partly reflecting and partly transmitting mirror.

f) A common reading lens

Focused the light from the object beam expander on two cylindrical lenses.

g) The cylindrical lenses

One biconcave and another bi-convex, were used because the object to be viewed was of rectangular shape. These lenses expanded the light to the required height of the object.

9. The Holographic Plate Holder

The holographic plate was kept in position in a grooved metal frame by means of a screw. The metal frame itself was supported from above by a massive stand designed to allow free access from below to the movable baths of processing liquids. The plate was not moved during the process of taking and developing the hologram because insitu development was performed.

The containers with the developing materials were raised toward the holographic plate, until it was submerged in the fluid bath. This arrangement is shown in (Figure 4.7).

Fig. 4.4 : The Optical Table

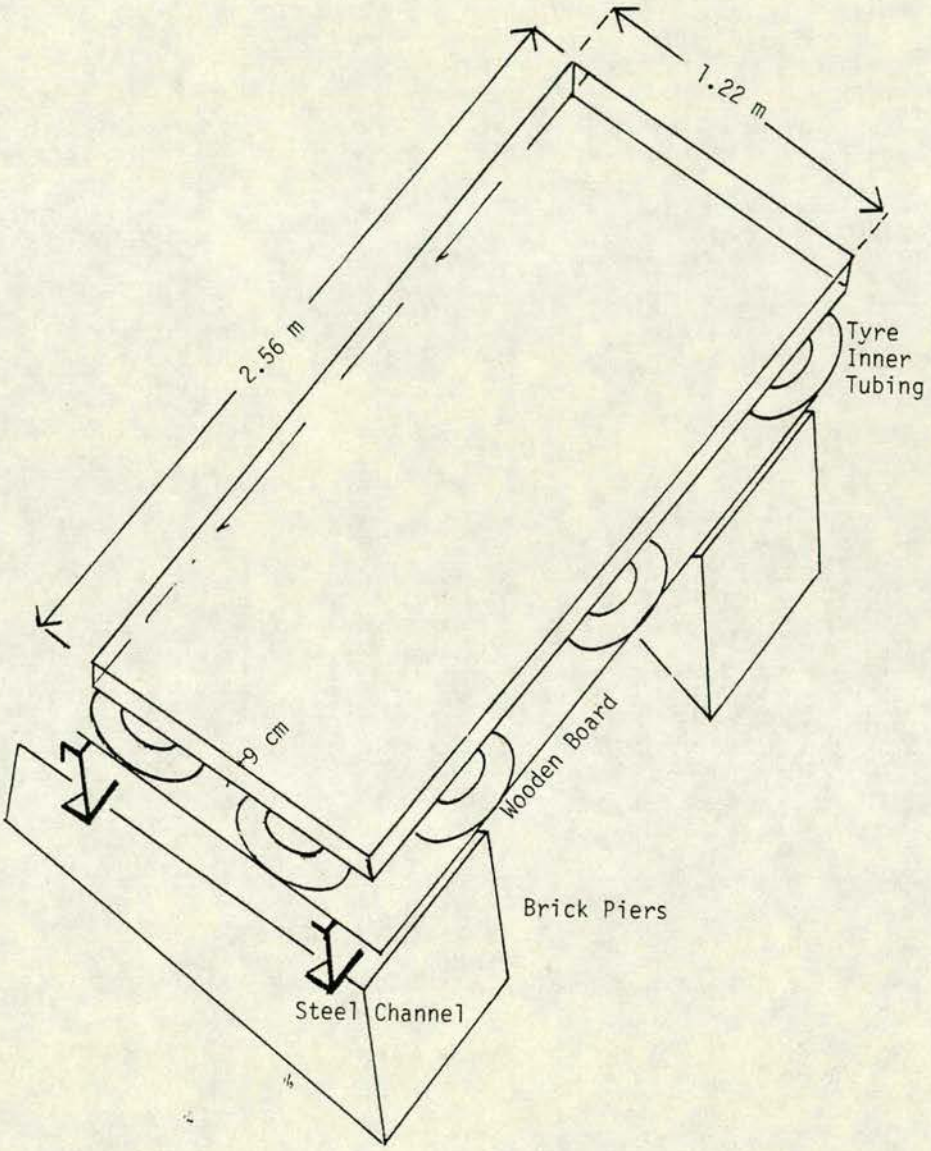

10. Object Stand

This support is made of mild steel and was designed in such a way that the polymer coated glass plate, the rectangular channels and the calming section can be assembled together. (Figure 4.8) shows the support. The glass plate goes into the gap at the point of the figure, resting on two supports at the bottom, and it is held in position by means of three screws, one in one side and two in the other side to ensure the stability of the plate.

The channel is held against the polymer by three screws situated at the centre of each of the three C-brackets fixed on the two vertical square pillars.

11. Perspex Prism: 45^{o} base angles

12. Suction Pump: Power 0.5 H.P. Provided by C.A. Morton, U.K.

13. Rotameters: Metric 24A and Metric 14 XA, provided by M.F.G. & Co. Ltd.,

14. Still Camera: Nikkon

15. Cine Camera: Bolex

16. Holographic Plates: Agfa Gaevert 86 75 (9 x 12 cm, 1.2 - 1.4 mm)

17. Lightmeter: Lunasix 3

18. Inner tyre tubes: For BMC Mini cars

Substances Used

Polymer G.E. RTV 602, no longer available in Britain, replaced by the G.E. RTV 615A, which was used in later experiments, with good results. Catalysts: SRC-05 (G.E.) used with G.E. RTV 602 and Primer: SS-4120 (G.E.), used with both polymers.

Isobutyl benzoate: used as swelling aspect. Supplied by ICN Pharmaceutical, Inc. N.Y.

Canada Balsam: Provided by BDH, Chem. Ltd. Used as cement, for the gluing of the perspex prism to the glass plate, after being diluted with Ortho-xylene, which together with the Canada Balsam cemented the prism to the glass plate. Provided by, BDH, Chem. Ltd.

Fig. 4.5 The Interferometer

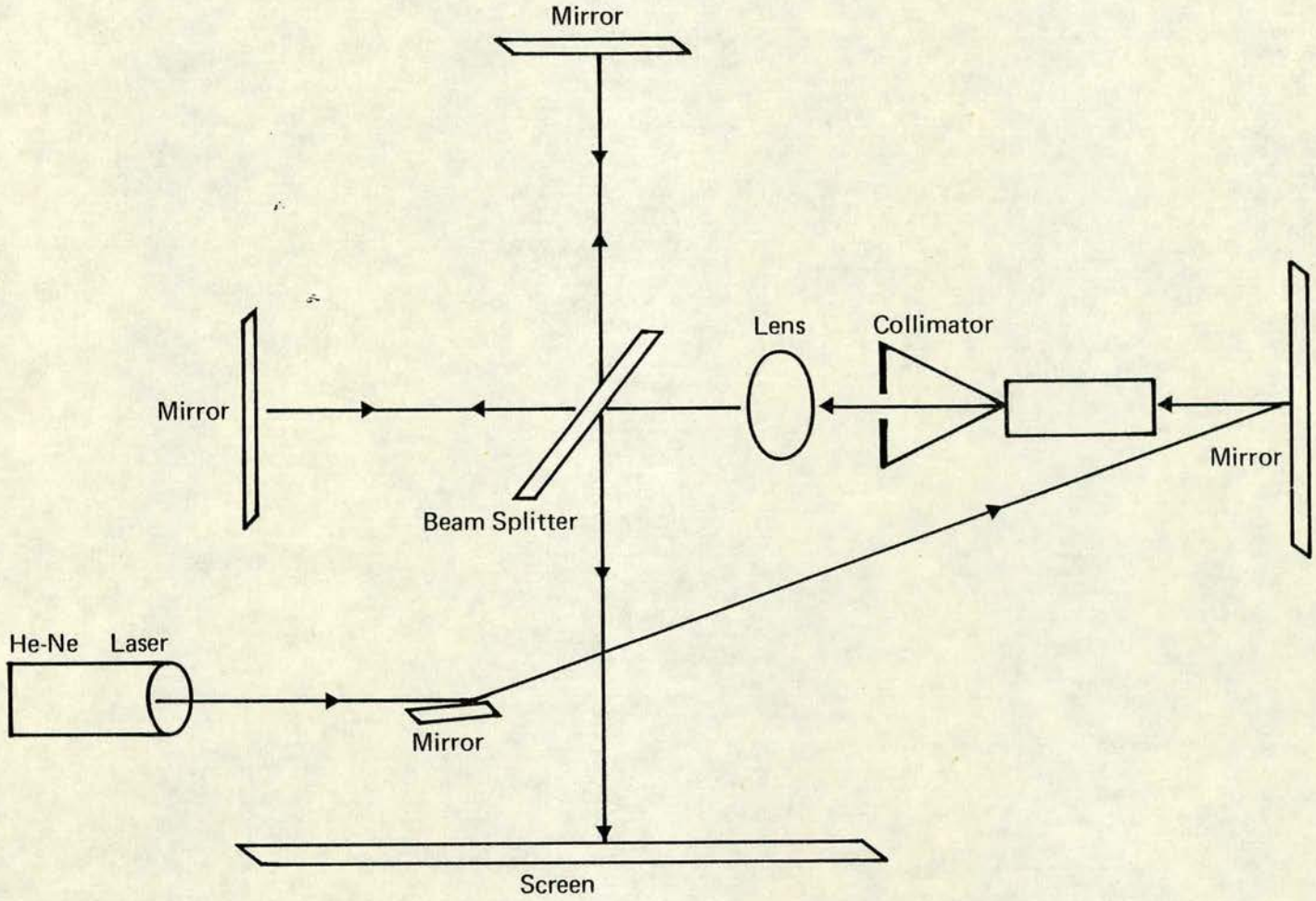

Developer: Kodak D19.

Fixer: Made by May & Baker.

Isopropyl alcohol: Used for accelerating the drying of the holographic plates.

4.2 Techniques Involved

4.2.1 The taking of the holograms

Two techniques were applied, namely, real-time and double-exposure holography. These will be described separately:

(a) Real Time

Using this technique a hologram is taken, developed and processed insitu with the object undisturbed. Air is then passed through the channel while this is viewed, via the prism, through the developed hologram, so that the process of mass transfer can be seen as it happens and recorded by means of a cine camera, for further study. The intensity ratio required was found to be very high, the reference beam to object beam intensities being 128:1, as measured at the centre of the holographic plate by means of a light meter.

This high intensity was needed because total internal reflection is very efficient in reflecting the object beam light. This makes the object appear very bright and the fringes, due to the recession of the polymer caused by mass transfer, cannot be seen. Consequently, it was concluded that the intensity of the object beam should be lowered, raising thereby the relative intensity of the reference beam. However, it was found that, although the fringes could then be seen very clearly, the fact that the intensity of the object beam was very low made impossible their recording with the cine camera. It was necessary, then, to resort to the double exposure technique.

Fig.4.6 The Optical Circuit

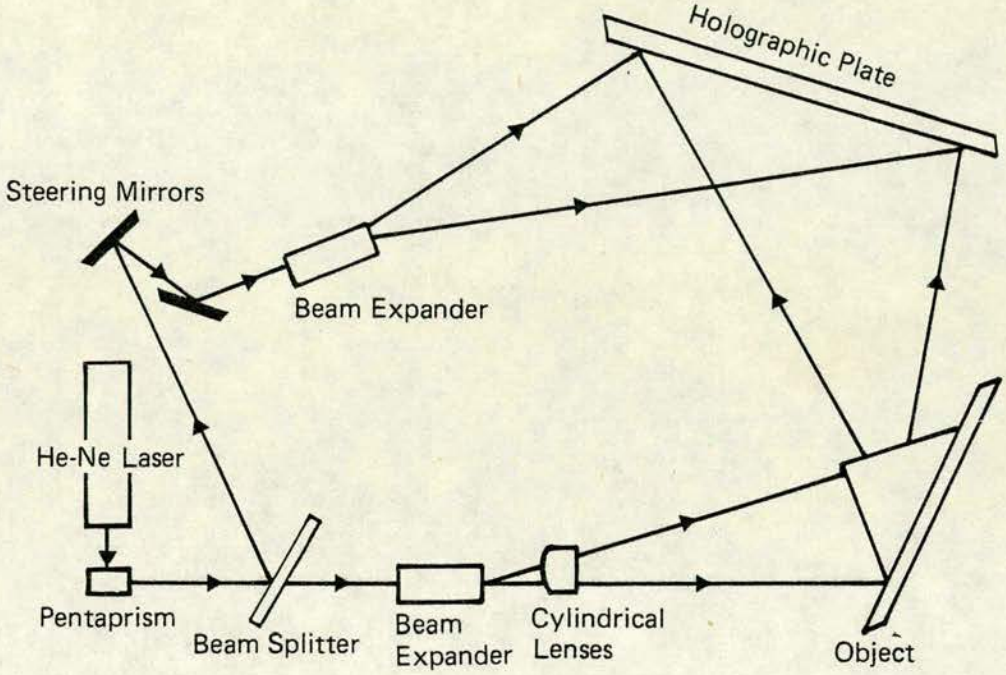

The attempt to record the formation of fringes in real time, was tackled in order to allow, through the cine film, the counting of the number of fringes passing a given point in a given time and thus to determine the mass transfer coefficient at that point. By such observations at different points on the channel wall, we could have obtained directly the variation of the mass transfer coefficient with distance from the leading edge of the channel from a single movie.

As it happened we have had to resort instead to the double exposure technique.

(b) Double exposure

The rationale behind the use of the double-exposure technique, for registering the process of mass being transferred from a swollen polymer to a stream of air, rests on the fact that when a hologram of an undisturbed object is taken, and the object itself remains illuminated insitu while its holographic reconstruction is reviewed, the light from both object and reconstruction travels the same distance to the observer; but when the object is disturbed, the light from the object (or from a second holographic reconstruction in the new position) travels now a different distance. When this path difference is equal to some integral multiple n of $\lambda/2$, a fringe will appear on the object and it will be bright if n is even or dark if n is odd. If the disturbance is produced by recessions of the polymer surface caused by mass being transferred from the polymer to the air stream, then every fringe will be the locus of all points with equal recession, i.e. with equal rate of mass transfer.

In this work, the reference to object intensity ratio was lowered to 64:1. It was possible to do this, and at the same time to get good fringes, because the technique involves, as said

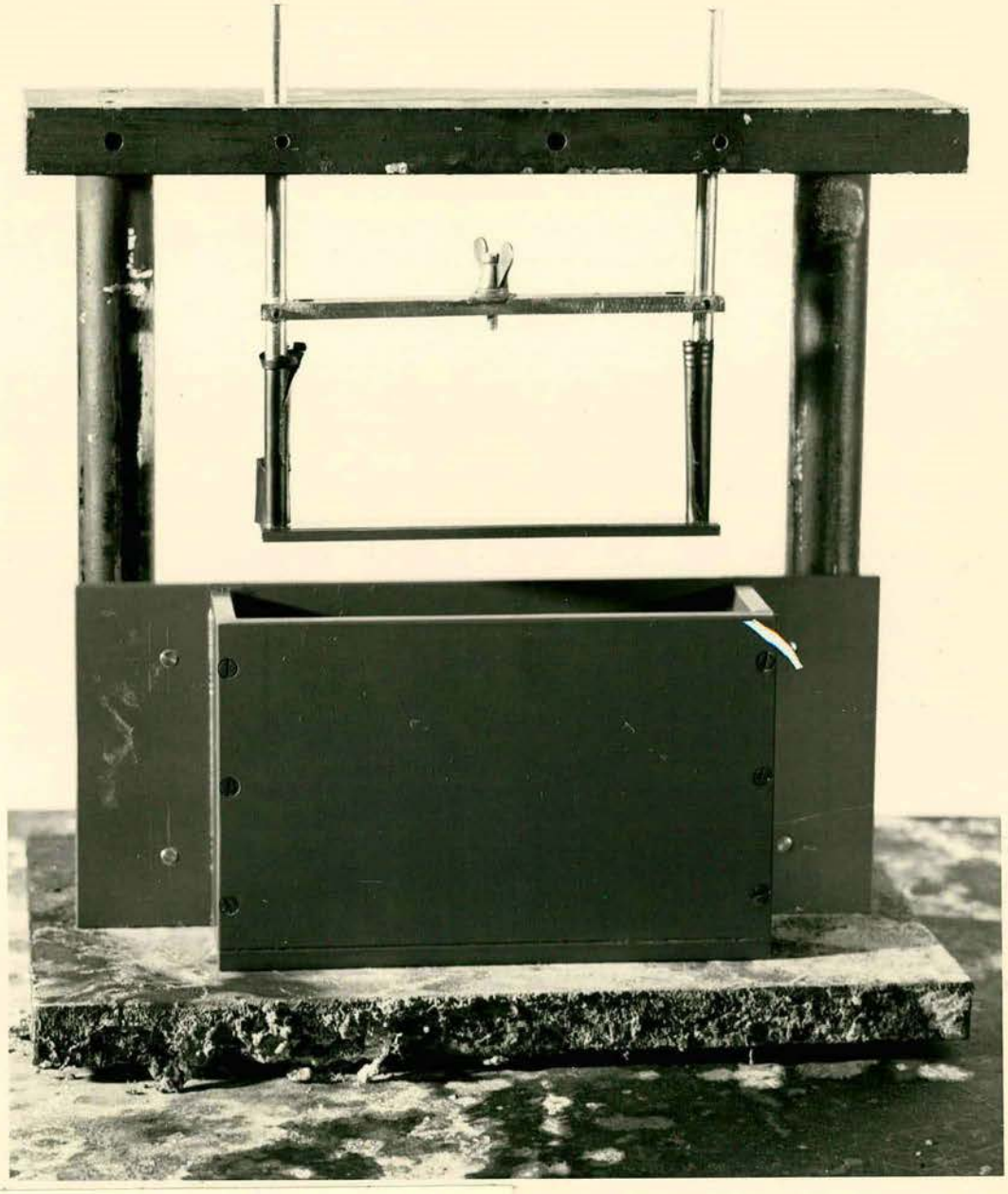

Fig. 4.7 The Holographic Plate Holder

above, the taking of two holograms on the same holographic plate, and whatever change occurs during the mass transfer process is recorded by the emulsion. In the case of the real time method, on the other hand, the fringes had to be detected by the eye, previous to the recording.

The first hologram is taken when the object is undisturbed. After this, air is run through the channel for a given time, and at the end of this time a second hologram is taken on the same holographic plate as the first one, the exposure times being the same for both holograms.

This procedure assures that if any positional change has occurred in the surface of the object between exposures, when the hologram is viewed using the reference beam, the change will be perceived as fringes on the object because the two images will not match.

4.2.2 Preparation of the glass plate

The glass plate was coated by the procedure described below with transparent polymer on one side, which formed one of the internal walls of the experimental channels. On the other side, a perspex prism was glued to the surface using Canada Balsam diluted with ortho-xylene as the cement. This side faces the object beam and the prism allows the rays to enter the polymer coating at such an angle as to undergo total internal reflection from its free surface, so permitting the recession of the polymer to be registered as the mass transfer process takes place.

A grid of parallel lines was ruled at one centimeter intervals on the face of the glass plate subsequently coated with polymer, in order to provide reference co-ordinates and to allow the scaling-up or down of the still pictures to be taken from the holograms.

Fig. 4.8 : The Object Stand

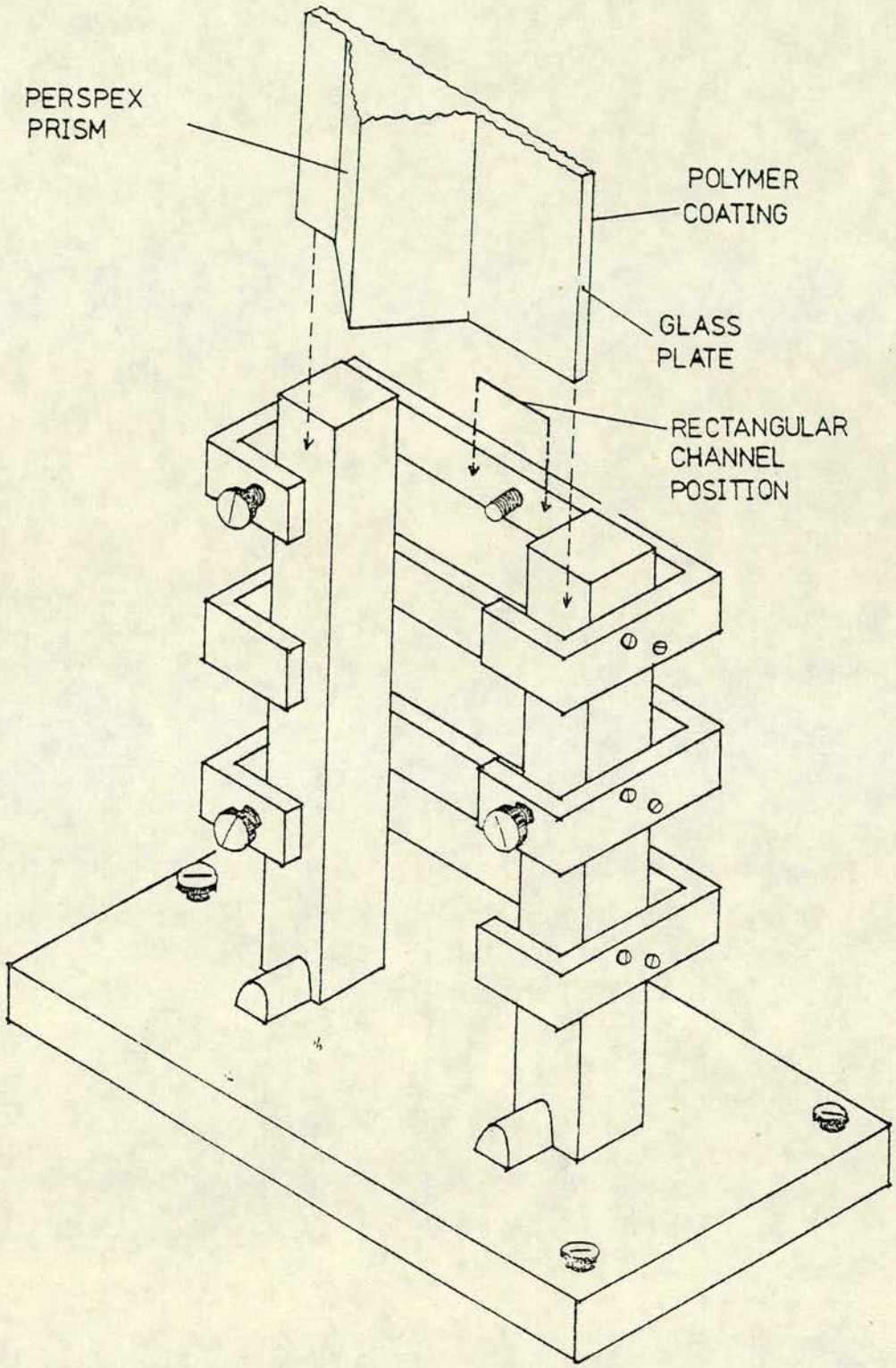

4.2.3 Polymer Coating

After the prism had been attached to the plate with the optically clear cement, the plate was leveled on wooden blocks, and brush-painted on the other side with the primer recommended by the manufacturers of the coating polymer (G.E., RTV 602, or G.E., RTV 615A) and then left to dry for half an hour. This operation was done to avoid the detachment of the polymer during swelling. Following this, ten ml. of the polymer was poured into a beaker and the makers recommended catalyst, specific for the type of polymer used, was added in the proportion of one per cent by weight.

The mixture was stirred vigorously, and the polymer spread with a knife on the plate surface. Afterwards the polymer (G.E. RTV 602) was allowed to set for a period of cure of twenty four hours at room temperature, following which it was ready to use.

There were some problems in following this procedure because of the ageing of the catalyst. This brought about either longer periods of cure, when the amount of catalyst was insufficient or a quick setting when, in an attempt to compensate for its reduced activity, it was added in excess. This caused the surface to suffer distortions and had to be discarded. With polymer G.E. RTV 615A, the curing took several days, at room temperature, and it was not even then totally complete, i.e., the polymer remained sticky. This situation demonstrated the need to accelerate the curing process by putting the glass plate, with the polymer already spread on it, inside an oven, where the temperature was kept at $60^{o}C$. Setting was achieved after 5 hours of this heat treatment. Also, with continuous use (swelling and re-swelling) the polymers detach from the plate or develop bubbles and have to be detached from the glass and re-cast anew.

4.2.4 Swelling of the Polymer

The swelling of the polymer was effected by immersing the coated glass plate in a shallow tray containing isobutyl benzoate and leaving it overnight. The isobutyl benzoate was held in a pad of porous absorbent cloth placed in the bottom of the tray and saturated with the liquid. This was done to prevent the poylmer from sticking to the bottom of the shallow tray. The glass plate was put with the coated side on the soaked cloth. Care was taken to avoid contact between the isobutyl benzoate and the Canada Balsam or the perspex prism at the back of the plate.

The swollen polymer-coated assembly was then removed from the tray and the surface dried thoroughly with a paper towel to remove surplus liquid. The glass plate assembly with the swollen polymer was then mounted on the heavy stand previously described, with the prism facing the laser. The carcass or body of the channel was then brought up to the plate, which formed its fourth wall, and pressed against the swollen polymer coating by clamping screws. To finish the drying of the surplus liquid from the swollen coating, air was made to pass through the channel for one minute.

The process of swelling, drying and clamping the channel body against the polymer was repeated for each complete run in the case of abrupt entrance with asymmetric transfer (both 3:1 and 2:1 ducts) and after two complete successive runs in the other flow situations. However, in a series of runs two complete successive runs were made without re-swelling in all flow situations.

The setting of the metal channel against the polymer was a laborious task which took from six to ten minutes. In abrupt entrance runs, setting the leading edge of the channel flush with that of the glass plate was done very carefully.

Clamping the plate likewise required to be done with great care, because if the channel presses the polymer too tight it may cut the surface of the polymer, but if it is too loose there will be leaks from the channel. The whole procedure is easier with the calming section because the end face of the latter automatically locates the upstreams edge of the glass plate.

4.2.5 The holographic plate

The photographic plate is set in the holographic plate support in the dark and it is prepared for the taking of the hologram in the real-time technique through these steps: (a) Washing with tap water for a minute, to allow the relaxation of stresses in the emulsion, (b) Washing with isopropyl alcohol for two minutes, to allow a faster drying (c) Drying in air for fifteen minutes. For double-exposure this preparation is not needed because, whatever change the emulsion suffers it will affect equally both holograms.

4.2.6 Exposure time and developing

The exposure time for making the original state hologram during the real time runs was 20 seconds. During the double exposure experiments the exposure time was 5 seconds for each exposure. The developer used was Kodak D19 and Amfix was used as a fixer.

After exposure, developing took place following these steps: a) one minute in Kodak D19 developer b) half a minute in water c) three minutes in the fixer and d) five minutes washing e) drying, which took from fifteen to twenty minutes, and was affected in the air. Sometimes, the process of drying was accelerated by washing the plate in isopropyl alcohol for one minute. This was done always when working with real time interferometry.

4.2.7 Reconstruction and Photographing

The dry double-exposed hologram was mounted in the holographic plate holder, then the object beam was blocked and the hologram viewed with the reference beam to check if the fringes were good.

A still camera supported on a rigid stand to avoid unwanted movements, was put behind the holographic plate. (Fig. 4.9). The pictures were taken at a fixed position of the camera relative to the hologram, and the exposure time was between twnety and thirty seconds.

After photographing, the pictures were developed at the University Film Unit and the prints were used for measuring the distances from the edge of the channel to the fringes, by means of a graduated scale, knowing that the parallel lines drawn on the plate were one centimeter apart. This allows the scaling-up or down of the pictures. (See Figs. 4.10 to 4.13).

4.2.8 Total internal reflection

In conjunction with the technique of double-exposure and real-time interferometry, we used the principle of total internal reflection, given the fact that we were interested in looking at the recession of the polymer brought about by the mass transfer process at one of the internal walls of the rectangular channel. It is not possible to effectively examine or record the state of the coating by the front reflection technique without dismantling the channel, because of problems of stray reflections from observation windows. Total internal reflection occurs when the angle of incidence of the light proceeding from a denser medium to a lighter one is greater than a critical angle, given by: $\sin c = \mu_1/\mu_2$ where $\mu_2 > \mu_2$. At the critical angle the light will pass through the boundary of the two media, at lower angle value it will go through to the other medium and at angles bigger than the critical, the light will be

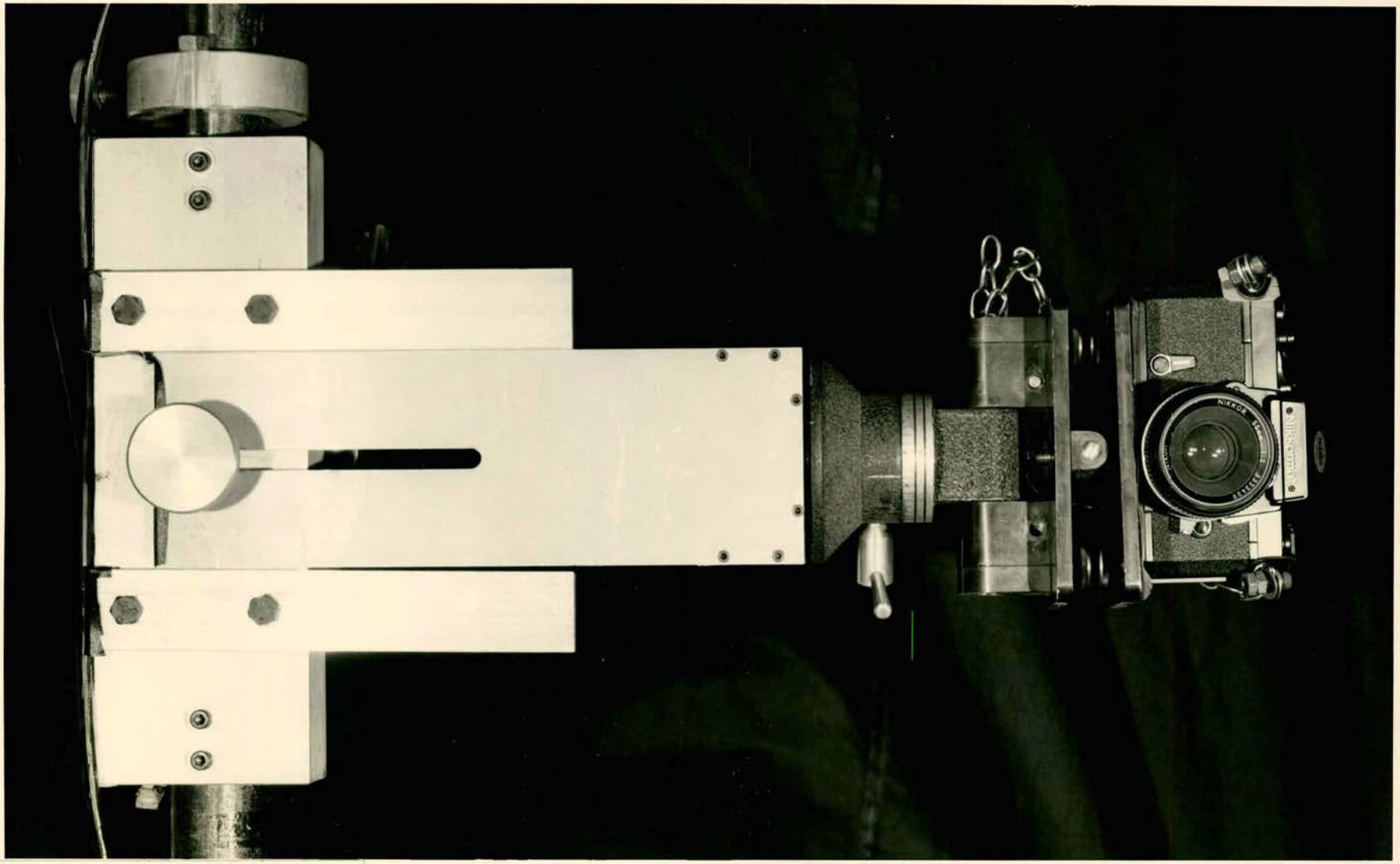

Fig. 4.9 The Camera Stand.

reflected back from the boundary of the two media. In our specific case, the angle C was found to be 44.29°; the angle of incidence actually used was 51.48°, which indicates that total internal reflection was achieved. (See Appendix B).

A related difficulty, although not inherent in the total reflection technique, manifested itself during the set up of the optical circuit. The prism only allows a narrow strip for viewing and because of the brightness due to specular reflection, the viewing was restricted to a given angle from where the fringes can be seen against an attenuated background. The fact that the eye or the camera has to be positioned at a particular angle, for the fringes to be seen, imposes a restriction in the value of the angle between beams at the holographic plate, because in our case the beam expanders give a small angle of divergence and therefore both the object and the holographic plate must be placed far from them. In these circumstances, the angle between beams cannot be made wider or smaller because of other restrictions, e.g. that the optical path difference should not be bigger than the coherence length of the laser.

In this work, the angle between beams was about 60° which gave a fringe spacing of 632 μm, corresponding to a resolution of 1580 lines/mm.

4.2.9 Identification of the Absolute Fringe Order

The measurement of local mass transfer coefficients has been historically a difficult task. In this present work we use a relatively novel technique to achieve this end, which employs holographic interferometry to measure the dimensional changes due to the convective transfer of volatile solvent from a swollen polymer to a stream of air. The local mass transfer coefficients are

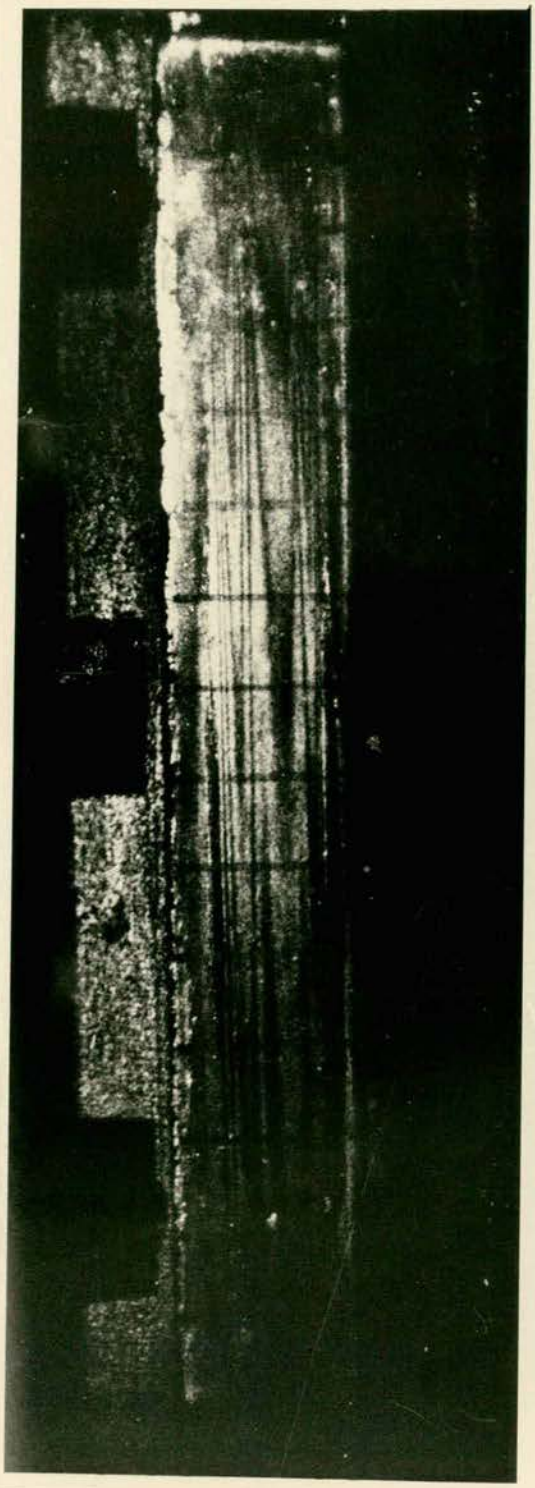

Fig. 4.10

Duct 2:1, dh = 1.27 cm.
Calming Section Abrupt Entrance.

Re = 3770, t = 10 min.

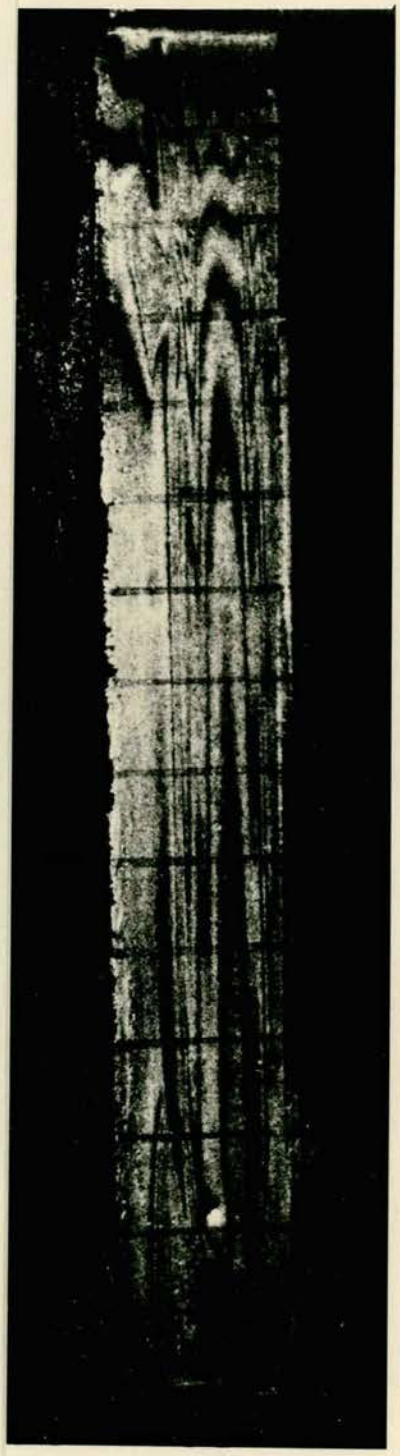

Fig. 4.11

Duct 2:1, dh = 1.27 cm.
Abrupt Entrance, Asymmetric Transfer.

Re = 5815, t = 7 min.

calculated from knowledge of the absolute orders of the fringes, which are found using a new method of coincidences. Interferometric holography has previously been applied to measure mass transfer coefficients for the impingement of a jet of air on a flat surface, for both laminar and turbulent flow by Kapur and Macleod (1974). Also Masliyah and Nguyen (1977, 1979) and Grosse-Wilde and Uhlenbush (1978) used holographic interferometry to measure local mass transfer coefficients from flat surfaces. However, in all these cases the absolute order of the fringes was known, only by reference from non-optical observations. Furthermore, at the time of this work we do not know of any publication dealing with the measure of local mass-transfer coefficients in ducts or dealing with the systematic determination of the absolute order of fringes produced as the result of mass transfer operations.

The technique employed requires the use of a polymer which is swollen by a suitable low vapour pressure swelling agent; in this case, isobutyl-benzoate. The polymer coats a glass plate which constitutes one of the walls of the duct used in these mass transfer experiments. The advantages of this technique are a) the coating can act as a mass transfer source or sink b) the polymer can be reswollen as many times as required, making the whole system a re-usable one, and c) the Schmidt number can be changed by changing the swelling agent.

Macleod and Todd (1973) give the conditions which must be fulfilled if the rates of recession of the polymer are to be proportional to the different air-side coefficients of mass transfer. Those conditions must hold during the periods of measurement and they are: a) the change in thickness of the swollen polymer is proportional to the mass of swelling agent transferred b) the vapor pressure of the

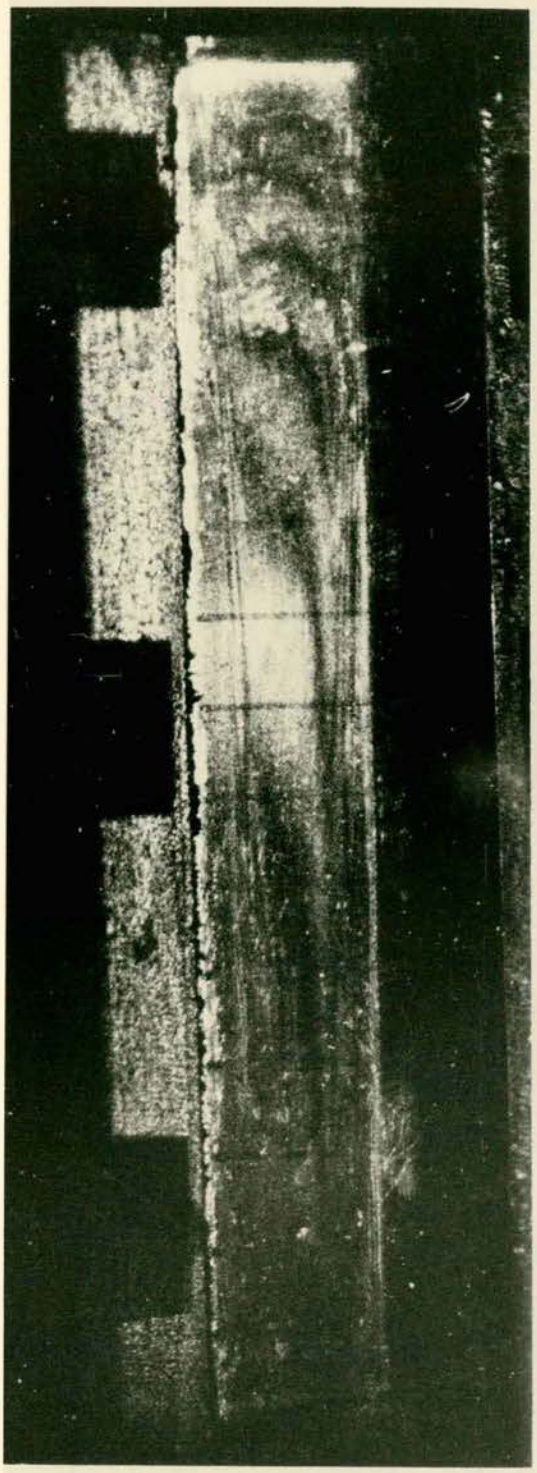

Fig. 4.12

Duct 3:1, dh = 1.43 cm.
Abrupt Entrance, Symmetric Transfer

Re = 4598, t = 10 min.

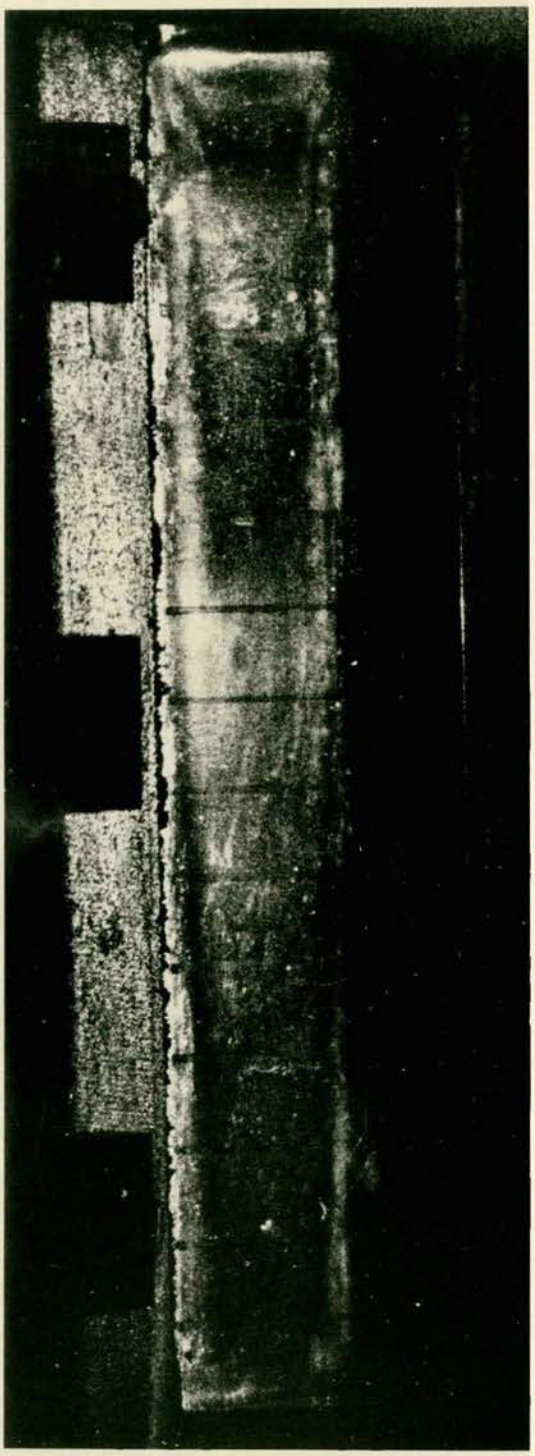

Fig. 4.13

Duct 3:1, dh = 1.43 cm.
Calming Section, Symmetric Transfer.

Re = 528, t = 10 min.

swelling agent over the surface is everywhere the same initially, and remains sensibly constant as the transfer proceeds c) the overall resistance to mass transfer is predominantly in the gas phase d) the behaviour of the coating at any given point must be governed only by the local situation, and lateral diffusion or differential stress effects must not affect it e) in spite of any inequalities in the original coating thickness, the relationship between mass transfer and shrinkage rate should be uniform over all the polymer . The same authors were able to show also, that all these conditions can be met in practical cases using rubber coatings a few tenths of a millimeter thick, swollen with suitable ester.

The results of the application of this technique to measurement of mass transfer rates in a rectangular duct are the theme of this thesis and they will be discussed later in more detail.

Previous experience had shown that one of the principal difficulties in measuring mass transfer coefficients holographically is that of identifying the absolute order of the interference fringes and hence of determining absolute mass transfer rates. Before the study of mass transfer in rectangular ducts was started, we experimented with an absolute method for determining local mass transfer coefficients from an aluminium alloy plate coated with a swollen polymer, using the swelling agent isobutyl benzoate and using a jet of air impinging normally in a set up similar to the one used by Kapur. The technique employed in these preliminary trials was that of real-time holography, using a cine camera to record the fringes in time-lapse photography.

The idea was to examine the pictures obtained, using a film analyser, and by means of it to count the number of fringes passing a given point. With this knowledge, the mass transfer coefficient

could be known at that point and by proceeding in the same fashion with other points it would be possible to know the variation of the mass transfer coefficients from the centre of the plate radially, the fringes in this type of experiment being circular. (Figs. 4.14-4.15).

Good fringes were obtained with this method but the rate of passage of the fringe through a given point, did not give good results and this was partly due to the imperfect mechanical stability of the system, i.e. to the deterioration of the antivibration pads on which the optical table rested.

After this problem was solved by making the top of the table rest on car tyre inner tubes we attempted time-lapse photography using the rectangular duct, and although we were able to get good fringes in real-time visible to the naked eye, it was not possible to record them cinematically for optical reasons. This was principally because the object beam had to be attenuated due to high specular reflectivity of the total inter al reflection set up.

The identification of the absolute odd fringe order comprises two main steps:

a) The construction of the master curve for a given run,

b) The calculation by trial and error of the absolute odd order.

a) <u>The master curve</u>

For a given run is constructed by the following procedure:

1) All the data, corresponding to each of the different times involved in the run in question, are plotted as graphs of nominal (odd) fringe order (N) vs distance (x) of the fringes from the leading edge of the test section.

2) An arbitrary point on the curve corresponding to the highest time (tk) is chosen as the reference or crossing point for all the curves.

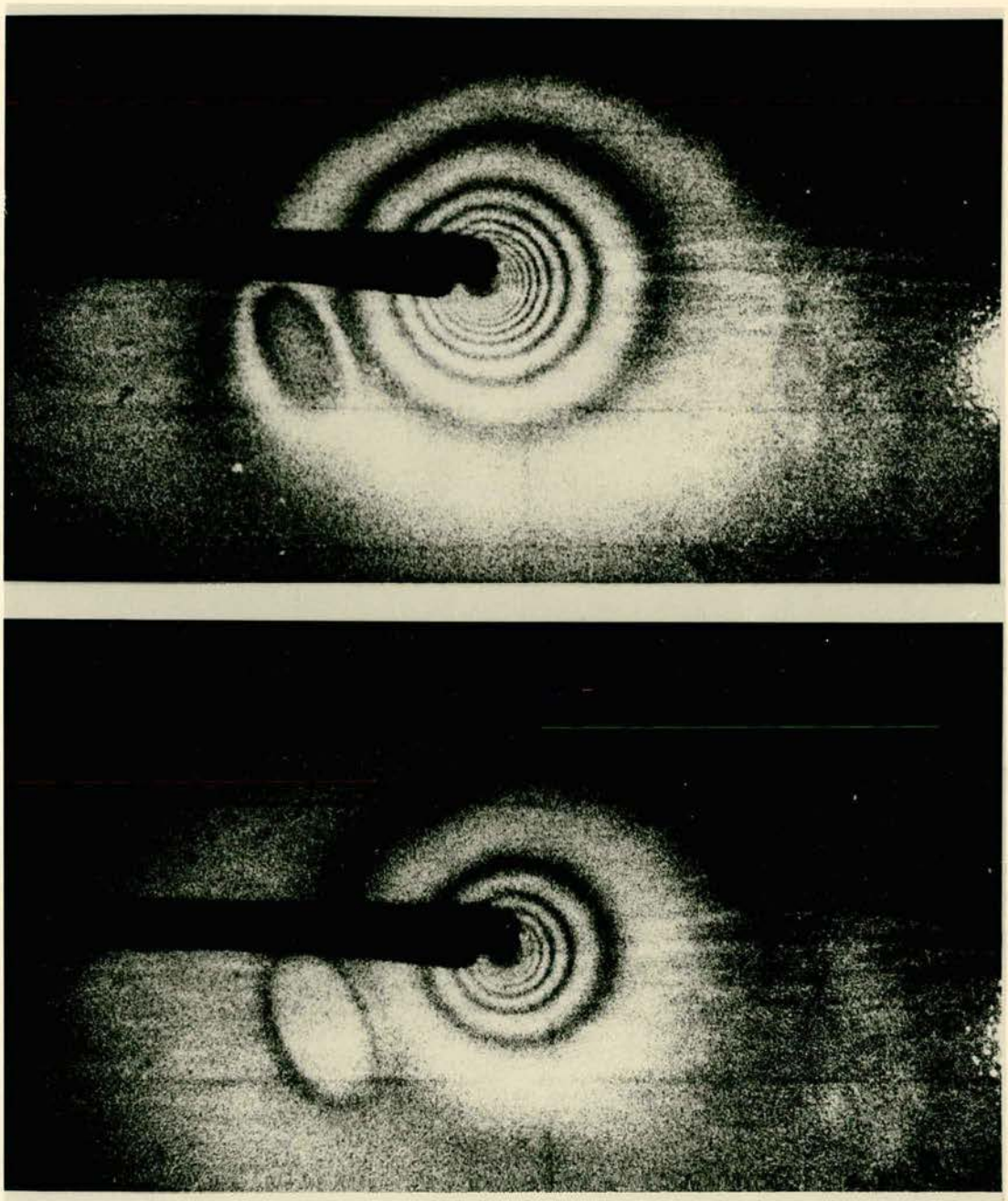

Fig. 4.14 (up) and Fig. 4.15 (down) **Flat Plate Experiments**

Fringes obtained by holographic interferometry, recording mass transfer of methyl salicylate from a flat plate, exposed to a normal air jet.

Fig. 4.14 (up) $Re = 288, t = 5\,min.$
Fig. 4.15 (down) $Re = 288, t = 3\,min.$

3) All the other curves of the run are translated so as to pass through the crossing point. This is done by adding to the ordinate of every point on a given curve, the difference between the ordinate of the reference crossing point and the ordinate on the given curve at the same abcissa.

4) From each of these new ordinates is subtracted the ordinate of the crossing point and the result is multiplied by the ratio of the highest time to the particular time for this curve. However, if the temperatures for the runs in question are different, then the multiplier is the ratio of the times as above times the ratio of the vapour pressures at the temperatures.

5) Finally, to the results of the above operation is added the co-ordinate of the crossing point, to give the ordinates of the points on the master curve. After these operations have been carried out for every point on all the curves, the degree of scattering, around the curve which corresponds to the highest time is considered. If the degree of scattering is low, then the curve already drawn for the highest time becomes the master curve of that run. If the scaled-up points mostly agree among themselves but show a systematic deviation for one of the curves of the run, that curve is excluded from the construction of the master.curve. The whole procedure is repeated for the other runs.

b) Calculation by trial and error of the absolute odd fringe order

The above described procedures serve to consolidate and average all the data for given flow conditions and to verify the expected proportionality between the ratios of times and the ratios of corresponding recessions for a given run.

If one point on the master curve, for $t = t_K$, has an ordinate n_K then the above operations ensure that the co-ordinate system is such that:

$$\frac{n_K}{n_{K-1}} = \frac{t_K}{t_{K-1}} \; ; \; \frac{n_K}{n_{K-2}} = \frac{t_K}{t_{K-2}} \; , \text{ etc.}$$

This proportionality is the basis for calculating the absolute odd fringe order. The value of n_K is not in general an integral number of fringes. The relationship between n_K and the next odd fringe value, $\bar{n}_K$, is:

$$n_K = \bar{n}_K \pm \nu_K$$

where the sign will depend on the choice of n_K

If the $\bar{n}_K$ corresponds to the next odd integer above n_K, it will be negative, and if it corresponds to the next odd integer below n_K it will be positive. Bearing all this in mind, the procedure for the trial and error operation is as follows:

1) An arbitrary n_K is chosen as a reference on the master curve. For convenience, n_K is taken to coincide with an odd n value of the ordinate, corresponding to a dark fringe, so that $\nu_K = 0$ and $n_K = \bar{n}_K$.
2) Going from $n_K = \bar{n}_K$ down, at the same abicissa (x_k), the next curve for $t = t_{K-1}$ is encountered and this point at x_k will be n_{K-1} In general n_{K-1} will not be integral.
3) An odd value of n is chosen ($\bar{n}_{K-1}$) next to n_{K-1} on the t_{K-1} curve.
4) The equation to be solved by trial and error or set up in the following manner: Taking into account the above discussion, it follows that:

$$\frac{n_K}{n_{K-1}} = \frac{t_K}{t_{K-1}} \quad \text{or} \quad \frac{\bar{n}_K}{\bar{n}_{K-1} \pm \nu_{K-1}} = \frac{t_K}{t_{K-1}}$$

5) The other equations which correspond to the times t_{k-2} t_{k-3} etc, are set up in a similar fashion.

6) Odd trial values are given to $\bar{n}_{k-1}$. $\bar{n}_{k-2}$. $\bar{n}_{k-3}$ etc, and at the end all values of n_k are compared. A consistent, repeated value of $\bar{n}_k$ through the calculation will ensure that that is the correct value of $\bar{n}_k$.

7) Once $\bar{n}_k$ is found, all other absolute odd fringe order values are automatically fixed.

4.2.10 Graphical Explanation of the Procedure to Determine the Absolute Fringe Order

Supposing the situation to be as depicted below, we take the following steps:

Fig. 4.15 Nominal Fringe Order (N) vs Distance (x)

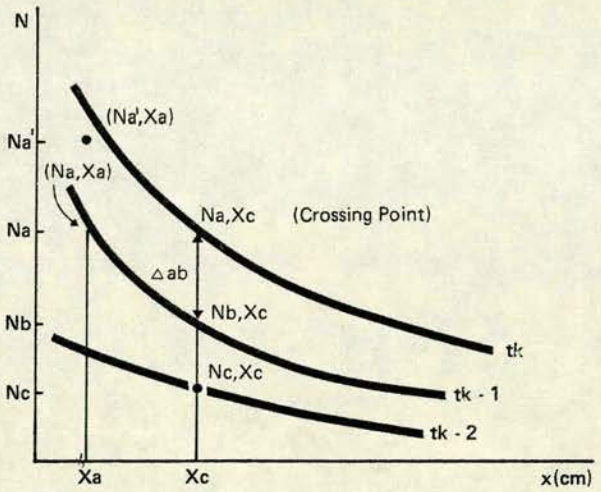

1) Na - Nb = Δab, this operation gives us Δab which is the amount to be added to each point on curve t_{k-1} to accomplish the translation of the whole curve t_{k-1}. whose point (Nb, x_c) will then become (Na, x_c).

2) For a given point (Na, x_a) the procedure is as follows:
Na + Δab = Na', this operation accomplishes the translation of this point.

3) Na' - Na, this gives the co-ordinate of Na' corresponding to Na = Nb as the new zero for the plotting of the points of curve t_{K-1}

4) The next scaling procedure will translate the point under consideration up to the curve at t_K or close to it depending on how good is the point. To achieve this, (Na' - Na) is multiplied by t_K/t_{K-1} but if this run is at a different temperature than the run at t , then the vapour pressure at both temperatures must be taken into account, so that the operation now reads:

$$(Na' - Na)\ \frac{t_K\ P_K}{t_K\ P_{K-1}}$$

5) $(Na' - Na)\ t_K/t_{K-1} + Na$, restores the original zero of the N vs x plot. As before, if the temperatures are different the vapour pressures must be taken into account.

The same procedure is repeated for each point on the curve t_{K-1} and then on the curve t_{K-2} etc. Once the master curve is constructed, being the best curve for the scaled points, the situation now will be handled as follows

Fig. 4.16 Absolute Fringe Order (n) vs Distance (x)

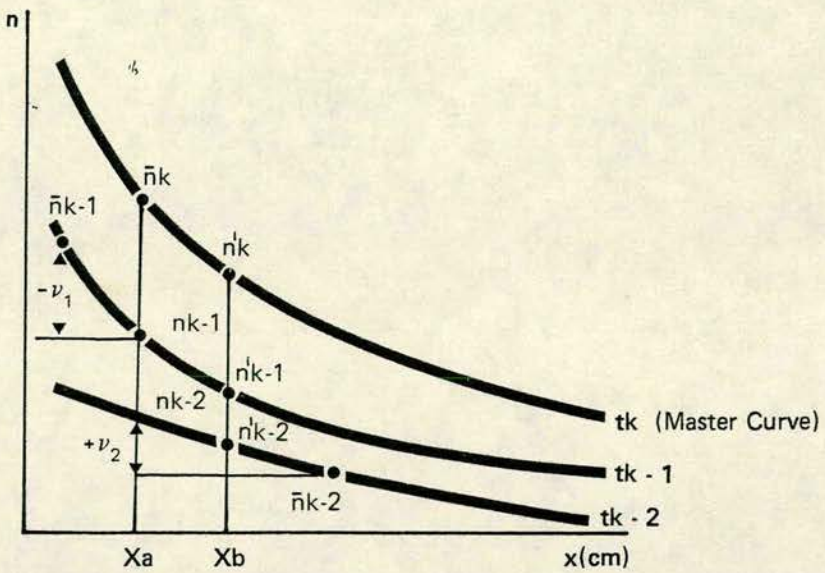

The above operations ensure that

$$\frac{n'_k}{n'_{k-1}} = \frac{t_k}{t_{k-1}} \quad \text{and} \quad \frac{n'_k}{n'_{k-2}} = \frac{t_k}{t_{k-2}}, \quad \text{also} \quad \frac{n'_{k-1}}{n'_{k-2}} = \frac{t_{k-1}}{t_{k-2}}$$

If we choose one of the n_k values (ordinates) on curve t_k to coincide with a dark fringe, i.e., to have an odd value and call it $\bar{n}_k$ then it follows from the graph that:

$$\frac{\bar{n}_k}{n_{k-1}} = \frac{t_k}{t_{k-1}} \quad \text{but} \quad n_{k-1} = \bar{n}_{k-1} - \nu_1, \text{ therefore}$$

$$\frac{\bar{n}_k}{\bar{n}_{k-1} - \nu_1} = \frac{t_k}{t_{k-1}}, \text{ the same with: } \frac{\bar{n}_k}{n_{k-2}} = \frac{t_k}{t_{k-2}}$$

but: $n_{k-2} = \bar{n}_{k-2} + \nu_2$, then: $\dfrac{\bar{n}_k}{\bar{n}_{k-2} + \nu_2} = \dfrac{t_k}{t_{k-2}}$

The equations: $\bar{n}_k = \dfrac{t_k}{t_{k-1}} (\bar{n}_{k-1} - \nu_1)$ and

$\bar{n}_k = \dfrac{t_k}{t_{k-2}} (\bar{n}_{k-2} + \nu_2)$ are used to find by trial and error the value of n_k, and consequently the value of $\bar{n}_{k-1}$ and $\bar{n}_{k-2}$.

Knowing these values, all others are known because being dark fringes they differ by two from the next one above or below it. An example of the practical application of this method is given in Appendix C.

4.3 Design of the Experiments

The aim of developing a general method of fringe interpretation of use for determining mass transfer coefficients from a volatile substance to air, by means of holographic interferometry, was achieved through several experiments. After a number of preliminary trials in which the feasibility of real time measurements was explored, the main experiments were undertaken on a system of both scientific and practical

interest. In these experiments, three rectangular ducts of aspect ratios 1:1, 2:1 and 3:1 were used.

Four flow situations were examined at different Reynolds numbers, giving laminar and transitional flow regimes. The flow situations were:

a) Abrupt entrance, asymmetric mass transfer

b) Abrupt entrance, symmetric mass transfer

c) Developed flow, asymmteric mass transfer

d) Developed flow, symmetric mass transfer

The transferring surface consisted of a polymer, cast on a glass plate and swollen by an agent of low vapour pressure, used under conditions assuring a good spacing between the fringes.

Mass transferthus occurred between an air stream provided by a vacuum pump and a solid surface to which a three-sided enclosure was clamped to form a rectangular channel which remained constant in shape. To perform the symmetric transfer runs a channel with a second detachable wall was used, so that both opposed walls of this channel could be coated with polymer. For experiments with hydrodynamically developed flow, a calming section of the same internal dimensions as the test section of the duct, but having plain uncoated walls, was fitted to the entrance of the flow system.

Finally, care of the stability of the system, which is paramount in holographic interferometry, was taken by the design of an antivibratory system, which kept the top of the optical table resting on tyre inner tubes.

4.4 Experimental Procedures

In order to make a run the procedures were as follows:

1) The object (channel plus glass plate) is put in position, clamped in the object stand, facing the laser.

2) The level of the table was checked to see that it was clear of the wooden stops and resting evenly on the pneumatic tubes by means of a level and eye inspection. If the table was not level, the tubes were inflated accordingly to achieve this.

3) The laser is turned on and allowed a warm-up period of at least half-an-hour. The readiness of the laser was ascertained by measuring, at the centre of the plate, the intensity ratio of reference to object beam by means of the Lunasix 3 light meter. The check was against a previous value of the intensity ratio determined by trial as the best one.

4) After this checking is finished and the room temperature is read from a thermometer, the laser light is blocked by means of a shutter and the holographic plate is put in the holographic plate holder, with the emulsion facing the object. If the real time technique is to be used, the holographic plate is soaked in tap water for one minute, to free the emulsion of 'frozen' stresses which produce unwanted movements in it, giving rise to unwanted fringes. Then isopropyl alcohol is used for two minutes to ensure fast drying. Drying takes between fifteen and twenty minutes. If, however, double exposure is to be used, after the holographic plate is in position, a minute is allowed to elapse, to assure the accommodation to the mechanical stresses and heating that may develop during manipulation of the plate. Whatever movements the emulsion will have during development will affect both holograms in the same degree cancelling out any side effects. Once the holographic plate is ready, the shutter is opened and the object is exposed to the laser light. Exposure time is 20 seconds for real-time holography. For double-exposure holography an exposure time of 5 seconds was allowed for each hologram.

5) After exposure, the light from the laser is blocked by the shutter and the vacuum pump is turned on. The pump will deliver a preset air flow, as controlled by a valve and measured by a rotameter. The pump is run for a chosen time, which again is checked by a clock. Because all this happens in the dark, a torch whose light intensity has been attenuated is used to illuminate the clock.

6) The pump is turned off at the chosen time, the laser light is unblocked and a new exposure, again for 5 seconds is effected for the real-time case, the plate is developed immediately after the exposure and the pump is run after drying.

7) Developing insitu with both techniques is carried out as explained before: the plate is kept in the developer for one minute, then the plate is washed for half a minute. Fixing takes three minutes and drying between fifteen and twenty minutes.

8) After the plate is dry, the fringes are viewed with both reference and object beams as they occur (real-time) or they are viewed using only the reference beam while the object beam is blocked (double-exposure).

9) Photographing is now carried out. The hologram is exposed to the reference beam while a still camera records the fringes in it. Exposure time was 15 to 20 seconds. The camera rested on a very heavy stand to avoid vibrations while photographing was taking place. Once the camera was in the right position, the stand nsures that the camera is always at the same position even if days elapsed between shots.

10) The whole process was repeated for every run.

CHAPTER 5

5.1 Discussion of Results

The values of the mass transfer coefficient (k) and therefore those of the Sherwood number (Shx) along the centre line of the transferring wall of the rectangular duct were first obtained under the assumption that the air-stream concentration of the swelling agent, isobutyl benzoate, does not change along the duct. Appendices D and E and Fig. 5.1 to Fig. 5.8. These values were then corrected where necessary by a factor:

$$F = 1/(1 - \frac{4A}{ReSc}),$$

the whole expression being: Shx = F Sh'x (Appendix F). The area (A) in this expression is the area under the curve Sh'x vs x/dh.

The correction introduced by this factor was important mainly at the exit end of the duct and it ranged from 5% to 30% (laminar flow). The results so corrected gave a better picture of the change of Shx vs x/dh, in the sense the curves are seen to level off as x/dh increases, except in the case of Run 5, Re = 528, duct 3:1, calming section, symmetric transfer. (Fig. 5.9 to Fig. 5.20 and Appendix G).

For this specific run the log-log plot of Shx vs x/dh gives a curve, with the values of the Sherwood number decreasing without apparent limit. This may be explained by the fact that this is a case of symmetric transfer at the lowest Reynolds number obtained for this situation and consequently the building up of the concentration in the air downstream is bigger than in other cases (symmetric or asymmetric transfer runs).

For Reynolds numbers in the turbulent and transition regimes, it was found that, in the case of both the 2:1 and 3:1 ducts with calming sections, the Sherwood number gives a linear log-log plot with x/dh whose slope is approximately invariant with Re for both asymmetric and symmetric transfer (Figs. 5.17 - 5.20). The slopes in these cases are found for the 2:1 duct to be - 0.1 ± 0.03 (asymmetric transfer) and - 0.20 ± 0.05 (symmetric transfer) and for the 3:1 duct to be - 0.14 ± 0.03 (asymmetric transfer) and - 0.08 ± 0.02 (symmetric transfer).

For the 3.1 duct, cross-plots from Figs. 5.19 and 5.20 indicate that the Sherwood number at any fixed value of x/dh varies as $Re^{0.83}$, as might be expected from the correlation of Linton and Sherwood (1950) for large x/dh Figs. (5.21 and 5.22), whereas for the 2:1 duct cross-plots from Figs. 5.17 and 5.18 indicate that

Fig. 5.1 : Consolidated Plot of Sh'x vs x/dh
Duct 2:1 dh = 1.27 cm
Abrupt Entrance, Asymmetric Transfer
Uncorrected Data

a) Run 1 Re = 5815
b) Run 2 Re = 5103
c) Run 3 Re = 3380
d) Run 4 Re = 2120
e) Run 5 Re = 704

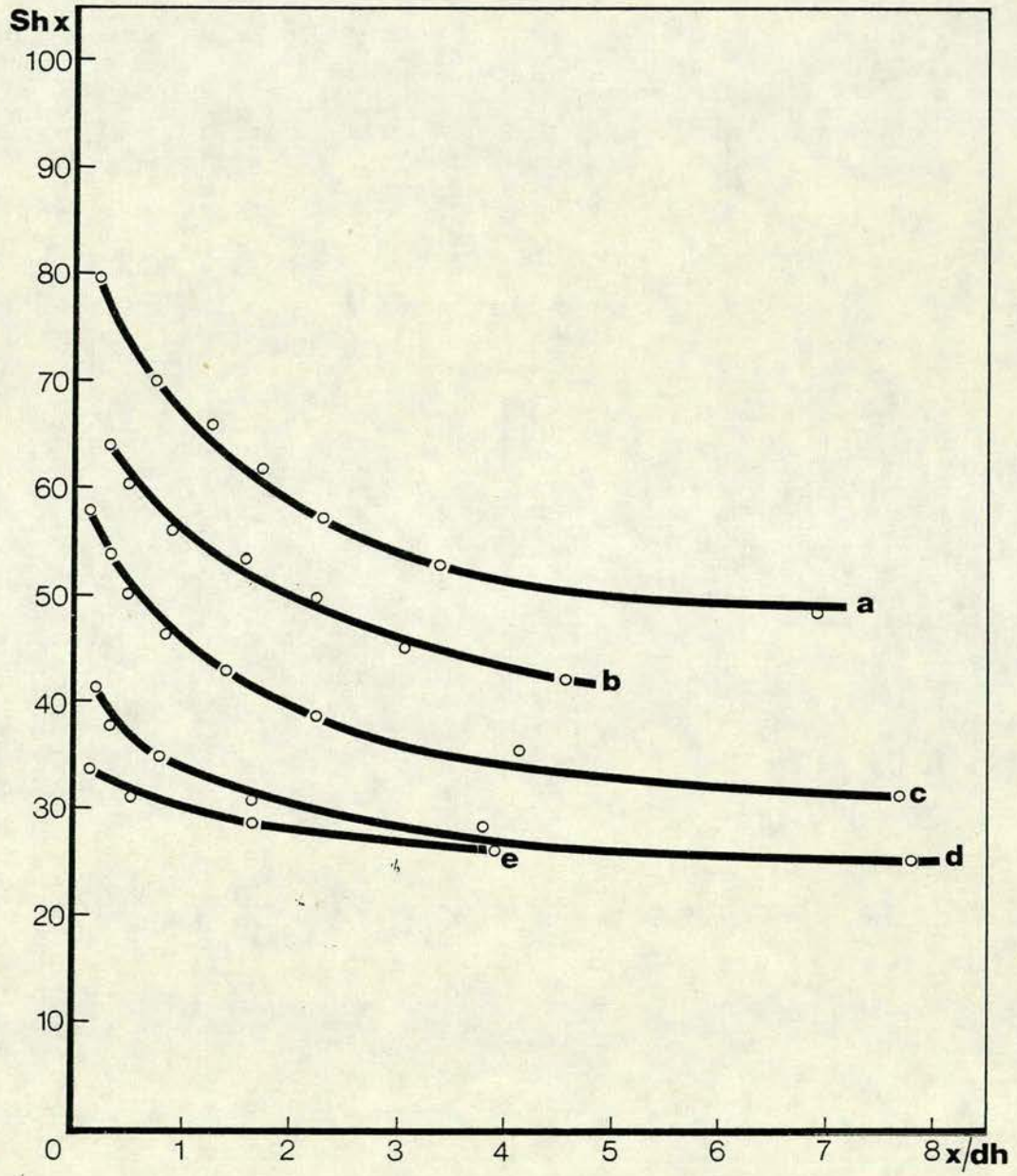

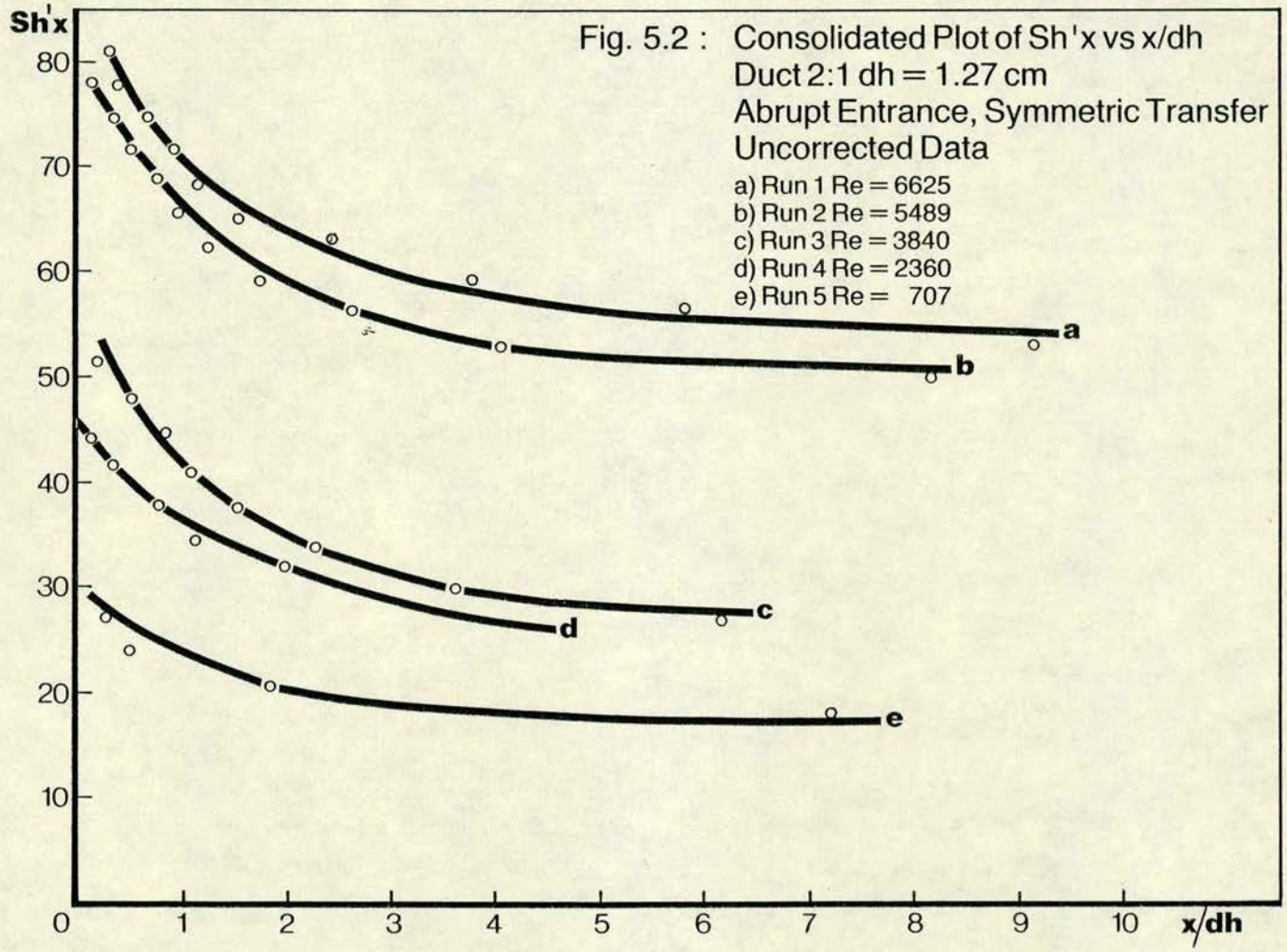

Fig. 5.2 : Consolidated Plot of Sh'x vs x/dh
Duct 2:1 dh = 1.27 cm
Abrupt Entrance, Symmetric Transfer
Uncorrected Data

a) Run 1 Re = 6625
b) Run 2 Re = 5489
c) Run 3 Re = 3840
d) Run 4 Re = 2360
e) Run 5 Re = 707

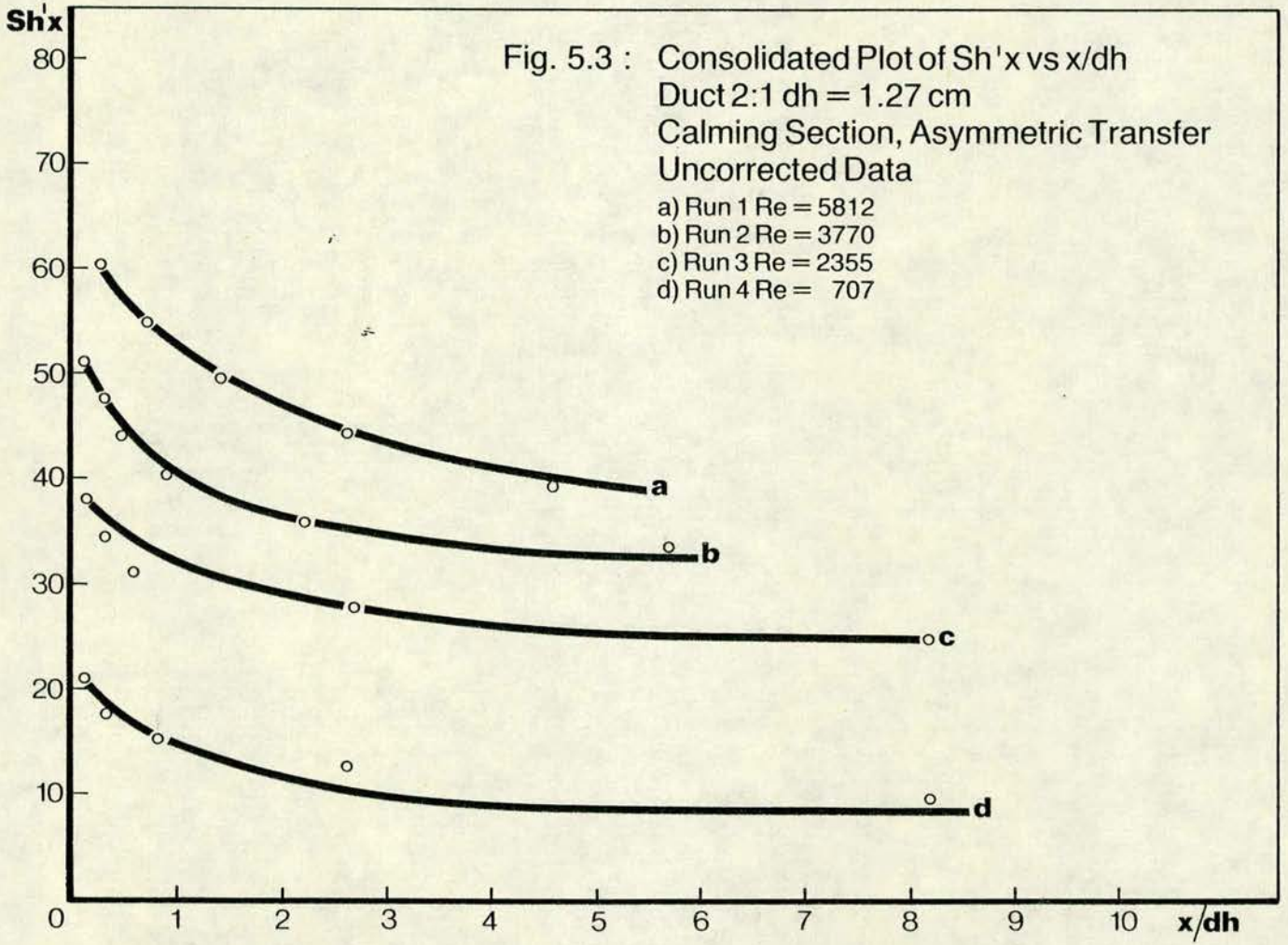

Fig. 5.3 : Consolidated Plot of Sh'x vs x/dh
Duct 2:1 dh = 1.27 cm
Calming Section, Asymmetric Transfer
Uncorrected Data

a) Run 1 Re = 5812
b) Run 2 Re = 3770
c) Run 3 Re = 2355
d) Run 4 Re = 707

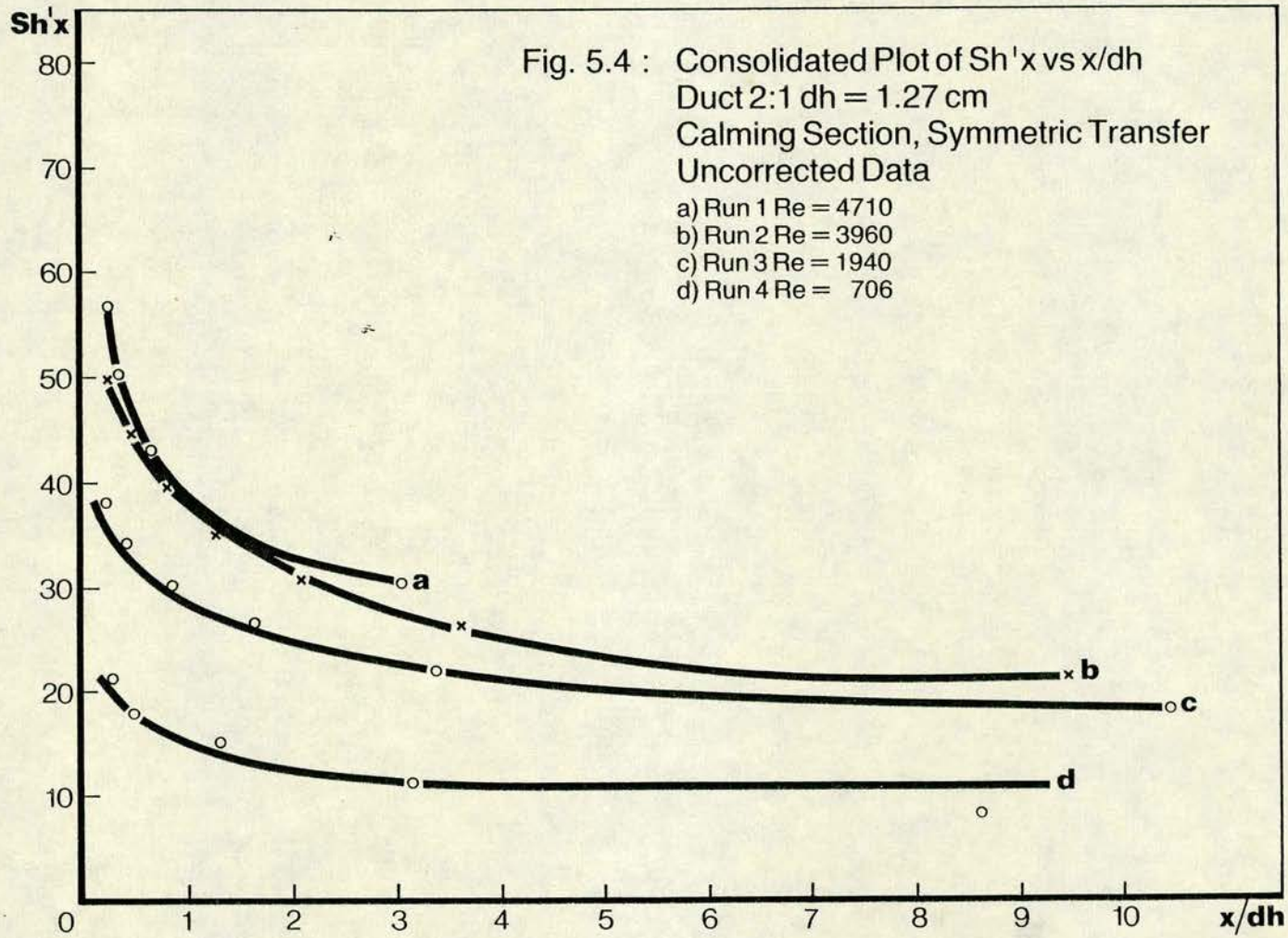

Fig. 5.4 : Consolidated Plot of Sh'x vs x/dh
Duct 2:1 dh = 1.27 cm
Calming Section, Symmetric Transfer
Uncorrected Data

a) Run 1 Re = 4710
b) Run 2 Re = 3960
c) Run 3 Re = 1940
d) Run 4 Re = 706

Fig. 5.5 : Consolidated Plot of Sh'_x vs x/dh
Duct 3:1 dh = 1.43 cm
Abrupt Entrance, Asymmetric Transfer
Uncorrected Data

a) Run 1 Re = 5710
b) Run 2 Re = 5120
c) Run 3 Re = 4470
d) Run 4 Re = 3700
e) Run 5 Re = 2590
f) Run 6 Re = 1760
g) Run 7 Re = 528

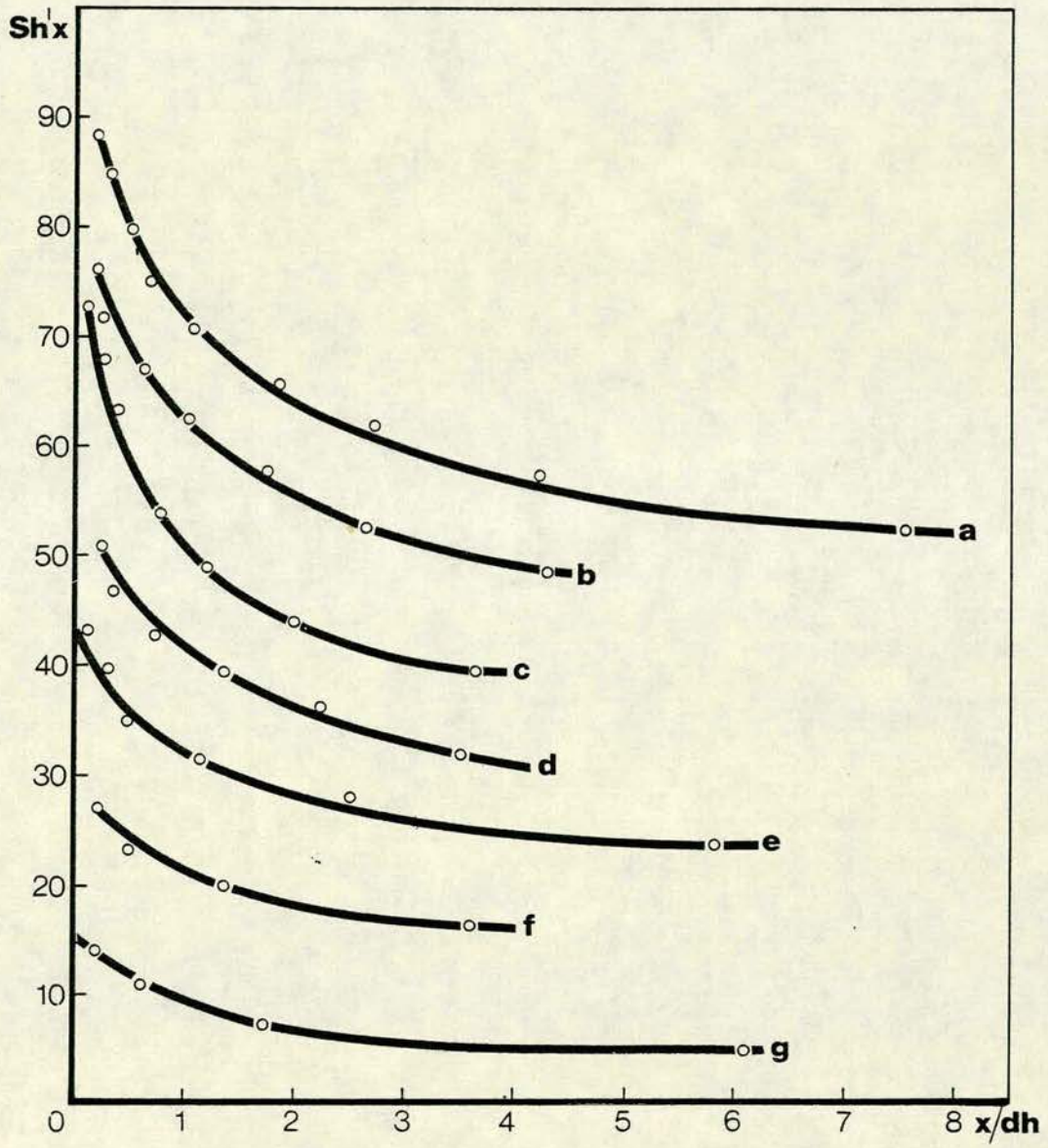

Fig. 5.6 : Consolidated Plot of Sh'x vs x/dh
Duct 3:1 dh = 1.43 cm
Abrupt Entrance, Symmetric Transfer
Uncorrected Data

a) Run 1 Re = 4610
b) Run 2 Re = 4420
c) Run 3 Re = 3830
d) Run 4 Re = 3240
e) Run 5 Re = 2538
f) Run 6 Re = 538

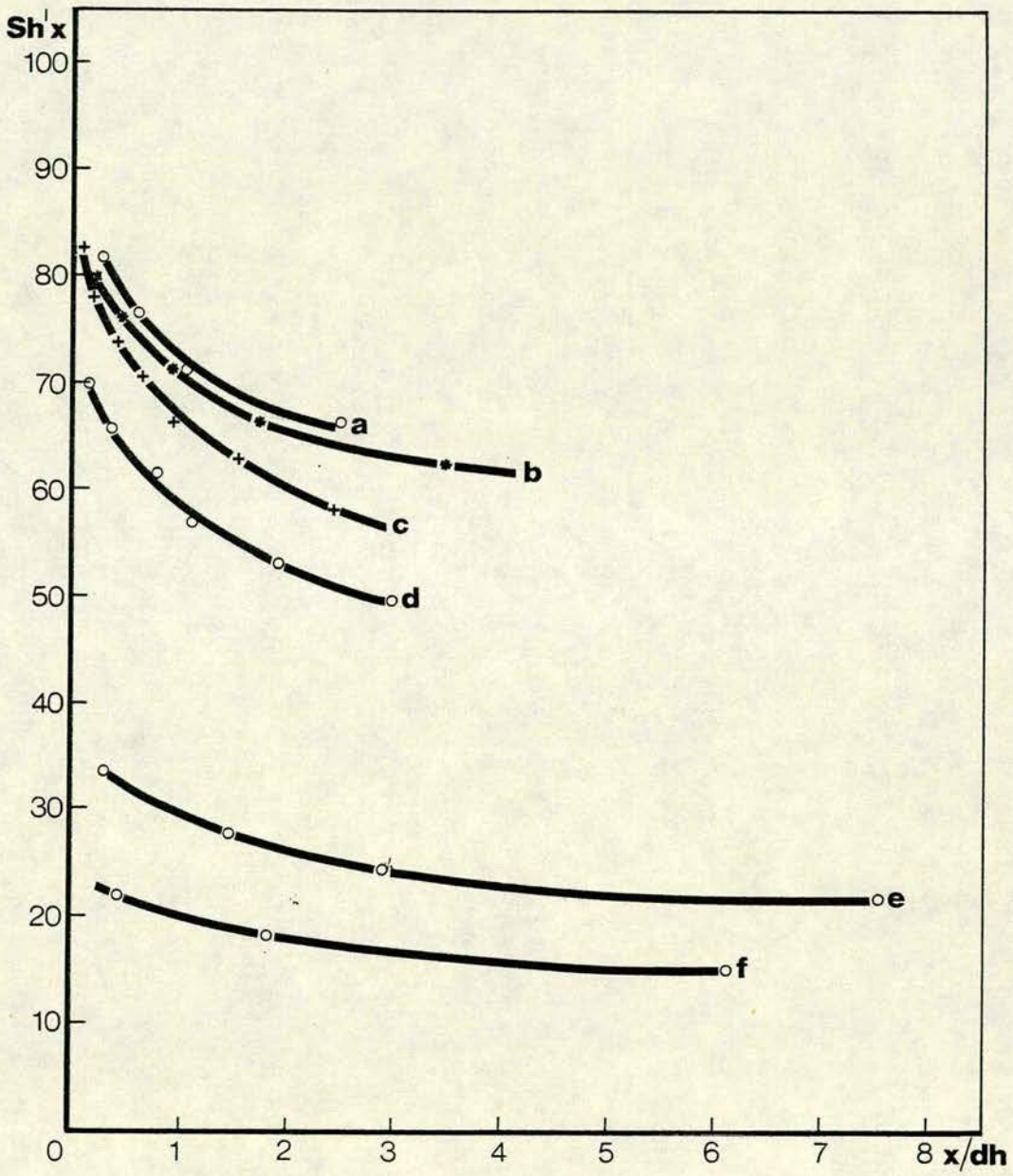

Fig. 5.7 : Consolidated Plot of Sh'x vs x/dh
Duct 3:1 dh = 1.43 cm
Calming Section, Asymmetric Transfer
Uncorrected Data

a) Run 1 Re = 4706
b) Run 2 Re = 3540
c) Run 3 Re = 2650
d) Run 4 Re = 528

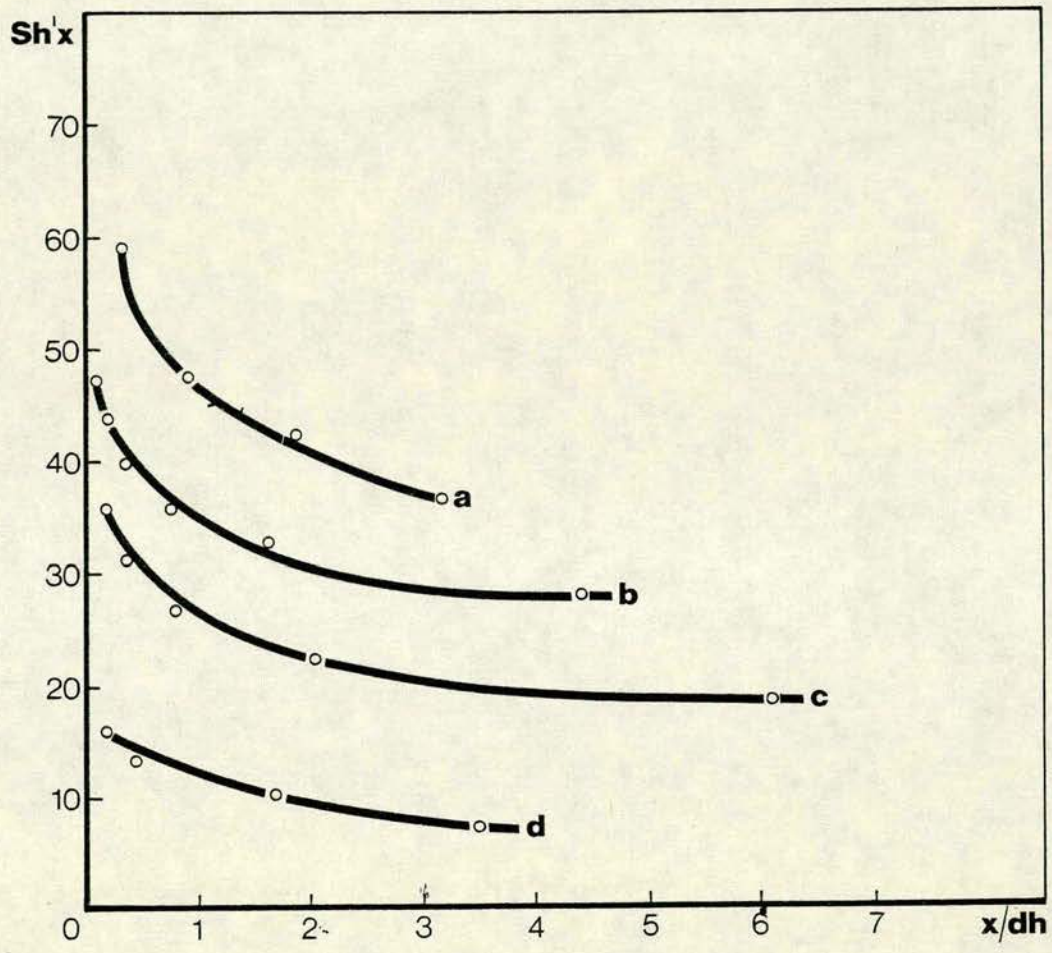

Fig. 5.8 : Consolidated Plot of Sh'_x vs x/dh
Duct 3:1 dh = 1.43 cm
Calming Section, Symmetric Transfer
Uncorrected Data

a) Run 1 Re = 4410
b) Run 2 Re = 3730
c) Run 3 Re = 3240
d) Run 4 Re = 2360
e) Run 5 Re = 528

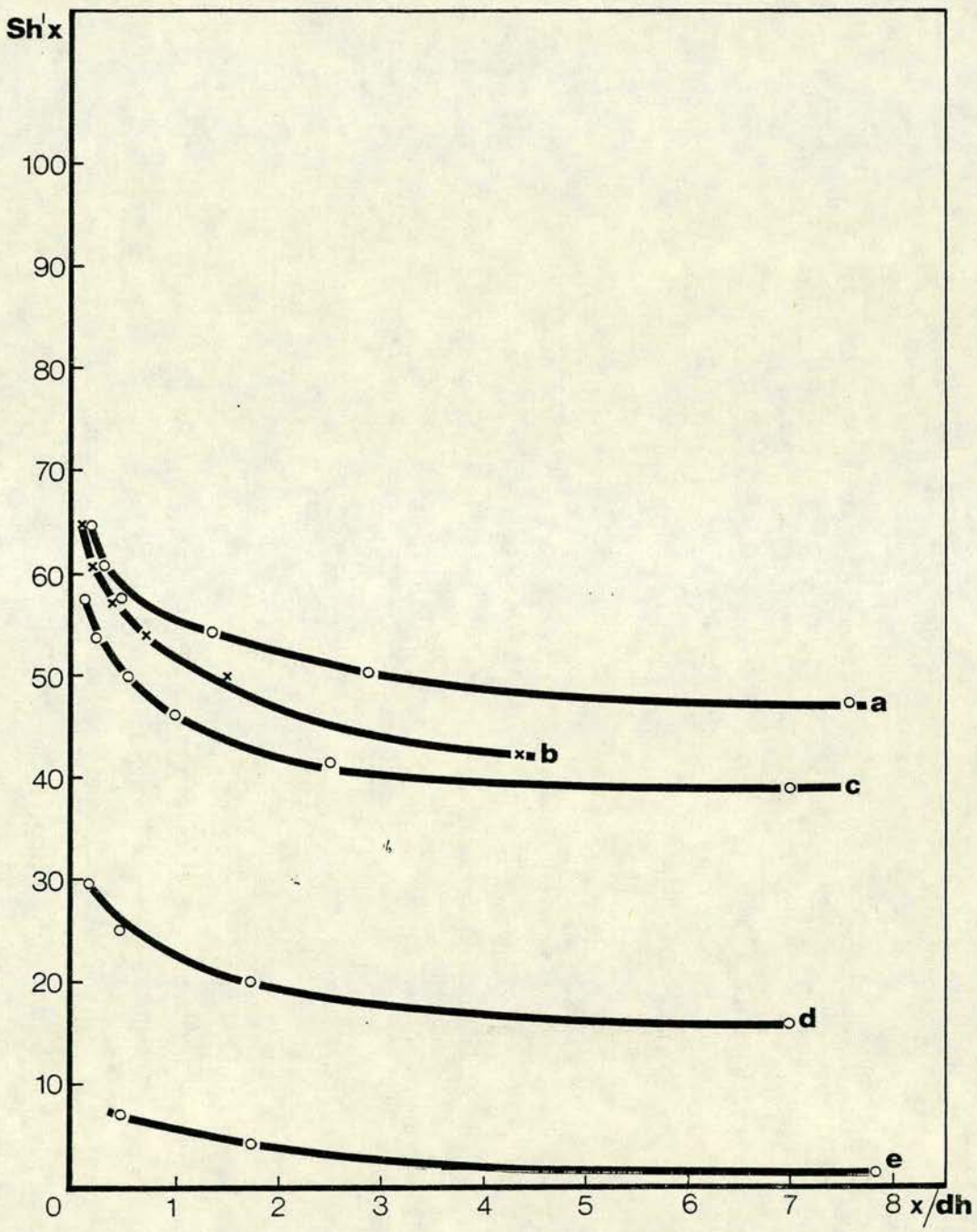

$Shx \propto Re^{0.6}$ (Figs. 5.23 - 5.24 and Appendix H). This surprising result, that the geometry of the ducts affects the relation between Sherwood and Reynolds numbers, may be explained in terms of secondary flow phenomenon. It must be borne in mind that the mass transfer coefficient k is that for points on the centre line of the transferring wall of the duct. For a sufficiently wide duct, it will be uninfluenced by the corner-flows, whereas this will be increasingly important as the duct is made narrower.

For the flow situation of calming section symmetric and asymmetric transfer (both ducts), the results were checked against an equation given by Legkiy and Markarov (1971). The original equation

$$Nux = 0.029\ Rex^{0.8}\ (x/d)^{0.08}$$

(eq. 5.1.1) was modified (Appendix I) to read:

$$Nud = 0.03\ Red^{0.8}\ (^{x1}/_{d})^{-0.12}$$

(eq. 5.1.2). Equation 5.1.1 contains in the constant the term $Pr^{0.33}$; for our mass transfer application this is modified by use of the Schmidt number to read: $(Sc/Pr)^{0.33}$, so that the whole modified equation is:

$$Nud = 0.03\ Red^{0.8}\ (^{x1}/_{d})^{-0.12}\ (sc/Pr)^{0.33} \qquad (5.1.3)$$

For asymmetric transfer, the agreement between the modified equation 5.1.3 and the results obtained for duct 3:1 was good, specially in the case of Re = 3540. The results were not so good for duct 2:1 except in the case of the run for Re = 5812 (Appendix G). This may be explained because of the different relationship between Sherwood and Reynolds numbers for this duct.

In the case of symmetric transfer Larson and Yerazunis (1973) cited various authors as finding Nusselts numbers higher by more than 20% for this case than for asymmetric heat transfer. On this basis, we compared our results with equation 5.1.3 multiplied by 1.2, to allow for 20% more in the Nusselt number for symmetric transfer (Appendix G). The ratio of the Sherwood number found experimentally, to the expected Nusselt was higher than in the previous mentioned asymmetric transfer comparison, which can be interpreted to mean that in rectangular ducts of the specific aspect ratios used in the present work, mass transfer is more sensitive to conditions at the other wall of the duct than in the experiments of the above mentioned authors, who studied turbulent mass transfer between parallel plates.

In all types of turbulent flow situations the furthest downstream values of Sh were compared with the turbulent flow correlation $Sh = 0.023\ Re^{0.8}\ Sc^{0.33}$. This was done taking the value of Shx for the purpose of comparison at the largest measured value of x/dh, with the idea of seeing how far this value was from the fully developed value of the Sherwood number (Sh_∞) far from the beginning of the test section. Of course, for the abrupt entrance case and even for the calming section case, the largest measured value of x/dh is comparatively small compared with that at which the transfer rate would be expected to approach its fully developed value. This comparison is nevertheless useful as a guide.

For laminar flow, we found a tendency for the Sherwood number to level off at short distances from the leading edge of the test section as expected, the largest distances where this occurs being 7.5 dh in the case of Run 5: Re = 528 duct 3:1, calming section, symmetric transfer, and 6 dh for Run 4, Re = 706, duct 2:1, calming section, symmetric transfer.

Fig. 5.9 : Consolidated Plot of Shx vs x/dh
Duct 2:1 dh = 1.27 cm
- Abrupt Entrance, Asymmetric Transfer
Corrected Data

a) Run 1 Re = 5815
b) Run 2 Re = 5103
c) Run 3 Re = 3380
d) Run 4 Re = 2120
e) Run 5 Re = 704

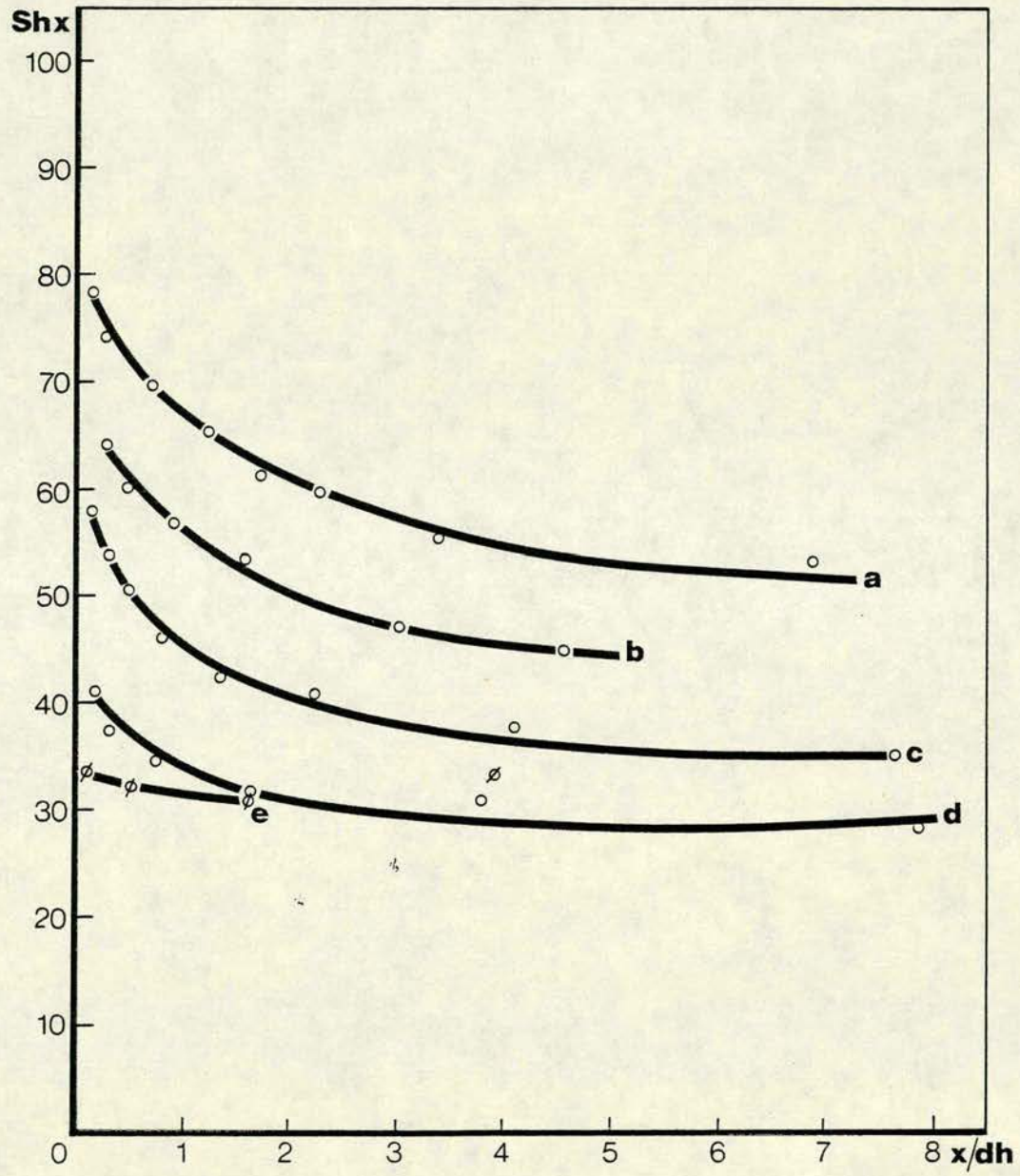

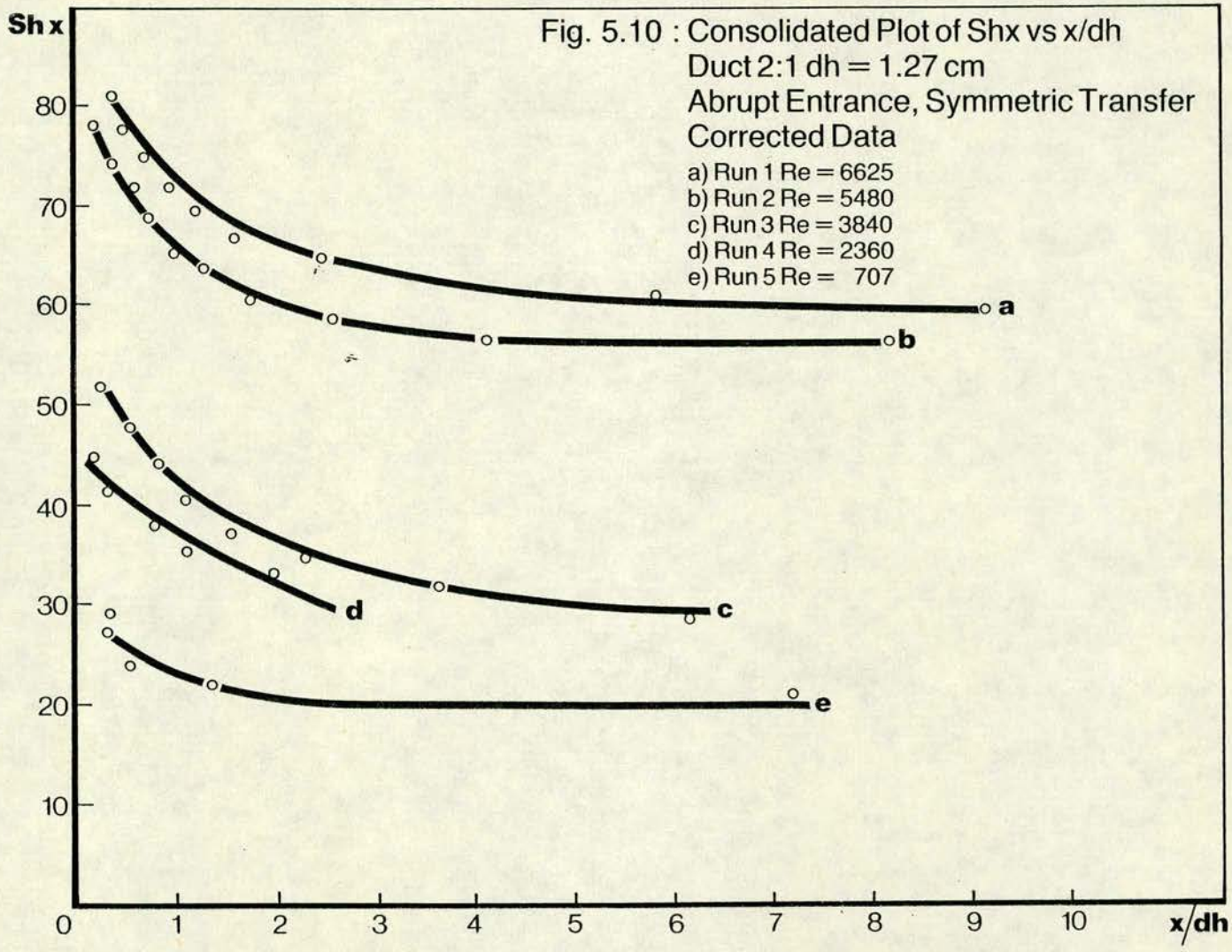

Fig. 5.10 : Consolidated Plot of Shx vs x/dh
Duct 2:1 dh = 1.27 cm
Abrupt Entrance, Symmetric Transfer
Corrected Data

a) Run 1 Re = 6625
b) Run 2 Re = 5480
c) Run 3 Re = 3840
d) Run 4 Re = 2360
e) Run 5 Re = 707

Fig. 5.11 : Consolidated Plot of Shx vs x/dh
Duct 2:1 dh = 1.27 cm
Calming Section, Asymmetric Transfer
Corrected Data

a) Run 1 Re = 5812
b) Run 2 Re = 3770
c) Run 3 Re = 2355
d) Run 4 Re = 707

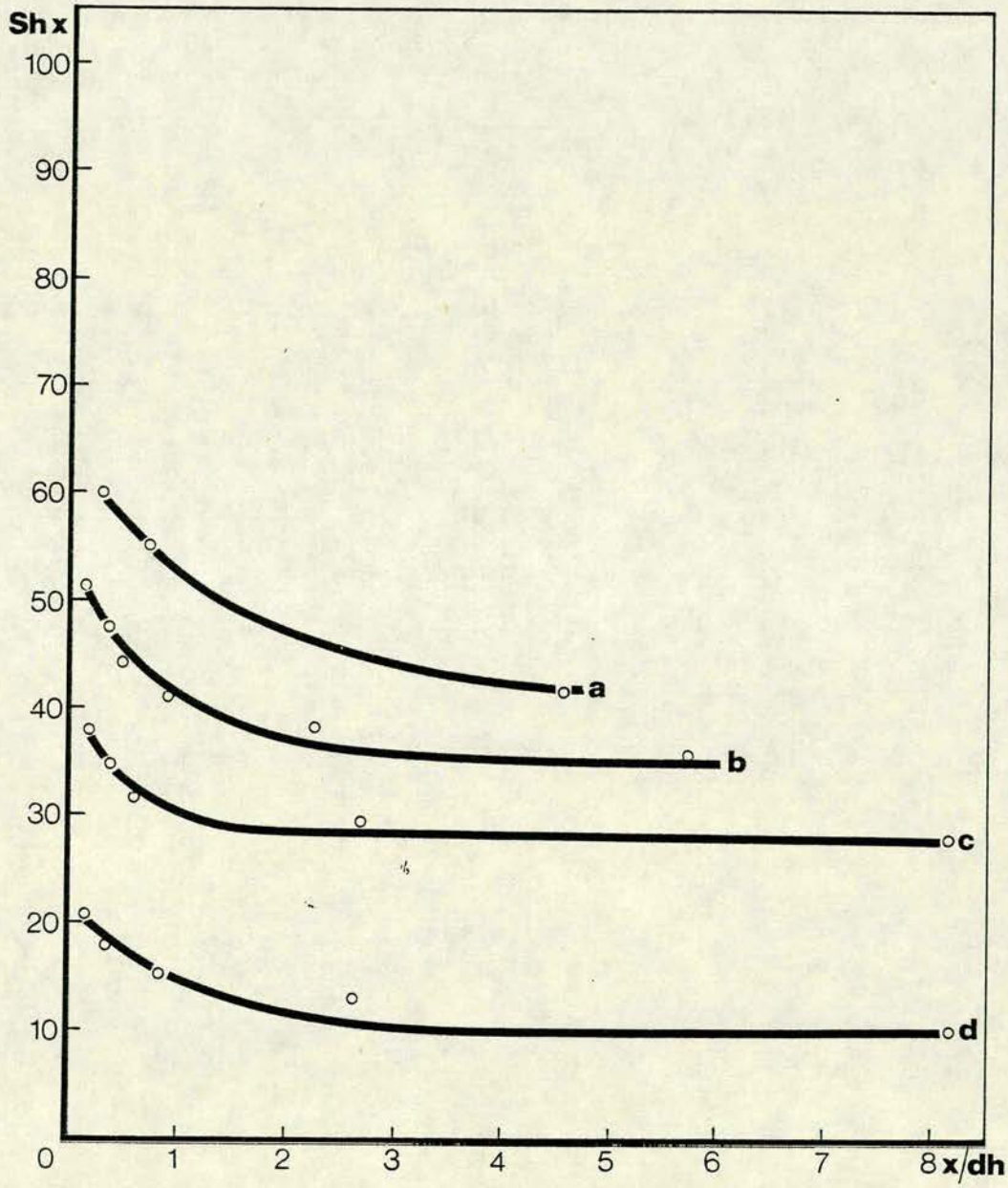

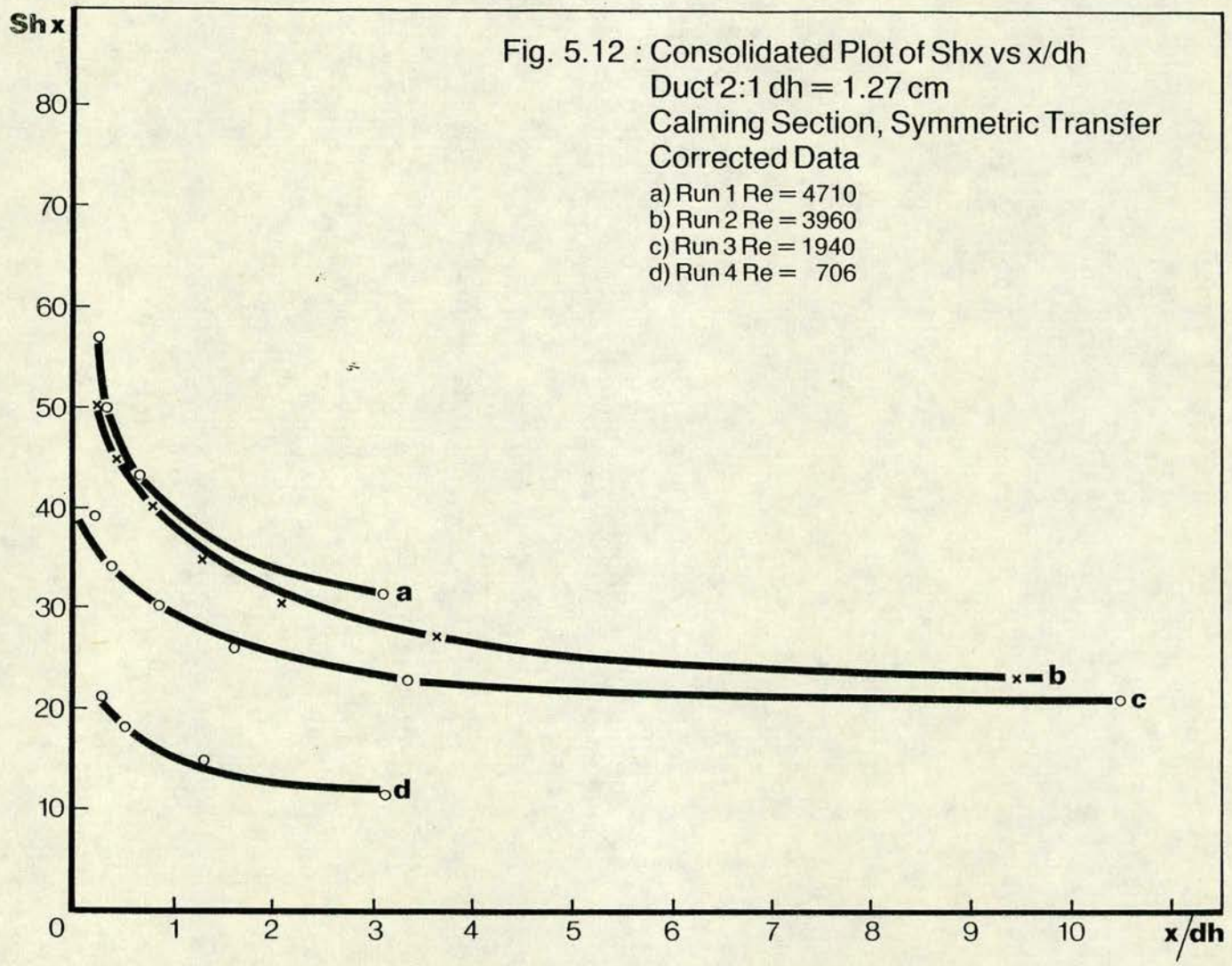

Fig. 5.12 : Consolidated Plot of Shx vs x/dh
Duct 2:1 dh = 1.27 cm
Calming Section, Symmetric Transfer
Corrected Data
a) Run 1 Re = 4710
b) Run 2 Re = 3960
c) Run 3 Re = 1940
d) Run 4 Re = 706

Fig. 5.13 : Consolidated Plot of Shx vs x/dh
Duct 3:1 dh = 1.43 cm
Abrupt Entrance, Asymmetric Transfer
Corrected Data

a) Run 1 Re = 5710
b) Run 2 Re = 5120
c) Run 3 Re = 4470
d) Run 4 Re = 3700
e) Run 5 Re = 2590
f) Run 6 Re = 1760
g) Run 7 Re = 528

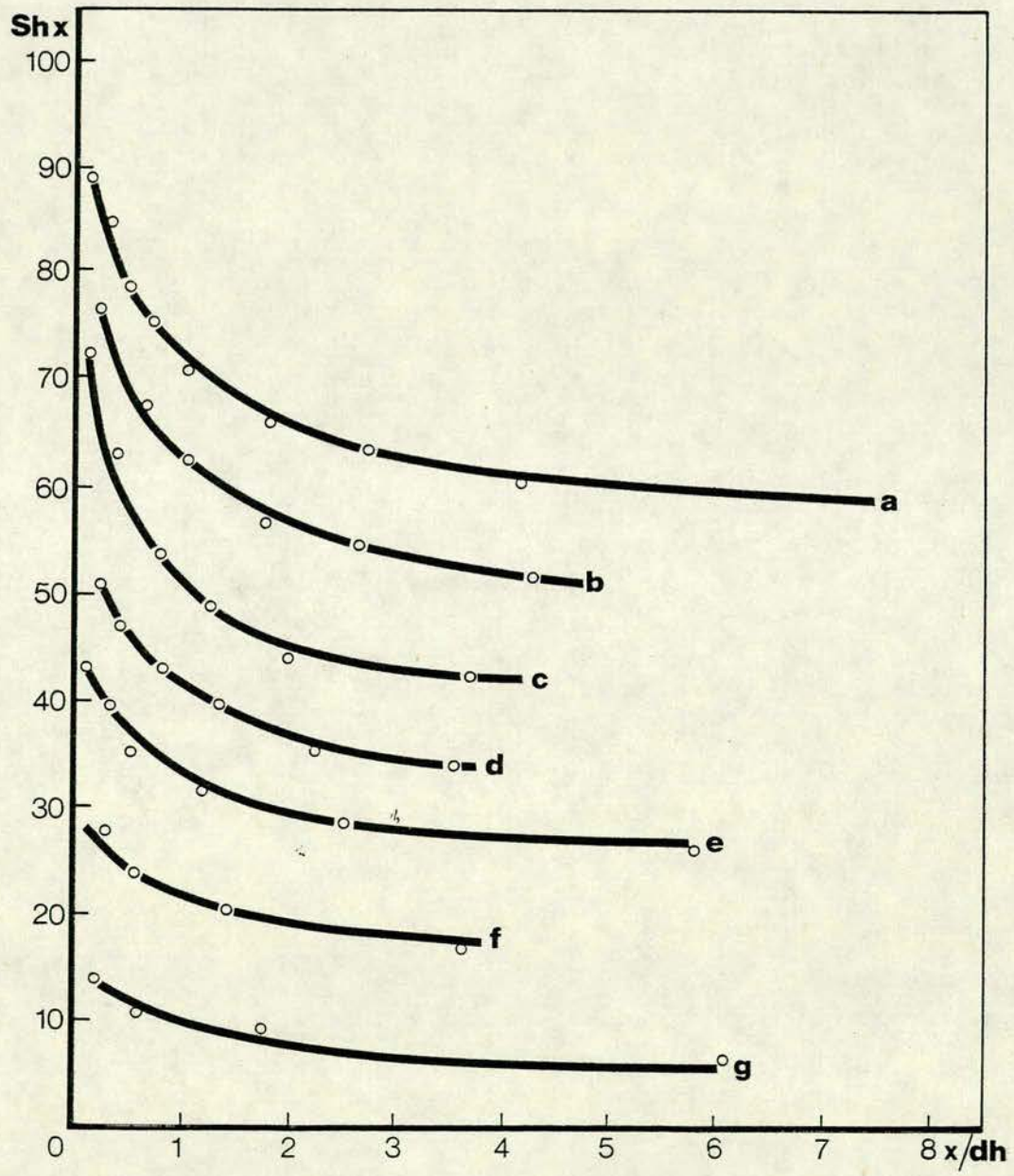

Fig. 5.14 : Consolidated Plot of Shx vs x/dh
Duct 3:1 dh = 1.43 cm
Abrupt Entrance, Symmetric Transfer
Corrected Data

a) Run 1 Re = 4610
b) Run 2 Re = 4420
c) Run 3 Re = 3830
d) Run 4 Re = 3240
e) Run 5 Re = 2538
f) Run 6 Re = 538

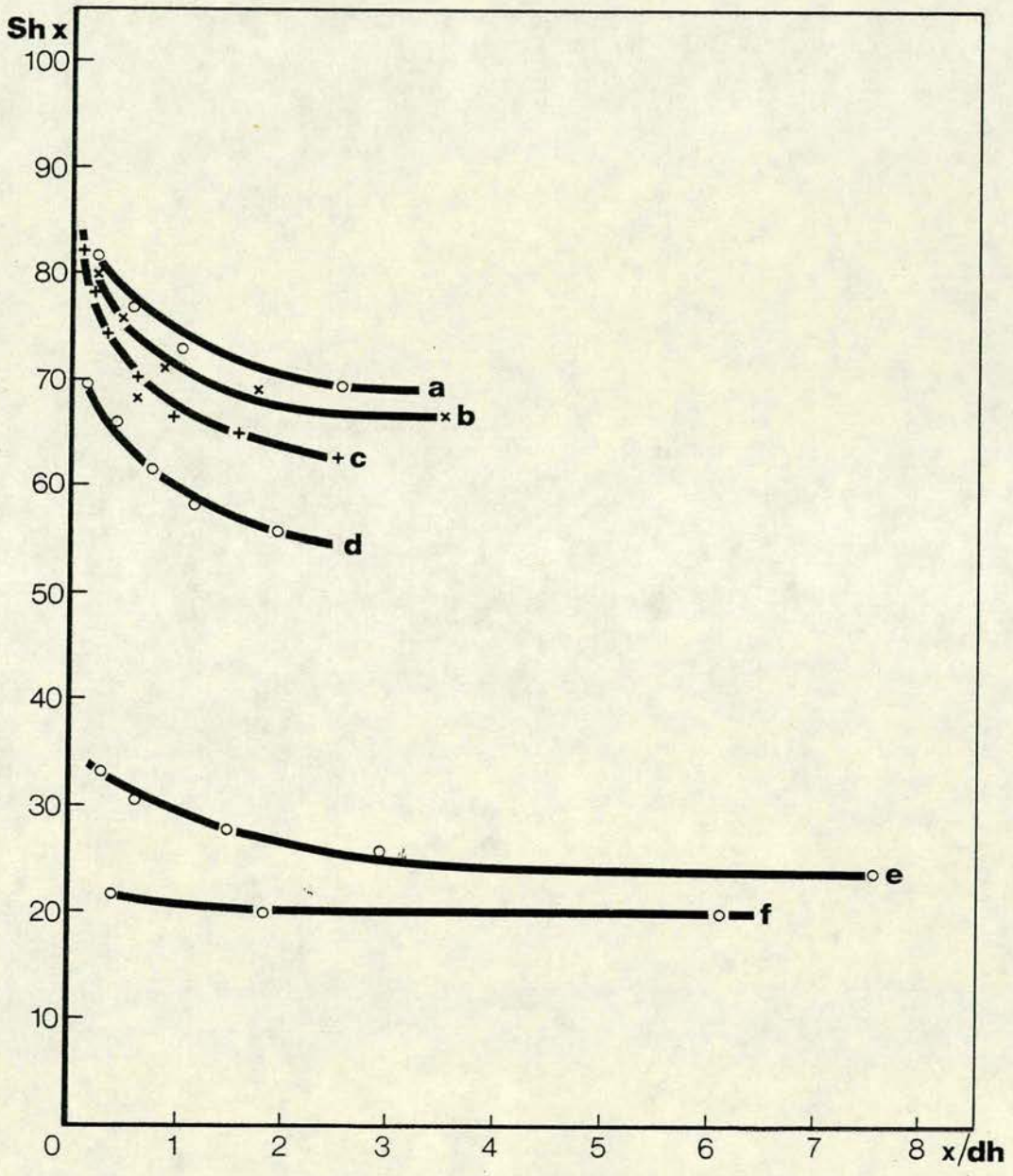

Fig. 5.15 : Consolidated Plot of Shx vs x/dh
Duct 3:1 dh = 1.43 cm
Calming Section, Asymmetric Transfer
Corrected Data
a) Run 1 Re = 4706
b) Run 2 Re = 3540
c) Run 3 Re = 2650
d) Run 4 Re = 528

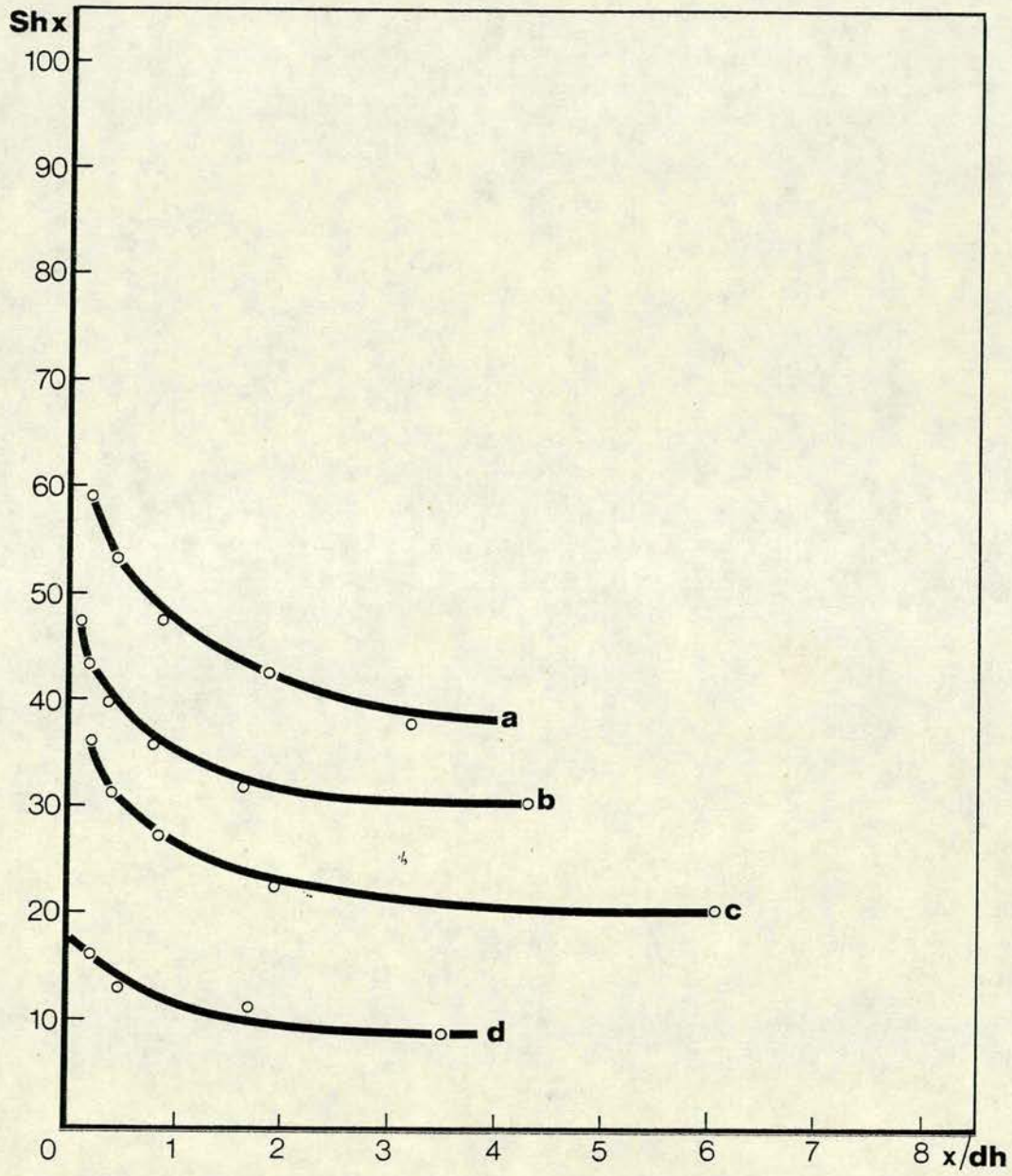

Fig. 5.16 : Consolidated Plot of Shx vs x/dh
Duct 3:1 dh = 1.43 cm
Calming Section, Symmetric Transfer
Corrected Data

a) Run 1 Re = 4410
b) Run 2 Re = 3730
c) Run 3 Re = 3240
d) Run 4 Re = 2360
e) Run 5 Re = 528

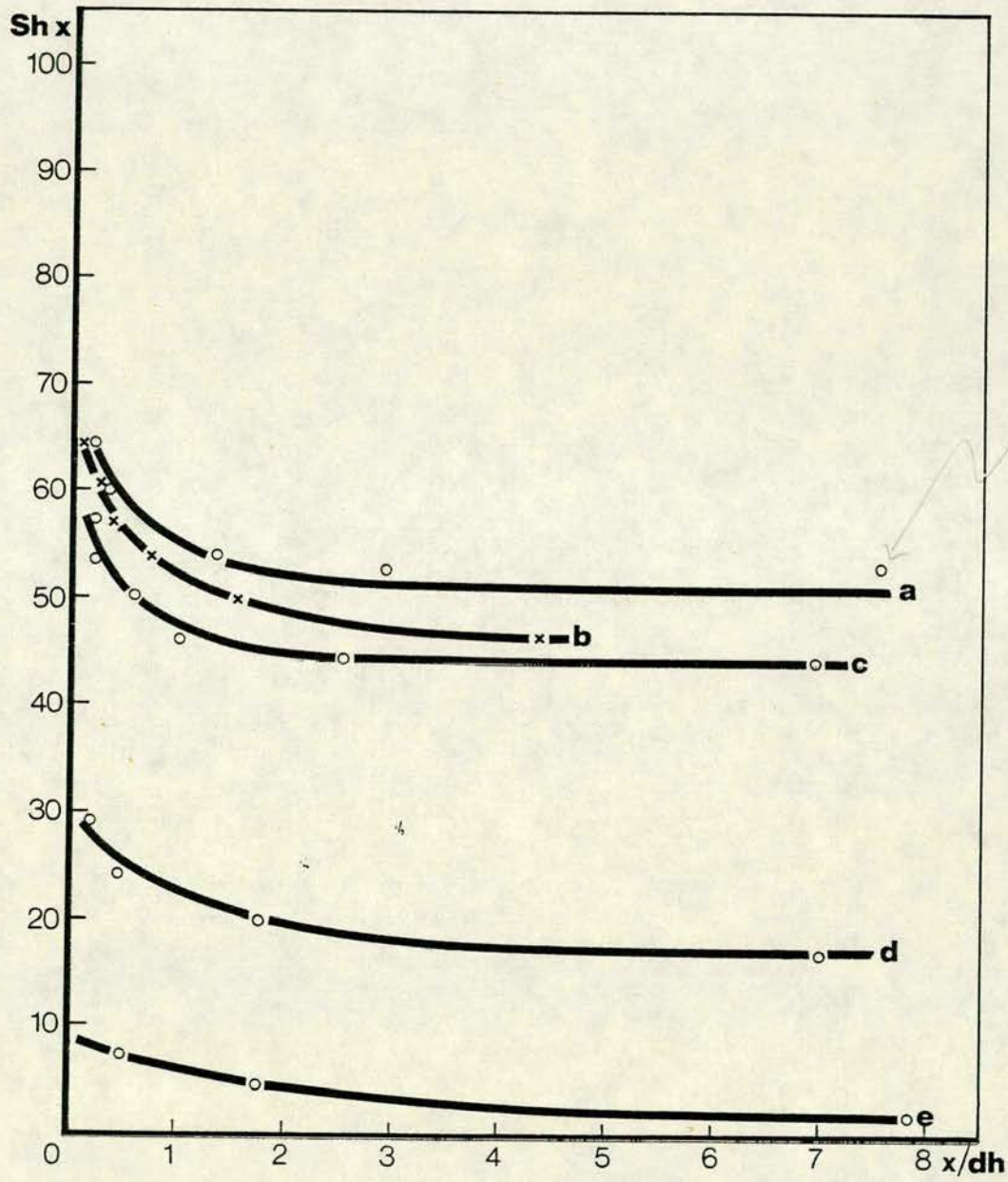

Fig. 5.17 : Consolidated Plot of Shx vs x/dh
Duct 2:1 dh = 1.27 cm
Calming Section, Asymmetric Transfer
Corrected Data
a) Run 1 Re = 5812
b) Run 2 Re = 3770
c) Run 3 Re = 2355
d) Run 4 Re = 707

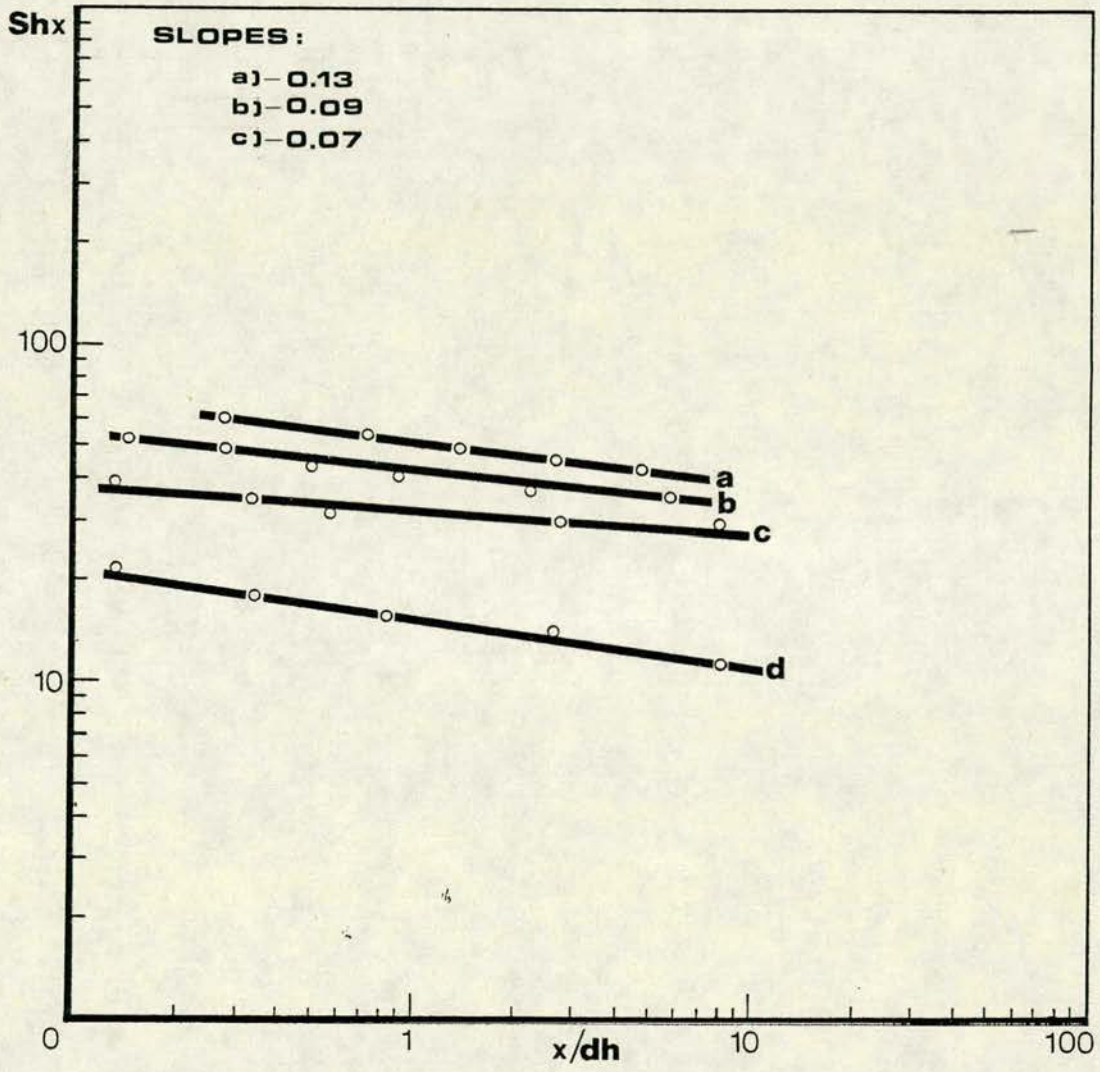

Fig. 5.18 : Consolidated Plot of Shx vs x/dh
Duct 2:1 dh = 1.27 cm
Calming Section, Symmetric Transfer
Corrected Data
a) Run 1 Re = 4710
b) Run 2 Re = 3960
c) Run 3 Re = 1940
d) Run 4 Re = 706

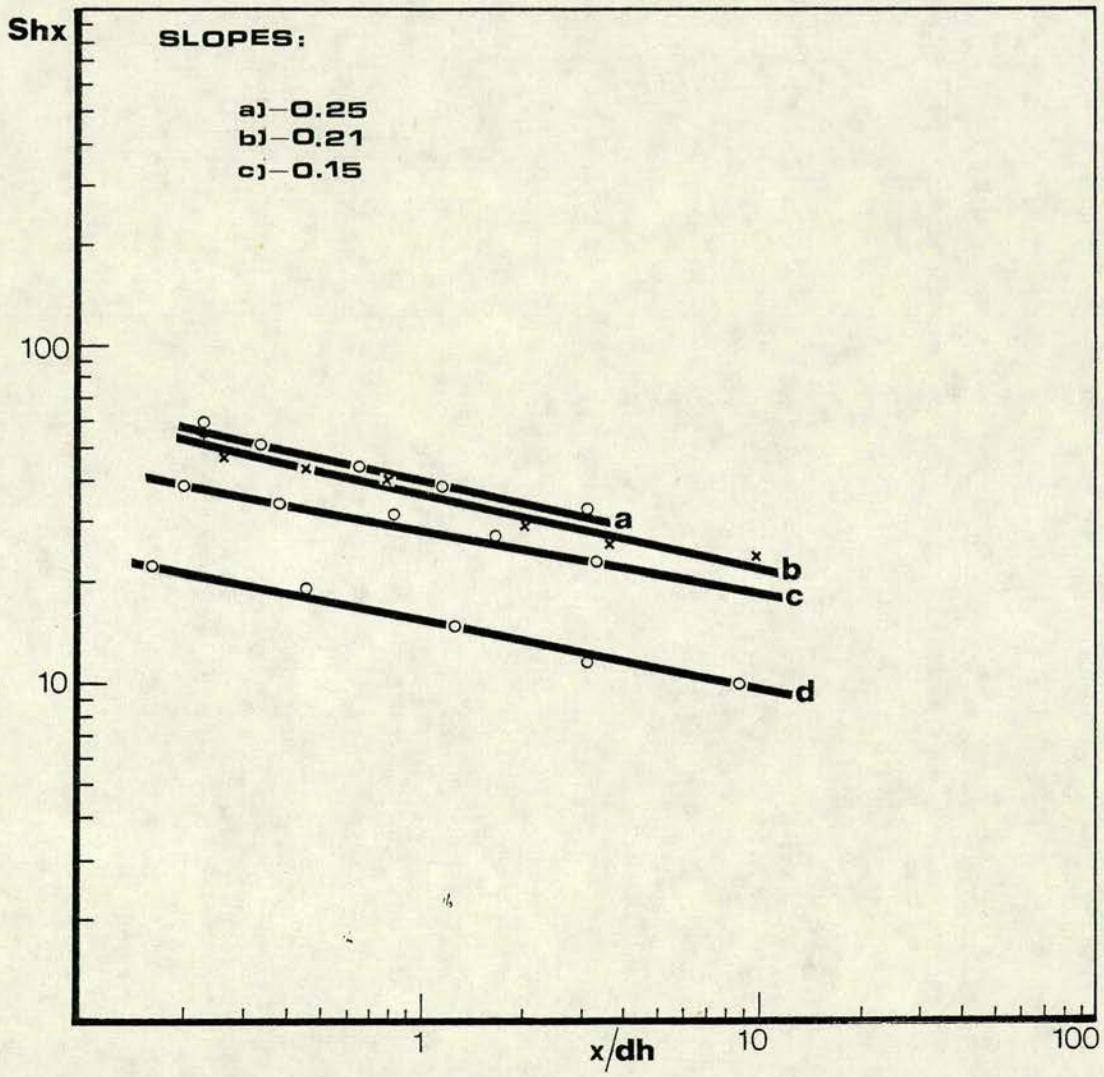

Fig. 5.19 : Consolidated Plot of Shx vs x/dh
Duct 3:1 dh = 1.43 cm
Calming Section, Asymmetric Transfer
Corrected Data
a) Run 1 Re = 4706
b) Run 2 Re = 3540
c) Run 3 Re = 2650
d) Run 4 Re = 528

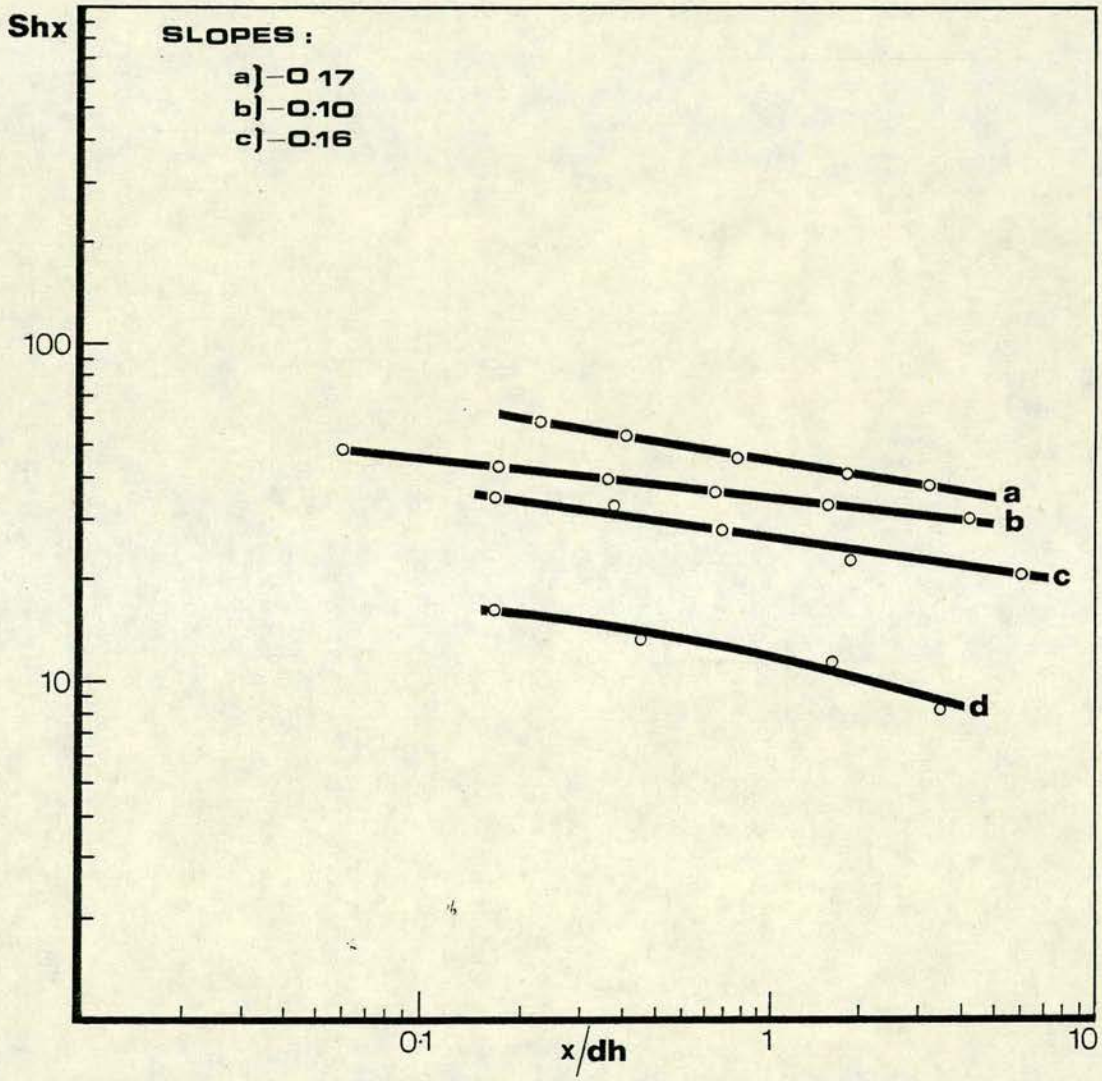

Fig. 5.20 : Consolidated Log-log Plot of Shx vs x/dh
Duct 3:1 dh = 1.43 cm
Calming Section, Symmetric Transfer
Corrected Data

a) Run 1 Re = 4410
b) Run 2 Re = 3730
c) Run 3 Re = 3240
d) Run 4 Re = 2360
e) Run 5 Re = 528

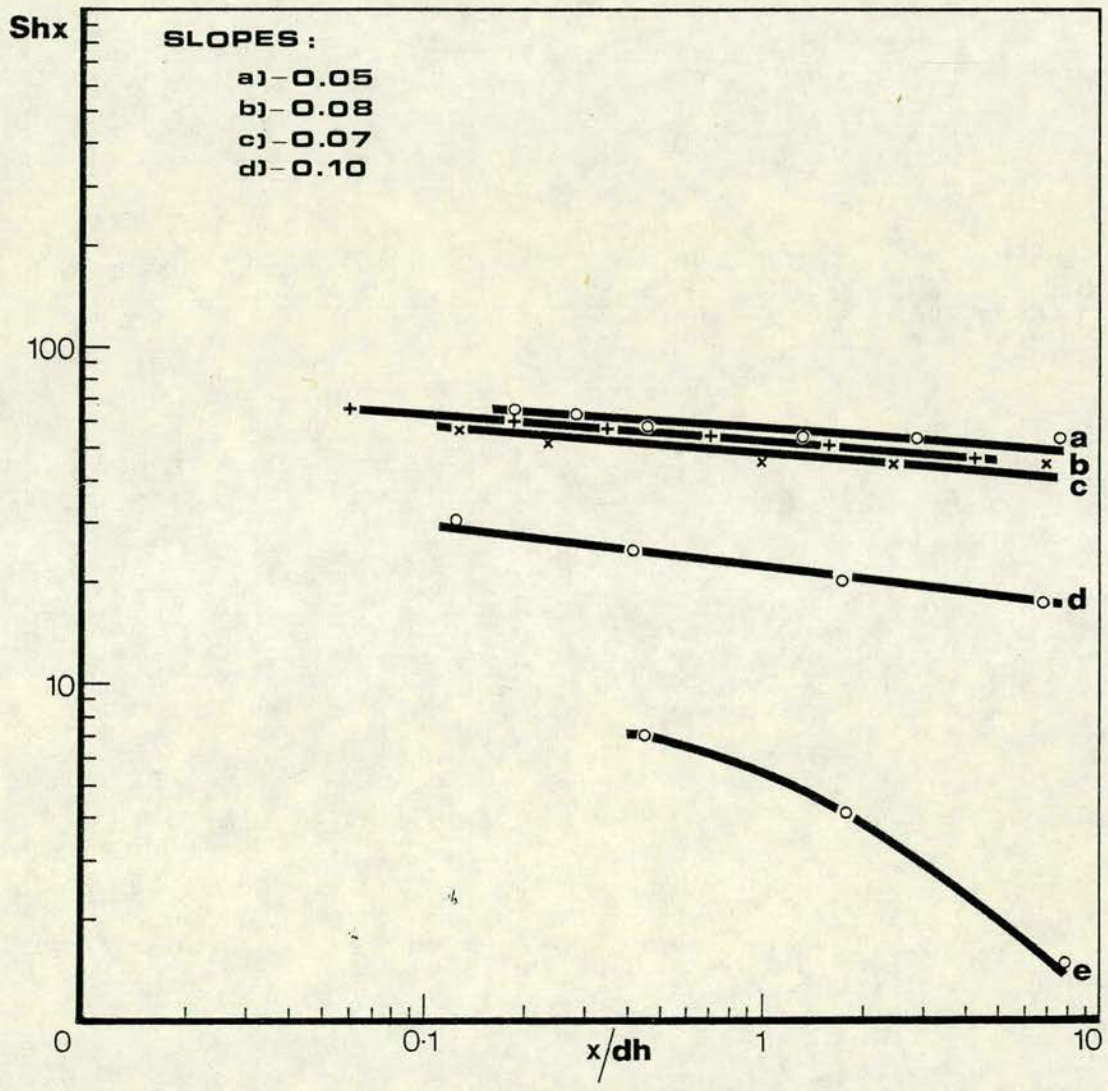

Knudsen and Katz (1958) give a relation proposed by Sellars et al (1956) for developed laminar flow in circular pipes, according to which:

$$Nu = 1.357 \left(\frac{x/rw}{Pe}\right)^{-0.33} \quad \text{for} \quad \frac{x/rw}{Pe} < 0.01$$

where x is a given length of pipe from the leading edge, rw the radius of the pipe and Pe = Re Pr (Peclet heat-transfer number).

Using this expression in a modified form, i.e. making Pe = Re Sc and using the hydraulic radius, rh = dh/4 instead of the radius of the pipe, we find a very high discrepancy between the predicted Nusselt number and the experimental Sherwood number the latter being much lower than the former for the case of ducts with calming section symmetric and asymmetric transfer. (Appendix J). However, for very long rectangular ducts and fully developed velocity profile, Knudsen and Katz (1958) present an experimental plot of limiting Nusselt number vs aspect ratio, and for the condition of constant wall temperature, the limiting value for the 2:1 duct is: 3.4 and for the 3:1 duct Nu = 4.10.

In this case, the values of the Sherwood number for duct 3:1, taking them at the largest value of x/dh, for calming section asymmetric transfer is almost twice this value and for the calming section, symmetric transfer run (Run 5 at Re = 528) almost 1/3 of this value. But it is obvious for the discussion that this is not a good run. For duct 2:1, symmetric and asymmetric transfer, calming section, the limiting values of the Sherwood numbers are above the predicted value, which would be expected given the prediction for very long ducts.

Knudsen and Katz give the equation:

Fig. 5.21 : Consolidated Plot of $Shx/Re^{0.83}$ vs x/dh
Duct 3:1 dh = 1.43 cm
Calming Section, Asymmetric Transfer
○ Run 1 Re = 4700
× Run 2 Re = 3540
+ Run 3 Re = 2650

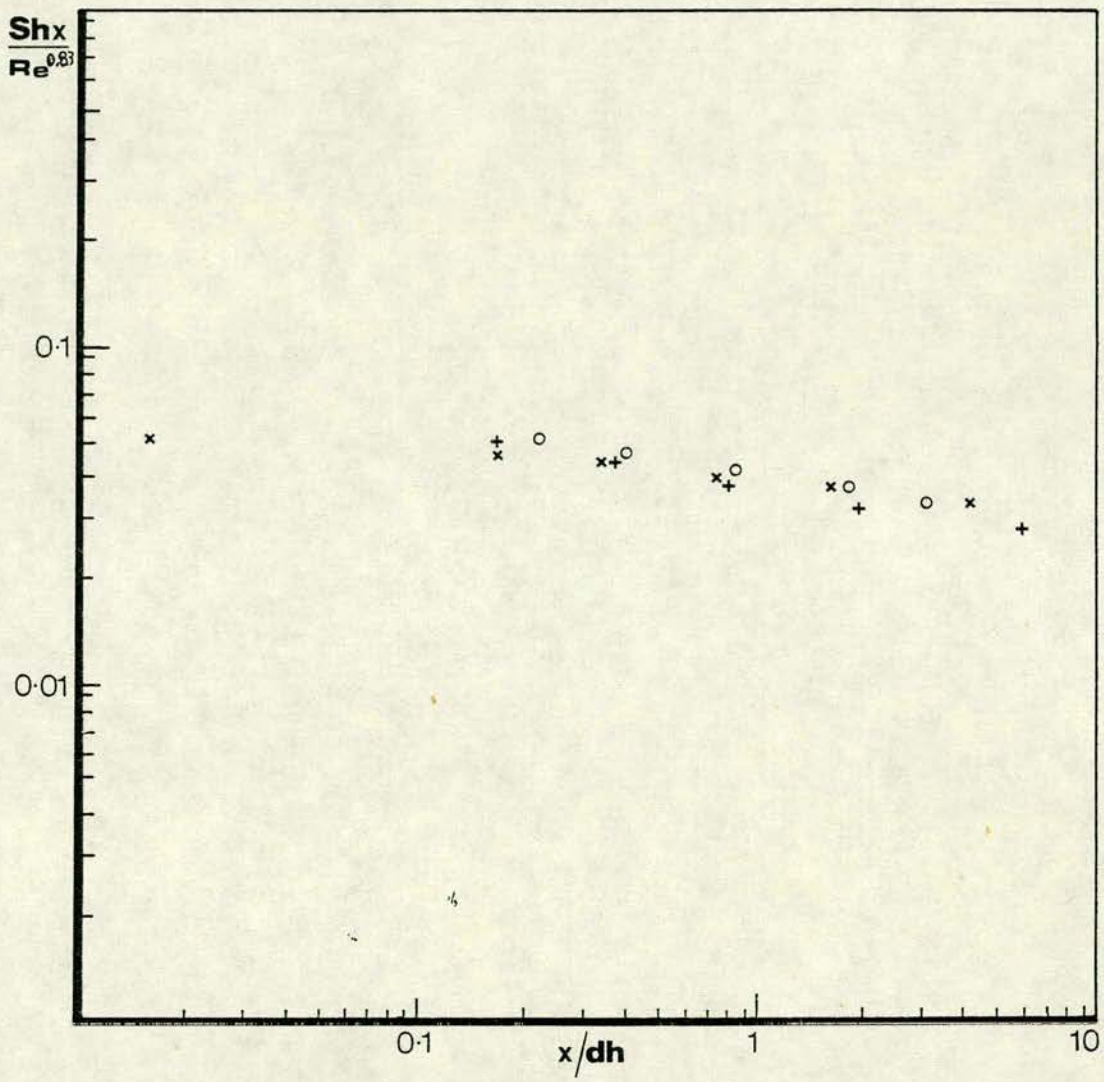

Fig. 5.22 : Consolidated Plot of $Shx/Re^{0.83}$ vs x/dh
Duct 3:1 dh = 1.43 cm
Calming Section, Symmetric Transfer
○ Run 1 Re = 4410
× Run 2 Re = 3730
+ Run 3 Re = 3240

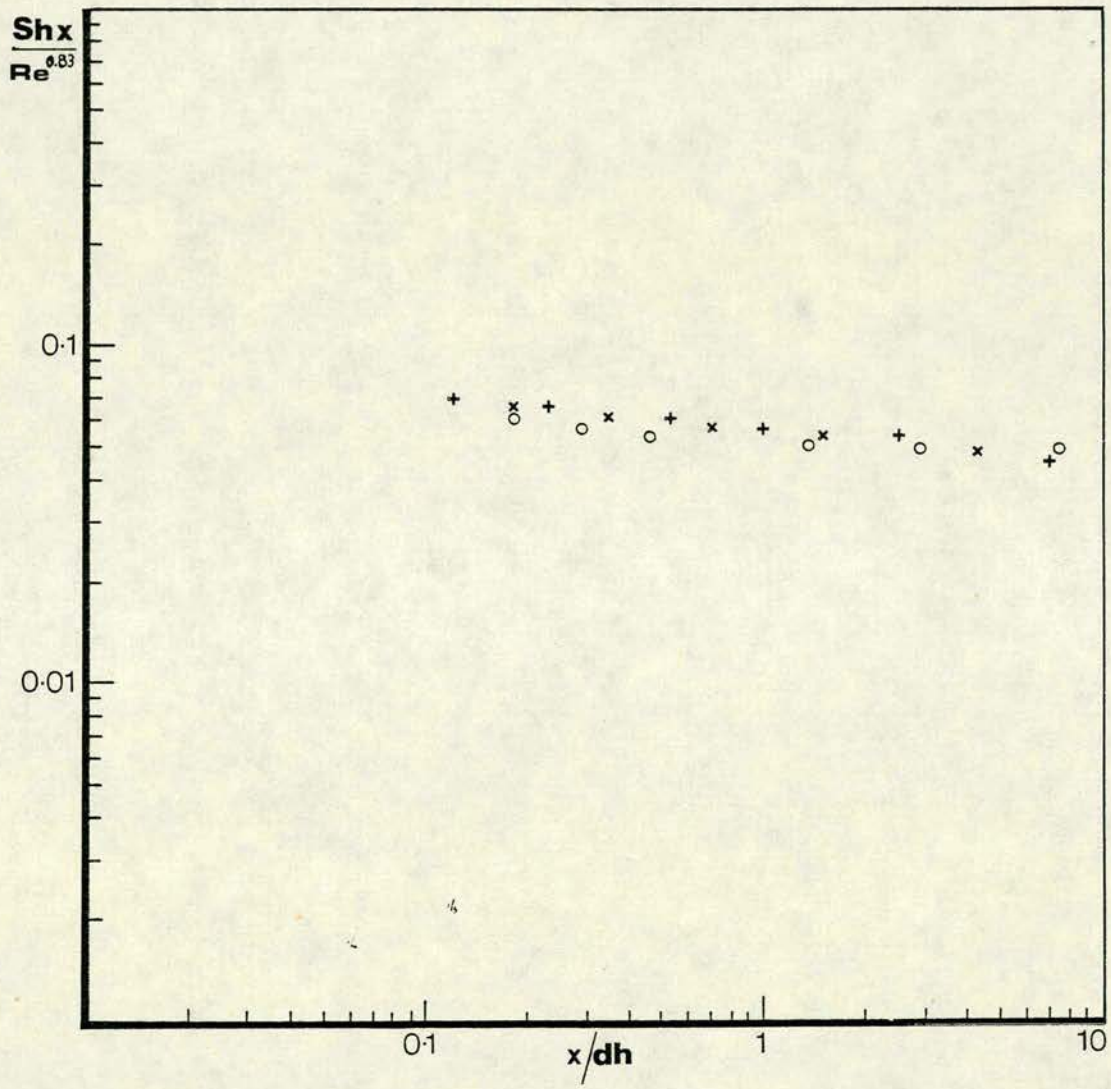

Fig. 5.23 : Consolidated Plot of $Shx/Re^{0.6}$ vs x/dh
Duct 2:1 dh = 1.27 cm
Calming Section, Asymmetric Transfer
Corrected Data
○ Run 1 Re = 5812
+ Run 2 Re = 3770
× Run 3 Re = 2355

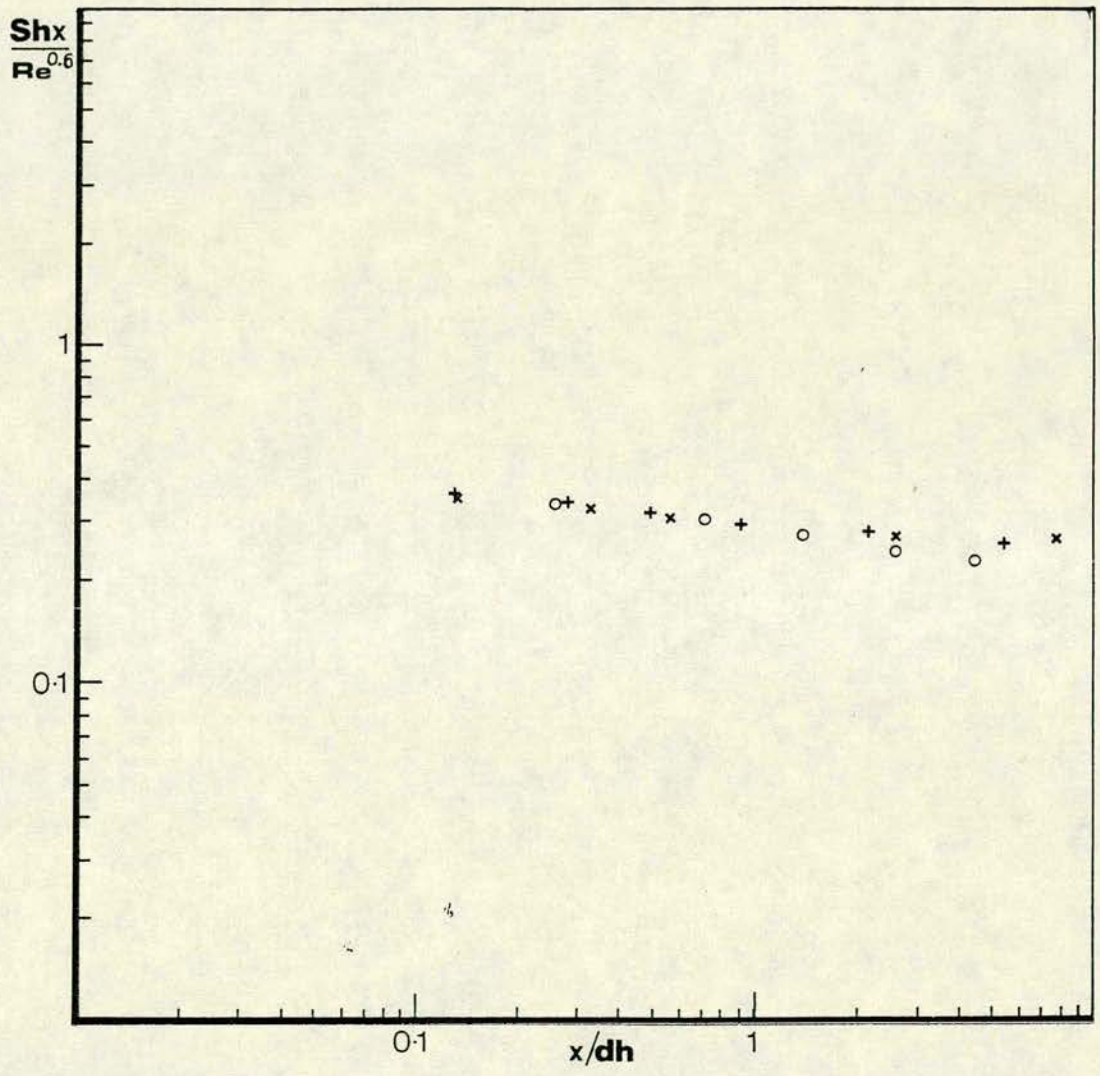

Fig. 5.24 : Consolidated Plot of $Shx/Re^{0.6}$ vs x/dh
Duct 2:1 dh = 1.27 cm
Calming Section, Asymmetric Transfer
○ Run 1 Re = 4710
+ Run 2 Re = 3960
× Run 3 Re = 1940

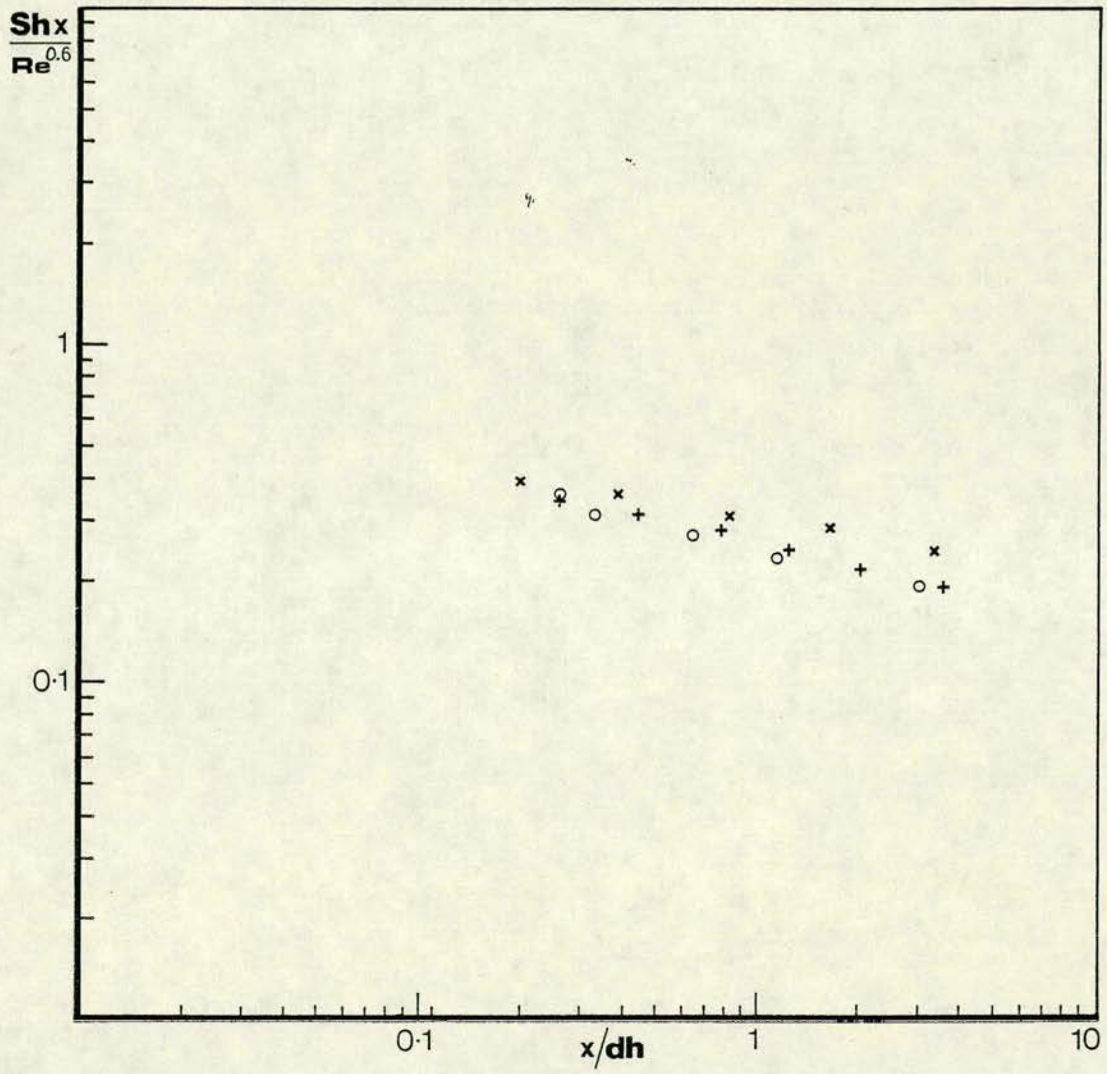

$$Num = \frac{0.664\ (Gz')^{0.5}}{Pr^{0.17}} \sqrt{1 + 6.27\ (\frac{Pr}{Gz'})^{0.44}}$$

where

$$G'z = \frac{Pe}{x/dh}$$

This equation is good for Pr > 2 and for laminar heat transfer between two parallel planes with heat being transferred through each plane. Again, exchanging Pr by Sc and applying it to our results, we find better agreement for the case of symmetric transfer from both ducts, as can be seen in Appendix J. For asymmetric transfer the results are not so good; this would be expected, since the equation is for symmetric transfer.

5.2 Conclusions

Given the state of research in mass transfer in rectangular ducts, which made us resort to literature data for heat transfer situations in most cases, we think our results are acceptable if we except the anomaly with Run 5, Re = 528, duct 3:1, calming section symmetric transfer. This means that the time-series method used in the determination of the absolute fringe order is sound and can be used in conjunction with holographic interferometry in other types of flow situations, in mass transfer determinations.

5.3 Recommendations

Through the experience gained in this work, we recommend to future investigators in this type of research, the following:

1) Modification of the flow system to allow attainment of higher Reynolds numbers. High air flow rates introduce compressibility effects and can bring about the detachment of the polymer from the

glass plate, so the attainment of high Reynolds numbers calls for ducts of larger diameter. Wider ducts would in any case make easier the recording and therefore the counting of the fringes, but will entail the use of a wider prism with the accompanying problems of making it and gluing it uniformly to the glass plate.

A fundamental difficulty about work at high Reynolds numbers may prove to be that the fringes, because of faster transfer, may be so numerous in an experiment of the shortest practical duration that they may not be properly countable. This difficulty should be overcome by suitable choice of swelling agent.

2) To avoid possible changes at the entrance of the duct when repositioning it in further abrupt entry experiments, a system should be devised by which the duct carcass is positively and accurately located flush with respect to the leading edge of the glass plate.

3) To avoid the uncertainty of locating the "true" centre of fringes and therefore the uncertainty of measuring the distance of the fringes from the leading edge of the test section, a micro-densitometer should be used. This will allow the obtaining of better and more precise results for the determination of the absolute order of the fringes.

4) Finally, the use of more sensitive film may make possible the performance of experiments in real time holography using the total internal reflection technique.

APPENDICES

APPENDIX A

Deduction of the Relationship between Fringe Spacing and Resolving Power of Photographic Film

Figure A1 shows two plane waves incident on a photographic plate, as the deduction shows the fringe spacing is given by:

$$d = \frac{\lambda}{\sin\theta}$$

The resolution of the photographic film being the inverse of this quantity or:

$$\text{Resolving Power (lines/mm)} = \frac{1}{d} = \frac{\sin\theta}{\lambda}$$

Fig. A1 : Fringe Spacing and Resolving Power of Photographic Film

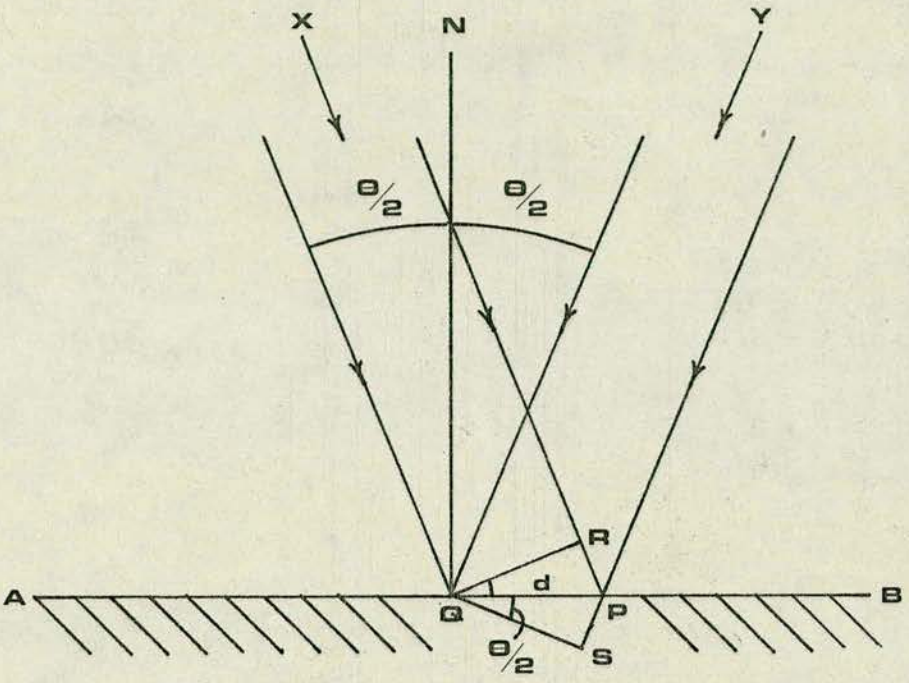

Suppose wave trains X and Y interfere at Q to form a dark fringe there. Other fringes such as P will form in the plane AB, whose normal N bisects the angle Θ between X and Y.

At the fringe P, next in sequence to Q, path length difference between X and Y $\equiv$ RP + PS must be equal to λ, wavelength. Hence

$$2d \sin \Theta/2 = \lambda \quad \therefore \quad d = \frac{\lambda}{2 \sin \Theta/2}$$

where d = fringe spacing. Thus, number of fringes/unit length on AB

$$\equiv \frac{1}{d} = \frac{2 \sin \Theta/2}{\lambda}$$

which is the required resolving power of the photographic film (lines/mm).

APPENDIX B

Prism Optics

Derivation of the Relationship between Polymer Recession and Fringe Order

Figure B1 shows the geometry of light passing through the prism. The angle of 101^{o} between P and Q was calculated by measuring a triangle whose vertices were at the beam splitter, the prism and the centre of the holographic plate.

From the figure (B1), taken the measure prism angles value of 44.9^{o} as being equal to 45^{o}, it follows that

$$\alpha = \frac{101^{o} - 90^{o}}{2} = \quad \text{or} \quad \alpha = 5.50^{o}$$

(since the angles of incidence and internal reflection at the point E are the same, so that the figure is symmetrical about the normal to the surface of the polymer at E).

From Snell's Law: $\sin \alpha \, \mu \text{ air} = \sin \beta \, \mu \text{ perspex}$

$$\sin \beta = \frac{0.10 \times 1.0}{1.496} = 0.07 \quad \therefore \beta = 3.900$$

The angle γ can be deduced from the figure below noticing that the geometrical situation depicted shows the following

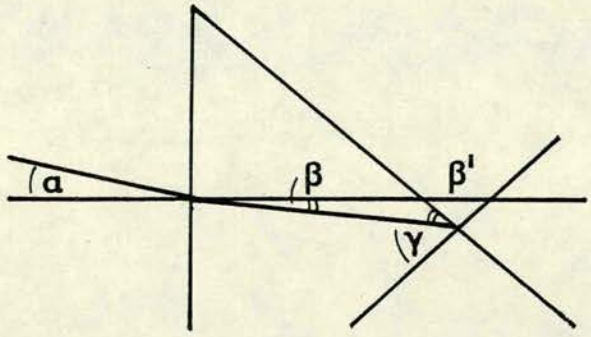

Fig. B1 : Prism Optics

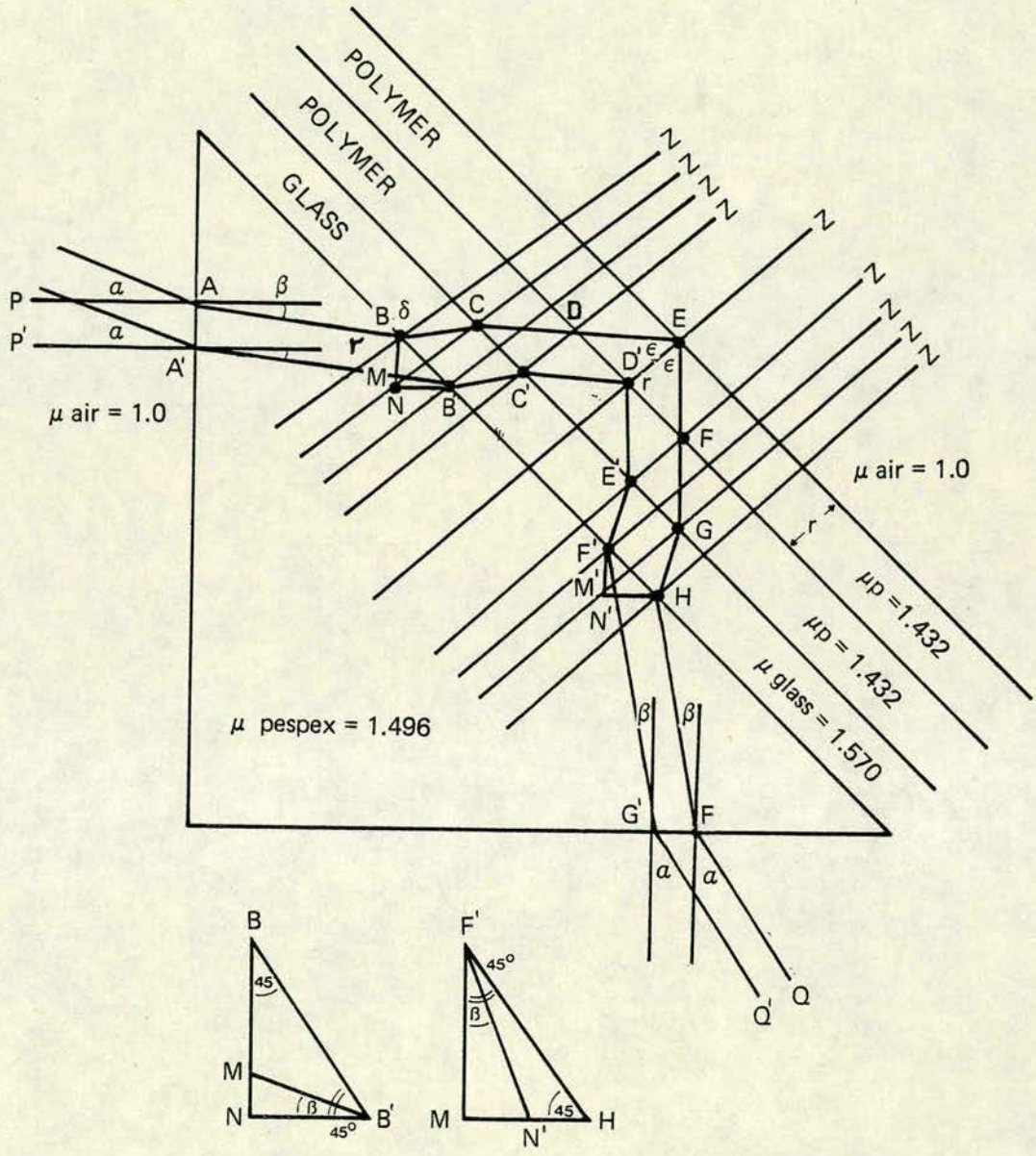

so that: $90^0 = \gamma + \beta'$

but $\beta' = 45^0 - \beta$; then : $\gamma = 90^0 - 45^0 + \beta$

$\gamma = 48.90^0$ or $\gamma = 45^0 + \beta$ $\therefore \gamma = 48.90^0$

For the critical angle:

$$\sin c = \frac{\mu \text{ air}}{\mu \text{ polymer}} = 0.698$$

$c = 44.29^0$. If ε is substantially greater than c therefore total internal reflection is achieved. Applying Snell's law again, we have:

$\sin \gamma \; \mu$ perspex = $\sin \delta$ / μ glass

$$\sin \delta = \sin \gamma \frac{\mu \text{ perspex}}{\mu \text{ glass}}$$

taking μ glass = 1.514 which corresponds to crown glass at a wavelength of 656 nm (laser wavelength is 633 nm), we have:

$$\sin \delta = 0.75 \times \frac{1.496}{1.514} = 0.74 \quad \text{or} \quad \delta = 47.82^0$$

By Snell's law again: $\sin \delta \; \mu$ glass = $\sin \varepsilon \; \mu$ polymer

$$\sin \varepsilon = \sin \delta \frac{\mu \text{ glass}}{\mu \text{ polymer}} \; ; \quad \sin \varepsilon = 0.72 \times \frac{1.514}{1.432} = 0.78$$

$\therefore \varepsilon = 51.48^0, > c$

Geometrical Path Change of Light in Perspex

$2(AB - A' B') = 2 M B'$

Geometrical Path Change of Light in Glass

$2(BC - B' C') = 0$

Geometrical Path Change of Light in Polymer

$2(CE - C' D') = 2 D E$ but $D E \cos \varepsilon = r$ $\therefore D E = \frac{r}{\cos \varepsilon}$

Total Geometrical Path Change

$2(DE - M B')$

Now:

$$\frac{M\,B'}{\sin 45} = \frac{B\,B'}{\sin(90 + \beta)} \quad \therefore\ M\,B' = \frac{B\,B'\sin 45}{\sin(90 + \beta)}$$

But $B\,B' = D\,D' \quad \therefore\ D\,D' = r \tan \varepsilon = B\,B'$

Therefore:

$$M\,B' = \frac{r \tan \varepsilon \sin 45}{\sin (90 + \beta)}$$

Total Optical Path Length Difference

$2\,(\mu \text{ polymer } D\,E - \mu \text{ perspex } M\,B')$, or

$$2\left(\mu \text{ polymer } \frac{r}{\cos \varepsilon} - \mu \text{ perspex } \frac{r \tan \varepsilon \sin 45}{\sin (90 + \beta)}\right.$$

The total optical path difference is also equal to: $n \frac{\lambda}{2}$, where n is the number of fringes generated by the recession n of the polymer surface from its initial position.

Consequently:

$$n \frac{\lambda}{2} = 2 r \left[\left(\frac{\mu \text{ polymer}}{\cos \varepsilon} - \frac{\mu \text{ perspex} \tan \varepsilon \sin 45^{o}}{\sin (90 + \beta)}\right.\right] \qquad \text{B1}$$

Substituting the values appropriate to the present case:

$$\frac{n\ 633 \times 10^{-7} \text{ cm}}{2} = 2 r \left[\frac{1.432}{\cos (51.48^{o})} - \frac{1.496 \tan 51.48^{o} \sin 45^{o}}{\sin (90^{o} + 3.90^{o})}\right]$$

$r = 1.64 \times 10^{-5}\ n\ (\text{cm})$ Eq. B2

$c = 1.64 \times 10^{-5}\ n\ (\text{cm}) \times 1\ (\text{gm/cm}^3)$ $\quad \frac{22400\ (\text{cm}^3/\text{g mol}) \times 760 \text{ mm Hg}}{273^{o}\text{K} \times 178\ (\text{gm/g mol})} \frac{1}{n} \frac{T}{P_s}$

$c = 571.25 \times 10^{-5} \left(\frac{T}{P_s}\right) \left(\frac{\text{mm Hg}}{\text{ok}}\right) \text{cm}$

The equation B1 can be put in function of the angle α so that we can know how the measure of the angle between P and Q (angle between the ray entering the prism and the ray emerging from it influences the calculated value of the constant in the expression for the recession of the polymer (r), equation B2.

Using: μ air = μa, μ polymer = μp, μ perspex = μpx and μ glass = μg and the following relationships:

$\tan \varepsilon = \sin \varepsilon / \cos \varepsilon$: $\sin \varepsilon = \sin \delta \, \mu g / \mu p$

$\cos \varepsilon = (1 - \sin^2 \varepsilon)^{\frac{1}{2}}$;

$\sin (90^o + \beta) = \sin 90^o \cos \beta + \sin \beta \cos 90^o = \cos \beta$

$\cos \beta = (1 - \sin^2 \beta)^{\frac{1}{2}}$; $\sin \beta = \sin \alpha \dfrac{\mu_a}{\mu_{px}}$

we get:

$$\frac{n\lambda}{4r} = \frac{1}{(1 - \sin^2 \delta \, \frac{\mu_g{}^2}{\mu_p{}^2})^{\frac{1}{2}}} \left[\mu p - \frac{\mu \, px \sin \delta \, \frac{\mu_g}{\mu_p} \sin 45}{(1 - \sin \alpha^2 \, \frac{\mu_a{}^2}{\mu_{px}{}^2})^{\frac{1}{2}}} \right]$$

But: $\sin \delta = \sin \gamma \dfrac{\mu_{px}}{\mu_g}$ and since $\gamma = 45^o + \beta$

we have $\sin \delta = \sin (45^o + \beta) \dfrac{\mu_{px}}{\mu_g}$

but $\sin (45^o + \beta) = \sin 45^o \cos \beta + \cos 45^o \sin \beta$, and from $\sin 45^o = \cos 45^o$, $\sin (45^o + \beta) = \sin 45^o (\sin \beta + \cos \beta)$

so that the above equation reads:

$$\frac{n\lambda}{4r} = \frac{1}{\left[1 - (\sin\beta + \cos\beta)^2 \sin^2 45 \, \frac{\mu_{px}{}^2}{\mu_p{}^2}\right]^{\frac{1}{2}}} \left[\mu p - \frac{\mu px \sin \delta \, \frac{\mu_g}{\mu_p} \sin 45}{(1 - \sin^2 \alpha \, \frac{\mu_a{}^2}{\mu_{px}{}^2})^{\frac{1}{2}}} \right]$$

Now: $(\sin \beta + \cos \beta)^2 = \sin^2 \beta + \cos \beta^2 + 2 \cos \beta \sin \beta$

or $(\sin \beta + \cos \beta)^2 = 1 + 2 \sin \beta \cos \beta$

Using again the expressions: $\sin \beta = (\mu_a / \mu_{px}) \sin \alpha$ and $\cos \beta = (1 - \sin^2 \beta)^{\frac{1}{2}}$ and replacing in the last expression, we get:

$$\frac{n\lambda}{4r} = \frac{1}{\{1 - \sin^2 45 \left[1 + 2\frac{\mu_a}{\mu_{px}} \sin\alpha \left(1 - \frac{\mu_a^2}{\mu_{px^2}} \sin^2\alpha\right)^{\frac{1}{2}}\right] \frac{\mu_{px^2}}{\mu_p^2}\}^{\frac{1}{2}}}$$

$$\left[\mu p - \frac{\mu_{px^2}}{\mu_p} \sin^2 45 \left[\frac{\mu_a}{\mu_{px}} \sin\alpha + \left(1 - \frac{\mu_a^2 \sin^2\alpha}{\mu_{px^2}}\right)^{\frac{1}{2}}\right]}{\left(1 - \sin^2\alpha \frac{\mu_a^2}{\mu_{px^2}}\right)^{\frac{1}{2}}}\right]$$

Now: $\sin^2 45 = 0.5$ and $\mu a = 1$, so that the final equation reads:

$$\frac{n\lambda}{4r} = \frac{1}{\{1-0.5 \left[1 + \frac{2}{\mu_{px}} \sin\alpha \left(1 - \frac{1}{\mu_{px^2}} \sin^2\alpha\right)^{\frac{1}{2}}\right] \frac{\mu_{px^2}}{\mu_p^2}\}^{\frac{1}{2}}}$$

$$\left[\mu p - 0.5 \frac{\mu_{px^2}}{\mu_p} \frac{\left[\frac{1}{\mu_{px}} \sin\alpha + \left(1 - \frac{\sin^2\alpha}{\mu_{px^2}}\right)^{\frac{1}{2}}\right]}{\left(1 - \sin^2\alpha \frac{1}{\mu_{px^2}}\right)^{\frac{1}{2}}}\right] \qquad \text{B3}$$

Equation B3 is equivalent to equation B1, it shows that a variation of α from $\alpha = 5.5^o$ to $\alpha = 6^o$, for example, which means a variation in the value of $\sin\alpha$ of 9.1% would mean a negligible variation in the value of the constant in equation B2.

APPENDIX C

Sample Calculation of the Absolute Fringe Order

Duct 3:1

Abrupt Entrance, Asymmetric Transfer

Run 2: Re = 5120 $\quad \Theta = 22.7^{o}C$

In this run the times involved in the determination of the absolute fringe order and hence in the construction of the master curve are: t = 6 min, t = 7 min and t = 8 min. The data for the X vs N curves, Fig. C1 was:

t = 8 min		t = 7 min		t = 6 min	
X (cm)	N	X (cm)	N	X (cm)	N
0.27	13	0.29	11	0.66	7
0.37	11	0.46	9	1.08	5
0.87	9	1.00	7	2.16	3
1.49	7	1.91	5	6.25	1
2.49	5	5.81	3		
3.82	3	9.71	1		
6.10	1				

The values of the distance from the leading edge of the test section (X) were read from the photographs of the fringes and corrected by a scaling factor of 0.83. The values of N are arbitrary satisfying the only condition that the furthest fringe downstream should be assigned the value one. The nominal values (N) are odd because we are dealing with dark fringes. For the scaling up, we have the following data:

Crossing point (C.P.) : X = 1.49 cm N = 7.0 (t = 8 min)

X = 1.49 cm N = 5.8 (t = 7 min)

X = 1.49 cm N = 4.2 (t = 6 min)

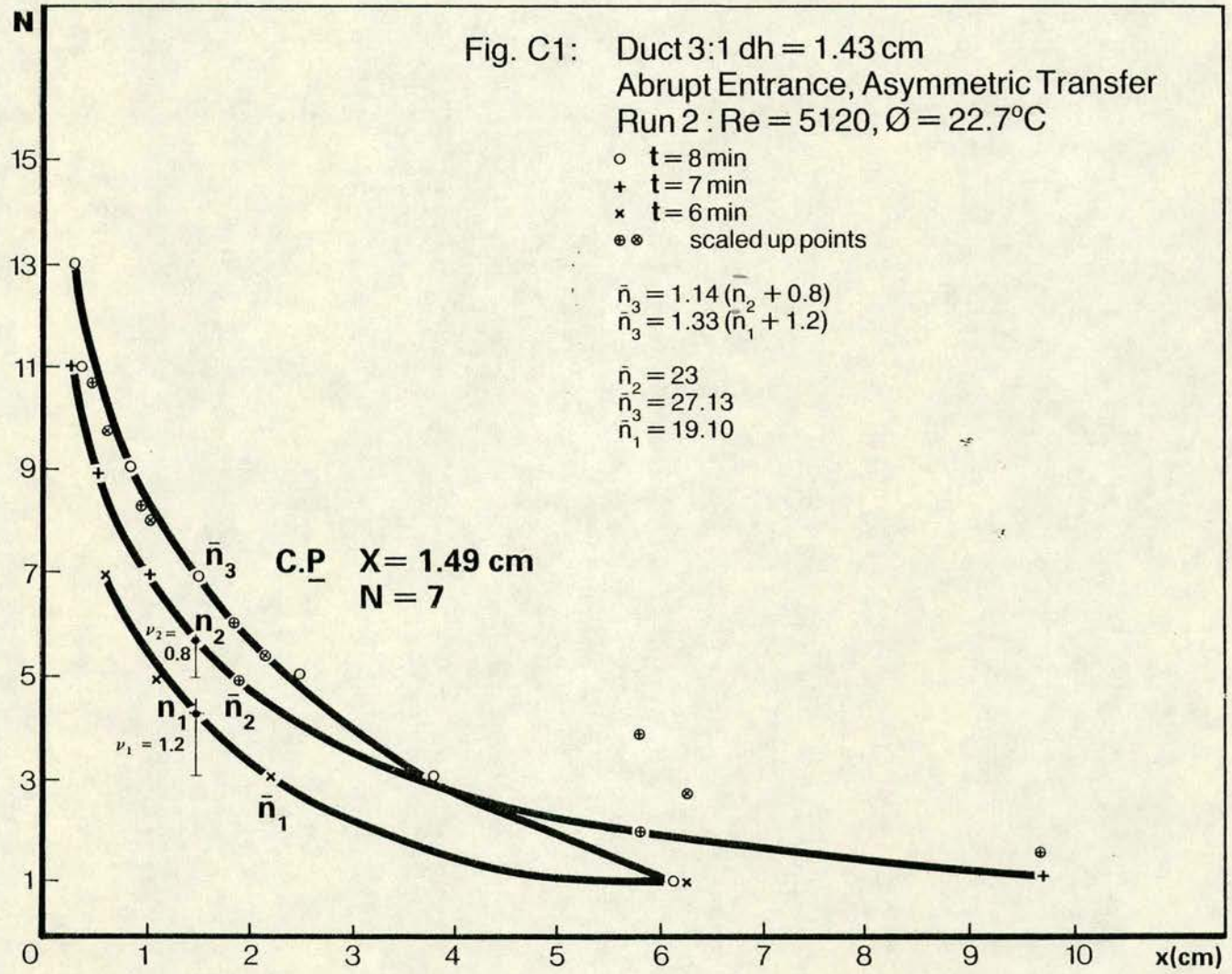
N
15
13
11
9
7
5
3
1
0
1
2
3
4
5
6
7
8
9
10
x(cm)
Fig. C1: Duct 3:1 dh = 1.43 cm
Abrupt Entrance, Asymmetric Transfer
Run 2 : Re = 5120, Ø = 22.7°C
o t = 8 min
+ t = 7 min
× t = 6 min
⊕⊗ scaled up points
$\bar{n}_3 = 1.14\,(\bar{n}_2 + 0.8)$
$\bar{n}_3 = 1.33\,(\bar{n}_1 + 1.2)$
$\bar{n}_2 = 23$
$\bar{n}_3 = 27.13$
$\bar{n}_1 = 19.10$
$\bar{n}_3$
C.P X= 1.49 cm
N = 7
n_2
$\nu_2 = 0.8$
n_1
$\bar{n}_2$
$\nu_1 = 1.2$
$\bar{n}_1$

so that the difference (Δ) to be added to each co-ordinate is:

Δ = 1.20 (t = 7 min) and Δ = 2.80 (t = 6 min).

The scaling up procedure will be illustrated using as an example the co-ordinates: N = 11 and N = 7 for t = 7 min and t = 6 min respectively.

The steps in the calculation are:

t = 7 min	t = 6 min
1. 11 + 1.20 = 12.20	1. 7 + 2.83 = 9.83
2. 12.20 - 7 = 5.20	2. 9.83 - 7 = 2.83
3. 5.20 (8/7) = 5.94	3. 2.83 (8/6) = 3.77
4. 5.94 + 7 = 12.94	4. 7 + 3.77 = 10.77

Therefore, the scaled up ordinates for these particular points are: 12.94 and 10.77. Proceeding in the same way with the other ordinates we get:

t = 7 min		t = 6 min	
X (cm)	N	X (cm)	N
0.29	12.94	0.66	10.77
0.46	10.65	1.08	8.06
1.00	8.37	2.16	5.40
1.91	6.09	6.25	2.74
5.81	3.81		
9.71	1.53		

These points give an acceptable scattering around the curve t = 8 min, except in the lower part of it, so that we can take this curve as the master curve itself. We now proceed to choose for trial an odd whole number value of n which we call n3 to set up the equations which will enable us to calculate the absolute order of the fringes.

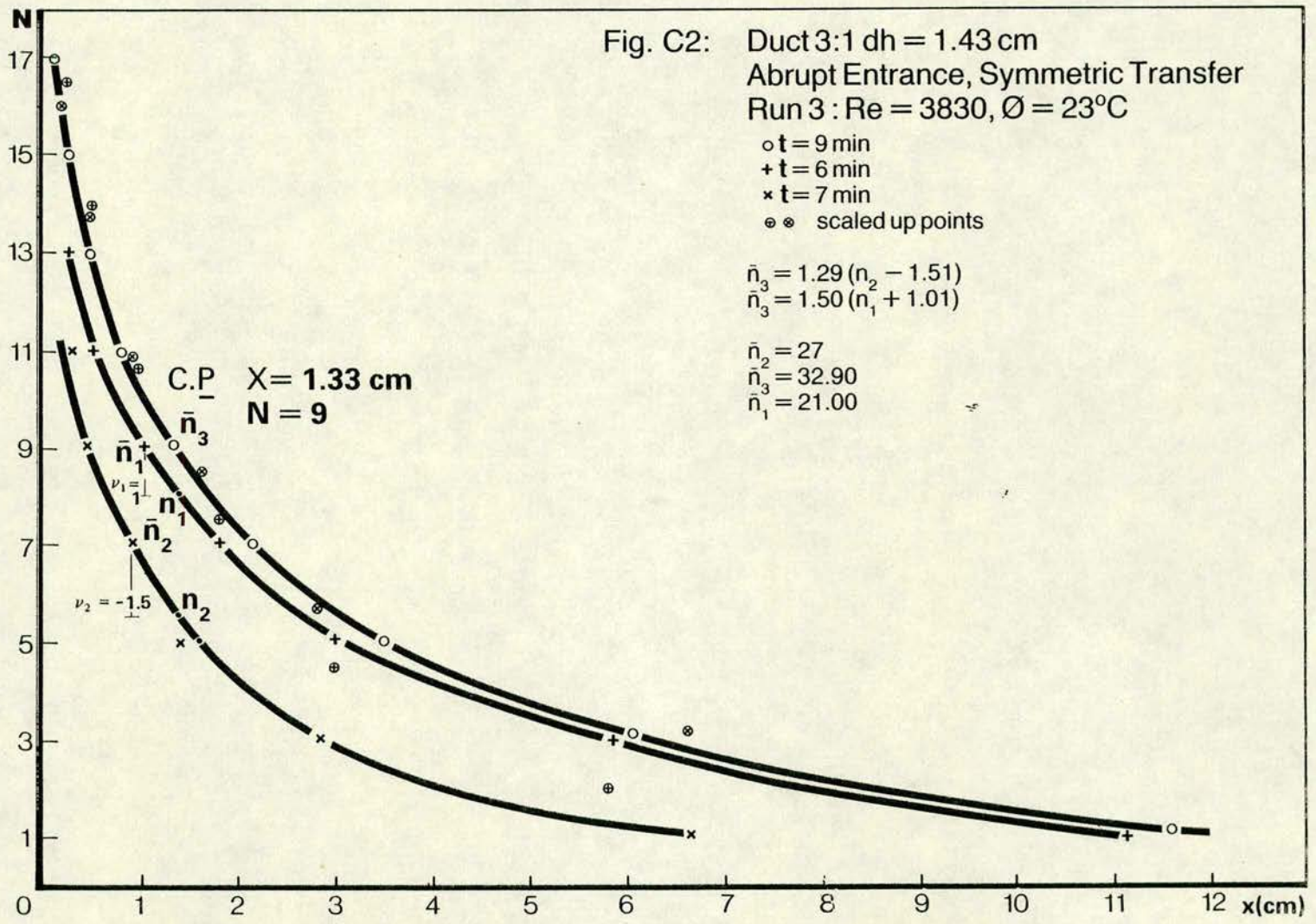

Fig. C2: Duct 3:1 dh = 1.43 cm
Abrupt Entrance, Symmetric Transfer
Run 3 : Re = 3830, Ø = 23°C

- o t = 9 min
- + t = 6 min
- × t = 7 min
- ⊕ ⊗ scaled up points

$\bar{n}_3 = 1.29\,(n_2 - 1.51)$
$\bar{n}_3 = 1.50\,(n_1 + 1.01)$

$\bar{n}_2 = 27$
$\bar{n}_3 = 32.90$
$\bar{n}_1 = 21.00$

From the figure we have:

$\bar{n}3 = 1.14\ (\bar{n}2 + 0.8)$ and

$\bar{n}3 = 1.33\ (\bar{n}1 + 1.2)$

We proceed to give odd trial values to n2 and we get the following corresponding sets of results for n_3 and n1:

$\bar{n}2$:	7	9	11	13	15	17	19	21	23	25
$\bar{n}3$:	8.89	11.17	13.45	15.73	18.01	20.29	22.57	24.85	27.13	29.41
$\bar{n}1$:	5.57	7.07							19.10	

Of these triads of values the ones enclosed by lines are the best approximations to whole odd numbers. The set: $\bar{n}2 = 9$, $\bar{n}3 = 11.17$ and $\bar{n}1 = 7.07$ will yield very low values for the mass transfer coefficient not compatable with the Reynolds number of 5120 for this run. Therefore, we have chosen the set of values: $\bar{n}2 : 23$, $\bar{n}3 = 27.13$ and $\bar{n}1 = 19.10$, so that the real values are: $\bar{n}2 = 23$, $\bar{n}3 = 27$ and $\bar{n}1 = 19$. Other values of the absolute fringe order follow from these.

Figures C2, C3, C4 are other examples of the scaling up method and the setting up of the equations of $\bar{n}$.

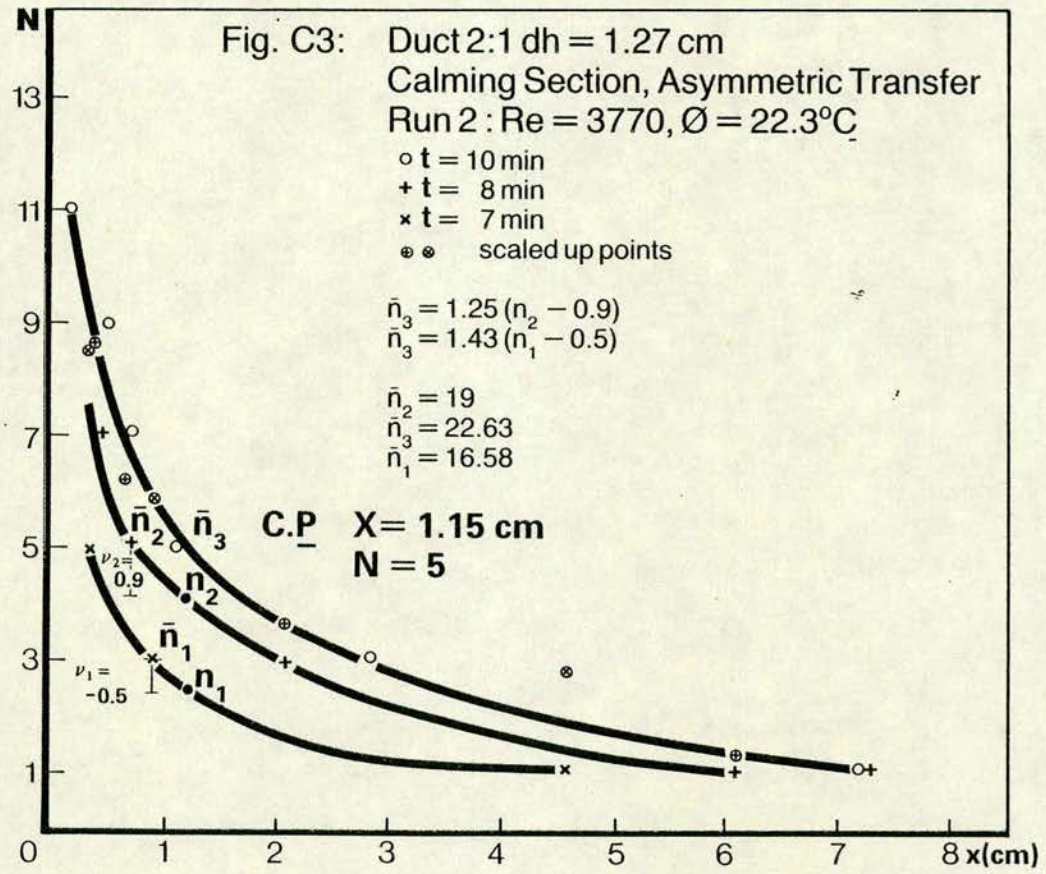
N
13
11
9
7
5
3
1
0
1
2
3
4
5
6
7
8 x(cm)
Fig. C3: Duct 2:1 dh = 1.27 cm
Calming Section, Asymmetric Transfer
Run 2 : Re = 3770, Ø = 22.3°C
o t = 10 min
+ t = 8 min
× t = 7 min
⊕ ⊗ scaled up points
$\bar{n}_3 = 1.25\,(n_2 - 0.9)$
$\bar{n}_3 = 1.43\,(n_1 - 0.5)$
$\bar{n}_2 = 19$
$\bar{n}_3 = 22.63$
$\bar{n}_1 = 16.58$
C.P X= 1.15 cm
N = 5
$\bar{n}_2$
$\bar{n}_3$
n_2
$\bar{n}_1$
n_1
$\nu_2 = 0.9$
$\nu_1 = -0.5$

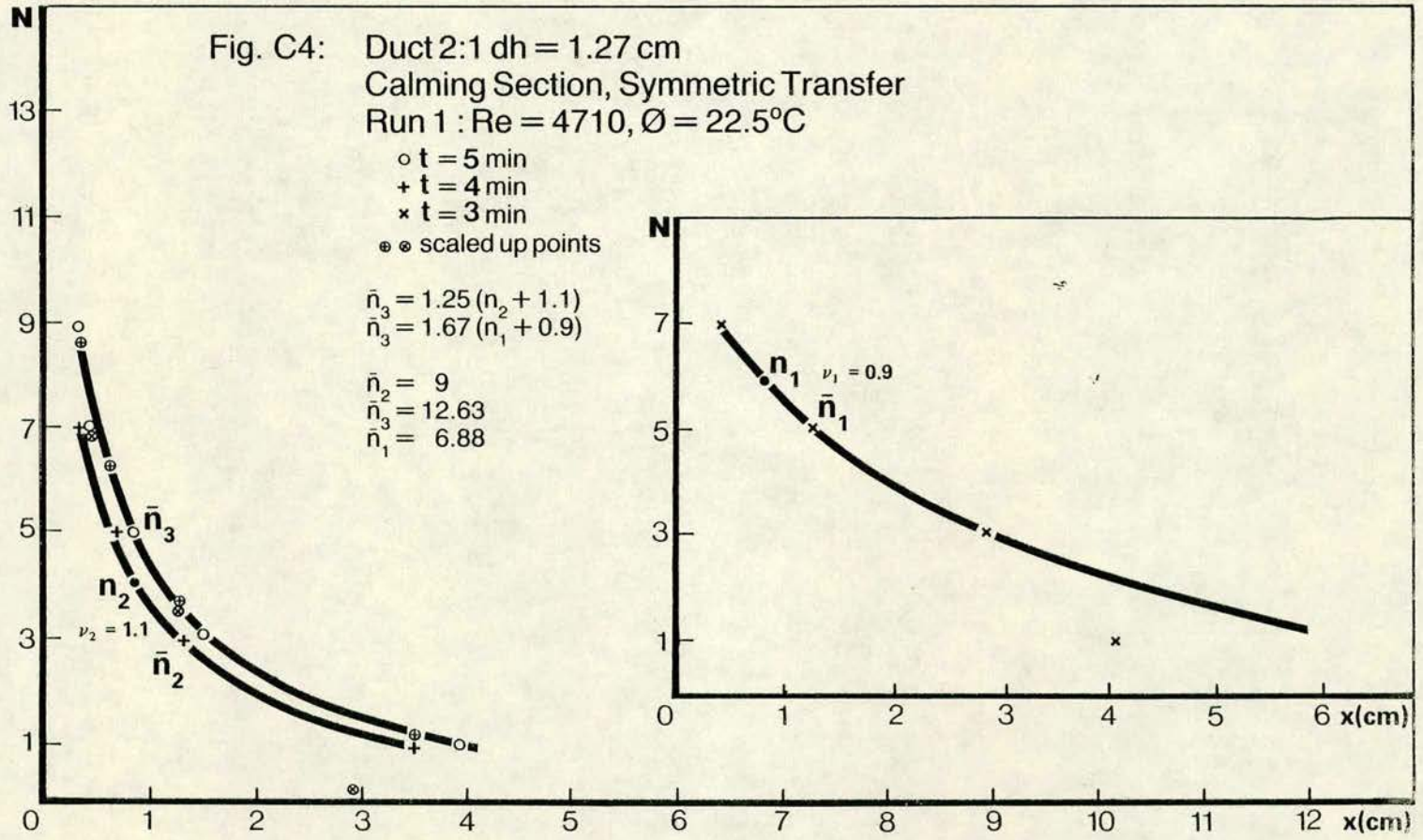
N
13
11
9
7
5
3
1
0 1 2 3 4 5 6 7 8 9 10 11 12 x(cm)
Fig. C4: Duct 2:1 dh = 1.27 cm
Calming Section, Symmetric Transfer
Run 1 : Re = 4710, Ø = 22.5°C
o t = 5 min
+ t = 4 min
× t = 3 min
⊕ ⊗ scaled up points
$\bar{n}_3 = 1.25\,(n_2 + 1.1)$
$\bar{n}_3 = 1.67\,(n_1 + 0.9)$
$\bar{n}_2 = 9$
$\bar{n}_3 = 12.63$
$\bar{n}_1 = 6.88$
$\bar{n}_3$
n_2
$\nu_2 = 1.1$
$\bar{n}_2$
N
7
5
3
1
0 1 2 3 4 5 6 x(cm)
n_1
$\nu_1 = 0.9$
$\bar{n}_1$

APPENDIX D

Sample Calculation of the Uncorrected Local Mass Transfer Coefficient and Sherwood number

Duct 3:1, dh = 1.43 cm

Abrupt Entrance, Asymmetric Transfer

Re = 5120, $\Theta = 22.7^{o}C$, t = 8 min

The equation for the calculation of the mass transfer coefficient (K) is: $K' = Cn/t$ (Appendix K). The expression for the constant C has been determined in Appendix B and reads:

$$C = 575.25 \times 10^{-5} \left(\frac{T}{P_s}\right) \left(\frac{\text{mm Hg. cm}}{^{o}K}\right)$$

$T = 22.7^{o}C + 273 = 295.7^{o}K$; $T = 295.7^{o}K$. The vapour pressure, P_s, is given by an empirical expression given by Kapur and Macleod (1976):

$$\ln P_s \text{ (mm Hg)} = - \frac{6983.74}{T} + 20.74$$

From that expression: $P_s = 0.04295$ mm Hg

therefore:

$$C = 575.25 \times 10^{-5} \frac{295.7}{0.04295} \left(\frac{ok}{\text{mm Hg}}\right) \left(\frac{\text{mm Hg}}{^{o}K} \text{ cm}\right)$$

C = 36.54 cm.

The time of this run was: $t = 8 \text{ min} \times 60 \frac{\text{sec}}{\text{min}}$

t = 480 sec. Consequently, c/t = 36.54 cm/480 sec, c/t = 0.0825 cm/sec.

We know from Appendix C that for this run the value of the absolute odd fringe order (n) at x = 1.5 cm is 27. Therefore, for that specific point the value of K' is:

$$K' = (27)\ (0.0825) \frac{\text{cm}}{\text{sec}}$$

K' = 2.23 cm/sec.

The remaining values of n for this run can be deduced from the previous one, because they have to be odd numbers, so for the point immediately to the left of X = 1.5 cm, the value of $\tilde{n}$ is 29, and for the one immediately to the right of the same point, $\bar{n}$ is 25. So with the use of the equation: K' = cn/t knowing all values of $n = \bar{n}$ we can make the following table:

X (cm)	K' (cm/sec)	n	c/t = 0.0825 cm/sec
0.27	2.73	33	
0.37	2.57	31	
0.87	2.40	29	
1.50	2.23	27	
2.49	2.06	25	
3.82	1.90	23	
6.11	1.73	21	

The data, however, has been given in terms of dimensionless numbers: the Sherwood number (Shx) and x/dh (distance for the leading edge of the test section/hydraulic diameter). To calculate the Sherwood number we proceed as follows:

$$Shx = \frac{K\ dh}{D} \left[\frac{(cm/sec)\ cm}{cm^2/sec}\right]$$

The diffusion coefficient (D) of isobutyl benzoate in air is given by Kapur (1973) for several temperatures, from his data D = 0.051 (cm /sec), so that for X = 1.50 cm

$$K = 2.23 \text{ cm/sec} \ ; \ Sh'x = \frac{2.23\ (cm/sec)\ 1.43\ (cm)}{0.051}$$

Sh'x = 62.53.

Proceeding in the same way we can find all values of Sh'x. These values are however uncorrected ones. From Appendix F we know

that Shx = F Sh'x and for this run correction was needed for the two last points, the factor, F, being: 1.06 (X = 3.82 cm) and 1.04 (X = 2.49 cm). By applying, then, the correction factor F to the last two points and dividing every distance (X) by the hydraulic diameter (dh) we finally get:

Duct 3:1, dh = 1.43 cm

Abrupt Entrance, Asymmetric Transfer

Re = 5120, Θ = 22.5°C, t = 8 min

X/dh	Shx
0.19	76.55
0.26	72.06
0.61	67.30
1.04	62.53
1.74	57.76
2.67	55.41
4.27	51.42

APPENDIX E

Uncorrected Data for Sherwood Number (Sh'x) and Mass Transfer Coefficient (K')

Duct 2:1, dh = 1.27 cm

Abrupt Entrance, Asymmetric Transfer

Run 1: Re = 5815

t = 6 min Θ = 22°C c/t = 0.1161 cm/sec

X(cm)	N	n	K'(cm/sec)	X/dh	Sh'x
0.17	15	29	3.37	0.13	83.91
0.33	13	27	3.13	0.26	77.93
0.58	11	25	2.90	0.46	72.21
1.08	9	23	2.67	0.85	66.48
1.83	7	21	2.44	1.44	60.75
2.66	5	19	2.21	2.09	55.03
4.32	3	17	1.97	3.40	49.05
11.79	1	15	1.74	9.28	43.32

$\frac{Sh'\left(\frac{x}{dh} = 9.28\right)}{Sh_\infty} = 1.27$

t = 7 min Θ = 22°C c/t = 0.0995 cm/sec

X(cm)	N	n	K'(cm/sec)	X/dh	Sh'x
0.17	15	33	3.28	0.13	81.67
0.33	13	31	3.08	0.26	76.69
0.75	11	29	2.89	0.59	71.96
1.41	9	27	2.69	1.11	66.98
2.08	7	25	2.49	1.64	62.00
2.91	5	23	2.29	2.29	57.02
4.40	3	21	2.09	3.46	52.04
10.13	1	19	1.89	7.98	47.06

$\frac{Sh'\left(\frac{x}{d_H} = 7.98\right)}{Sh_\infty} = 1.38$

APPENDIX E (Contd.)

Duct 2:1, dh = 1.27 cm

Abrupt Entrance, Asymmetric Transfer

t = 8 min Θ = 22.3°C c/t = 0.0851 cm/sec

X(cm)	N	n	K'(cm/sec)	X/dh	Sh'x
0.25	15	37	3.15	0.20	78.43
0.42	13	35	2.98	0.33	74.20
0.91	11	33	2.81	0.72	69.97
1.58	9	31	2.64	1.24	65.73
2.16	7	29	2.47	1.70	61.50
2.91	5	27	2.30	2.29	57.22
4.32	3	25	2.13	3.40	53.03
8.72	1	23	1.96	6.87	48.80

$$\frac{Sh'_{\left(\frac{x}{dh}=6.87\right)}}{Sh_\infty} = 1.43$$

$Sh_\infty = 0.023\ Re^{0.8}\ Sc^{0.33}$

Run 2: Re = 5103

t = 7 min Θ = 22.7 c/t = 0.0943 cm/sec

X(cm)	N	n	K'(cm/sec)	X/dh	Sh'x
0.42	11	27	2.55	0.33	63.40
0.83	9	25	2.36	0.65	58.70
1.66	7	23	2.17	1.31	54.01
2.99	5	21	1.98	2.35	49.31
5.23	3	19	1.79	4.12	44.61
8.72	1	17	1.60	6.87	39.92

$$\frac{Sh'_{\left(\frac{x}{dh}=6.87\right)}}{Sh_\infty} = 1.28$$

APPENDIX E (Contd.)

Duct 2:1, dh = 1.27 cm

Abrupt Entrance, Asymmetric Transfer

t = 8 min Θ = 22.7°C c/t = 0.0825 cm/sec

X(cm)	N	n	K'(cm/sec)	X/dh	Sh'x
0.42	13	31	2.56	0.33	63.68
0.71	11	29	2.39	0.56	59.57
1.58	9	27	2.23	1.24	55.46
2.32	7	25	2.06	1.83	51.36
3.32	5	23	1.90	2.61	47.25
4.57	3	21	1.73	3.60	43.14
8.96	1	19	1.57	7.06	39.03

$\frac{Sh'\left(\frac{x}{dh} = 7.06\right)}{Sh_\infty} = 1.27$

t = 9 min Θ = 22.7°C c/t = 0.0733 cm/sec

X(cm)	N	n	K'(cm/sec)	X/dh	Sh'x
0.42	13	35	2.57	0.33	63.99
0.66	11	33	2.42	0.52	60.26
1.16	9	31	2.27	0.91	56.52
1.99	7	29	2.13	1.57	53.08
2.82	5	27	1.98	2.22	49.30
3.82	3	25	1.83	3.01	45.57
5.81	1	23	1.69	4.57	42.08

$\frac{Sh'\left(\frac{x}{dh} = 4.57\right)}{Sh_\infty} = 1.38$

$Sh_\infty = 0.023\ Re^{0.8}\ Sc^{0.33}$

APPENDIX E (Contd.)

Duct 2:1, dh = 1.27 cm

Abrupt Entrance, Asymmetric Transfer

Run 3: Re = 3380

t = 7 min Θ = 22.5°C c/t = 0.0956 cm/sec

X(cm)	N	n	K'(cm/sec)	X/dh	Sh'x
0.25	9	23	2.20	0.20	54.75
0.58	7	21	2.01	0.46	49.99
1.25	5	19	1.82	0.98	45.23
2.08	3	17	1.63	1.64	40.47
4.15	1	15	1.43	3.27	35.71

$\frac{Sh'_{(\frac{x}{dh}=3.27)}}{Sh_\infty} = 1.62$

t = 8 min Θ = 22.5°C c/t = 0.0837 cm/sec

X(cm)	N	n	K'(cm/sec)	X/dh	Sh'x
0.21	11	27	2.26	0.17	56.27
0.46	9	25	2.09	0.36	52.10
0.87	7	23	1.93	0.69	47.93
1.58	5	21	1.76	4.24	43.77
2.74	3	19	1.59	2.16	39.60
5.48	1	17	1.42	4.31	35.43

$\frac{Sh'_{(\frac{x}{dh}=4.31)}}{Sh_\infty} = 1.61$

t = 9 min Θ = 22.5°C c/t = 0.0744 cm/sec

X(cm)	N	n	K'(cm/sec)	X/dh	Sh'x
0.17	15	31	2.31	0.13	57.52
0.33	13	29	2.16	0.26	53.78
0.58	11	27	2.01	0.46	50.05
1.04	9	25	1.86	0.82	46.31
1.74	7	23	1.71	1.37	42.58
2.82	5	21	1.56	2.22	38.84
5.23	3	19	1.41	4.12	35.11
9.71	1	17	1.26	7.65	31.37

$\frac{Sh'_{(\frac{x}{dh}=7.65)}}{Sh_\infty} = 1.42$

$Sh_\infty = 0.023\ Re^{0.8}\ Sc^{0.33}$

APPENDIX E (Contd.)

Duct 2:1, dh = 1.27 cm

Abrupt Entrance, Asymmetric Transfer

Run 4: Re = 2120

t = 8 min Θ = 22.7°C c/t = 0.0825 cm/sec

X(cm)	N	n	K'(cm/sec)	X/dh	Sh'x
0.21	7	21	1.73	0.17	43.14
0.75	5	19	1.57	0.59	39.03
2.24	3	17	1.40	1.76	34.92
5.40	1	15	1.24	4.25	30.81

$\frac{Sh'\left(\frac{x}{dh}=4.25\right)}{Sh_\infty}=2.03$

t = 9 min Θ = 22.7°C c/t = 0.0734 cm/sec

X(cm)	N	n	K'(cm/sec)	X/dh	Sh'x
0.42	7	19	1.39	0.33	34.74
1.00	5	17	1.25	0.79	31.07
2.49	3	15	1.10	1.96	27.41
7.14	1	13	0.95	5.26	23.76

$\frac{Sh'\left(\frac{x}{dh}=5.26\right)}{Sh_\infty}=1.57$

t = 10 min Θ = 22.7°C c/t = 0.0660 cm/sec

X(cm)	N	n	K'(cm/sec)	X/dh	Sh'x
0.21		25	1.65	0.17	41.09
0.42		23	1.52	0.33	37.85
0.95		21	1.39	0.75	34.61
2.08		19	1.26	1.64	31.37
4.81		17	1.13	3.79	28.14
9.96		15	0.99	7.84	24.65

$\frac{Sh'\left(\frac{x}{dh}=7.84\right)}{Sh_\infty}=1.62$

$Sh_\infty = 0.023\ Re^{0.8}\ Sc^{0.33}$

APPENDIX E (Contd.)

Duct 2:1, dh = 1.27 cm

Abrupt Entrance, Asymmetric Transfer

Run 5: Re = 704

t = 9 min $\Theta = 24^{o}C$ c/t = 0.0604 cm/sec

X(cm)	N	n	K'(cm/sec)	X/dh	Sh'x
0.33	7	21	1.39	0.26	34.72
0.75	5	19	1.26	0.59	31.42
2.05	3	17	1.13	1.61	28.11
8.72	1	15	1.00	6.87	24.80

t = 11 min $\Theta = 24^{o}C$ c/t = 0.0543 cm/sec

X(cm)	N	n	K'(cm/sec)	X/dh	Sh'x
0.17	7	25	1.36	0.13	33.80
0.66	5	23	1.25	0.52	31.10
2.32	3	21	1.14	1.83	28.40
8.72	1	19	1.03	6.87	25.69

t = 12 min $\Theta = 24^{o}C$ c/t = 0.0534 cm/sec

X(cm)	N	n	K'(cm/sec)	X/dh
0.17	7	27	1.34	0.13
0.66	5	25	1.25	0.52
2.08	3	23	1.15	1.64
4.98	1	21	1.05	3.92

APPENDIX E (Contd.)

Duct 2:1, dh = 1.27 cm

Abrupt Entrance, Symmetric Transfer

Run 1: Re = 6625

t = 7 min Θ = 23.7°C c/t = 0.0874 cm/sec

X(cm)	N	n	K'(cm/sec)	X/dh	S'hx
0.42	11	37	3.23	0.33	80.52
0.66	9	35	3.06	0.52	76.17
1.12	7	33	2.88	0.88	71.82
1.58	5	31	2.71	1.24	67.46
3.32	3	29	2.53	2.61	63.11
5.06	1	27	2.36	3.98	58.76

$\frac{Sh'\left(\frac{x}{dh} = 3.98\right)}{Sh''_{\infty}} = 1.30$

t = 9 min Θ = 23.7°C c/t = 0.0680 cm/sec

X(cm)	N	n	K'(cm/sec)	X/dh	S'hx
0.42	15	47	3.20	0.33	79.58
0.75	13	45	3.06	0.56	76.19
1.08	11	43	2.92	0.85	72.81
1.49	9	41	2.79	1.17	69.42
2.32	7	39	2.65	1.83	66.03
3.24	5	37	2.52	2.55	62.65
4.98	3	35	2.38	3.92	59.26
8.30	1	33	2.24	6.54	55.88

$\frac{Sh'\left(\frac{x}{dh} = 6.54\right)}{Sh''_{\infty}} = 1.23$

APPENDIX E (Contd.)

Duct 2:1, dh = 1.27 cm

Abrupt Entrance, Symmetric Transfer

t = 10 min Θ = 23.7°C c/t = 0.0612 cm/sec

X(cm)	N	n	K'(cm/sec)	X/dh	S'hx
0.42	19	53	3.24	0.33	80.77
0.54	17	51	3.12	0.43	77.72
0.83	15	49	3.00	0.65	74.67
1.16	13	47	2.88	0.91	71.62
1.49	11	45	2.75	1.17	68.57
1.99	9	43	2.63	1.57	65.53
3.10	7	41	2.51	2.44	62.48
4.8	5	39	2.39	3.78	59.43
7.4	3	37	2.26	5.83	56.38
11.62	1	35	2.14	9.15	53.23

$\frac{Sh'\left(\frac{x}{dh} = 9.15\right)}{Sh''_{\infty}} = 1.17$

$Sh'_{\infty} = 1.2\ Sh_{\infty}$

$Sh_{\infty} = 0.023\ Re^{0.8}\ Sc^{0.33}$

Run 2: Re = 5480

t = 7 min Θ = 23.7°C c/t = 0.0874 cm/sec

X(cm)	N	n	K'(cm/sec)	X/dh	S'hx
0.50	13	33	2.88	0.39	71.82
0.83	11	31	2.71	0.65	67.46
1.33	9	29	2.53	1.05	63.11
1.99	7	27	2.36	1.57	58.76
3.24	5	25	2.16	2.55	54.41
5.60	3	23	2.01	4.41	50.05
10.79	1	21	1.84	8.50	45.70

$\frac{Sh'\left(\frac{x}{dh} = 8.50\right)}{Sh''_{\infty}} = 1.17$

APPENDIX E (Contd.)

Duct 2:1, dh = 1.27 cm

Abrupt Entrance, Symmetric Transfer

t = 8 min Θ = 23.7°C c/t = 0.0764 cm/sec

X(cm)	N	n	K'(cm/sec)	x/dh	S'hx
0.17	17	39	2.98	0.13	74.19
0.42	15	36	2.83	0.33	70.39
0.75	13	35	2.67	0.59	66.58
1.20	11	33	2.52	0.94	62.78
1.58	9	31	2.37	1.20	58.97
2.24	7	27	2.06	1.76	51.36
3.50	5	25	1.91	2.76	47.56
10.79	1	23	1.76	8.50	43.75

$\frac{Sh'\left(\frac{x}{dh} = 8.50\right)}{Sh''_{\infty}} = 1.12$

t = 10 min Θ = 23.7°C c/t = 0.0612 cm/sec

X(cm)	N	n	K'(cm/sec)	x/dh	S'hx
0.17	19	51	3.12	0.13	77.72
0.42	17	49	3.00	0.33	74.67
0.66	15	47	2.88	0.52	71.62
0.91	13	45	2.75	0.72	68.57
1.25	11	43	2.63	0.99	65.53
1.59	9	41	2.51	1.25	62.48
2.24	7	39	2.39	1.75	59.43
3.32	5	37	2.26	2.61	56.38
5.15	3	35	2.14	4.06	53.34
10.38	1	33	2.02	8.17	50.29

$\frac{Sh'\left(\frac{x}{dh} = 8.17\right)}{Sh''_{\infty}} = 1.29$

APPENDIX E (Contd.)

Duct 2:1, dh = 1.27 cm

Abrupt Entrance, Symmetric Transfer

Run 3: Re = 3840

t = 6 min Θ = 21.3°C c/t = 0.1225 cm/sec

X(cm)	N	n	K'(cm/sec)	X/dh	Sh'x
0.42	9	17	2.08	0.33	51.85
0.83	7	15	1.84	0.65	45.75
1.66	5	13	1.59	1.31	39.65
2.99	3	11	1.35	2.35	33.55
7.06	1	9	1.10	5.56	27.45

$\frac{Sh'\left(\frac{x}{dh}=5.56\right)}{Sh''_\infty}=0.94$

t = 7 min Θ = 21.3°C c/t = 0.1050 cm/sec

X(cm)	N	n	K'(cm/sec)	X/dh	Sh'x
0.25	13	21	2.21	0.20	54.90
0.58	11	19	2.00	0.46	49.68
1.00	9	17	1.79	0.79	44.45
1.83	7	15	1.58	1.45	39.34
2.82	5	13	1.37	2.23	33.99
4.98	3	11	1.16	3.93	28.76
9.38	1	9	0.95	7.41	23.53

$\frac{Sh'\left(\frac{x}{dh}=7.41\right)}{Sh''_\infty}=0.81$

t = 10 min Θ = 21.7°C c/t = 0.0713 cm/sec

X(cm)	N	n	K'(cm/sec)	X/dh	S'hx
0.25	15	29	2.07	0.20	51.54
0.66	13	27	0.92	0.52	47.81
1.00	11	25	1.78	0.79	44.32
1.37	9	23	1.64	1.08	40.84
1.95	7	21	1.50	1.54	37.35
2.91	5	19	1.36	2.29	33.86
4.57	3	17	1.22	3.60	30.38
7.80	1	15	1.08	6.14	26.89

$\frac{Sh'\left(\frac{x}{dh}=6.14\right)}{Sh''_\infty}=1.10$

$Sh''_\infty = 1.2\ Sh_\infty$

$Sh_\infty = 0.023\ Re^{0.8}\ Sc^{0.33}$

APPENDIX E (Contd.)

Duct 2:1, dh = 1.27 cm

Abrupt Entrance, Symmetric Transfer

Run 4: Re = 2360

t = 6 min Θ = 22.5°C c/t = 0.1116 cm/sec

X(cm)	N	n	K(cm/sec)	X/dh	Sh'x
0.21	9	17	1.90	0.17	47.24
0.66	7	15	1.67	0.52	41.68
1.58	5	13	1.45	1.24	36.12
4.15	3	11	1.23	3.27	30.57
10.38	1	9	1.00	8.17	25.09

$\frac{Sh'\left(\frac{x}{dh}=8.17\right)}{Sh''_\infty}=1.26$

t = 8 min Θ = 22.5°C c/t = 0.0837 cm/sec

X(cm)	N	n	K(cm/sec)	X/dh	Sh'x
0.21	11	23	1.93	0.17	47.93
0.58	9	21	1.76	0.46	43.77
1.16	7	19	1.59	0.91	39.60
1.99	5	17	1.42	1.57	35.43
4.15	3	15	1.26	3.27	31.26
8.72	1	11	0.92	6.87	22.93

$\frac{Sh'\left(\frac{x}{dh}=6.87\right)}{Sh''_\infty}=1.16$

t = 10 min Θ = 22.5°C c/t = 0.0669 cm/sec

X(cm)	N	n	K(cm/sec)	X/dh	Sh'x
0.17	13	29	1.93	0.13	48.14
0.42	11	27	1.80	0.33	44.82
1.00	9	25	1.67	0.79	41.58
1.41	7	23	1.54	1.11	38.35
2.49	5	21	1.40	1.96	34.86
5.06	3	19	1.27	3.98	31.62
9.96	1	17	1.13	7.84	28.17

$\frac{Sh'\left(\frac{x}{dh}=7.84\right)}{Sh''_\infty}=1.42$

$Sh''_\infty = 1.2\ Sh_\infty$

$Sh_\infty = 0.023\ Re^{0.8}\ Sc^{0.33}$

APPENDIX E (Contd.)

Duct 2:1, dh = 1.27 cm

Abrupt Entrance, Symmetric Transfer

Run 5: Re = 707

t = 8 min $\Theta = 22.7^{o}C$ c/t = 0.0825

X(cm)	N	n	K'(cm/sec)	X/dh	Sh'x
0.42	7	13	1.07	0.33	26.71
1.00	5	11	0.91	0.74	22.60
2.82	3	9	0.74	2.22	18.49
8.72	1	7	0.58	6.87	14.38

t = 9 min $\Theta = 23^{o}C$ c/t = 0.0717

X(cm)	N	n	K'(cm/sec)	X/dh	Sh'x
0.42	7	15	1.08	0.33	26.78
1.04	5	13	0.93	0.82	23.21
2.91	3	11	0.79	2.29	19.62
8.72	1	9	0.65	6.87	16.07

t = 10 min $\Theta = 23^{o}C$ c/t = 0.0645

X(cm)	N	n	K'(cm/sec)	X/dh	Sh'x
0.33	7	17	1.10	0.26	27.30
0.66	5	15	0.97	0.52	24.09
2.32	3	13	0.84	1.83	20.88
9.13	1	11	0.71	7.19	17.67

APPENDIX E (Contd.)

Duct 3:1, dh = 1.43 cm

Abrupt Entrance, Asymmetric Transfer

Run 1: Re = 5710

t = 6 min Θ = 22.5°C c/t = 0.109 cm/sec

X(cm)	N	n	K(cm/sec)	X/dh	S'hx
0.21	11	29	3.17	0.15	88.76
0.42	9	27	2.95	0.29	82.64
0.91	7	25	2.73	0.64	76.52
1.91	5	23	2.51	1.34	70.40
3.24	3	21	2.24	2.27	64.28
5.98	1	19	2.07	4.18	58.16

$\frac{Sh'\left(\frac{x}{dh}=4.18\right)}{Sh_\infty}=1.73$

t = 7 min Θ = 22.5°C c/t = 0.0953 cm/sec

X(cm)	N	n	K(cm/sec)	X/dh	S'hx
0.08	17	37	3.46	0.06	97.07
0.21	15	35	3.27	0.15	91.83
0.29	13	33	3.09	0.20	86.58
0.46	11	31	2.90	0.32	81.33
0.79	9	29	2.71	0.53	76.08
1.37	7	27	2.53	0.96	70.84
2.41	5	25	2.34	1.69	65.59
3.98	3	23	2.15	2.78	60.34
8.13	1	21	1.96	5.69	55.10

$\frac{Sh'\left(\frac{x}{dh}=5.69\right)}{Sh_\infty}=1.64$

APPENDIX E (Contd.)

Duct 3:1, dh = 1.43 cm

Abrupt Entrance, Asymmetric Transfer

t = 8 min Θ = 22.8°C c/t = 0.0815 cm/sec

X(cm)	N	n	K(cm/sec)	X/dh	Shx
0.21	17	39	3.18	0.15	89.17
0.46	15	37	3.02	0.32	84.68
0.71	13	35	2.85	0.50	79.91
1.04	11	33	2.69	0.73	75.43
1.54	9	31	2.53	1.08	70.94
2.66	7	29	2.36	1.86	66.18
3.90	5	27	2.20	2.73	61.69
6.06	3	25	2.04	4.24	57.20
10.79	1	23	1.87	7.55	52.44

$Sh' \left(\frac{x}{dh} = 7.55\right) / Sh_\infty = 1.56$

$Sh_\infty = 0.023\ Re^{0.8}\ Sc^{0.33}$

Run 2: Re = 5120

t = 6 min Θ = 22.7°C c/t = 0.1106 cm/sec

X(cm)	N	n	K(cm/sec)	X/dh	Sh'x
0.66	7	23	2.54	0.46	71.33
1.08	5	21	2.32	0.76	65.13
2.16	3	19	2.10	1.51	58.92
6.25	1	17	1.88	4.37	52.72

$Sh' \left(\frac{x}{dh} = 4.37\right) / Sh_\infty = 1.72$

t = 7 min Θ = 22.7°C c/t = 0.0943 cm/sec

X(cm)	N	n	K(cm/sec)	X/dh	Sh'x
0.29	11	27	2.55	0.20	71.39
0.46	9	25	2.36	0.32	66.10
1.00	7	23	2.17	0.70	60.82
1.91	5	21	1.98	1.34	55.53
5.81	3	19	1.79	4.06	50.24
9.71	1	17	1.60	6.79	44.95

$Sh' \left(\frac{x}{dh} = 6.79\right) / Sh_\infty = 1.46$

APPENDIX E (Contd.)

Duct 3:1, dh = 1.43 cm

Abrupt Entrance, Asymmetric Transfer

t = 8 min Θ = 22.7°C c/t = 0.0825 cm/sec

X(cm)	N	n	K(cm/sec)	X/dh	Sh'x
0.27	13	33	2.73	0.19	76.55
0.37	11	31	2.57	0.26	72.06
0.87	9	29	2.40	0.61	67.30
1.49	7	27	2.23	1.04	62.53
2.49	5	25	2.06	1.74	57.76
3.82	3	23	1.90	2.67	53.28
6.10	1	21	1.73	4.27	48.58

$\frac{Sh'\left(\frac{x}{dh}=4.27\right)}{Sh_\infty}=1.58$

Run 3: Re = 4470

t = 6 min Θ = 22.5°C c/t = 0.1110 cm/sec

X(cm)	N	n	K(cm/sec)	X/dh	Sh'x
0.25	11	23	2.54	0.17	70.94
0.50	9	21	2.31	0.35	64.77
1.00	7	19	2.09	0.70	58.60
2.08	5	17	1.87	1.45	52.43
3.90	3	15	1.65	2.73	46.27
9.13	1	13	1.43	6.38	40.10

$\frac{Sh'\left(\frac{x}{dh}=6.38\right)}{Sh_\infty}=1.45$

t = 7 min Θ = 22.6°C c/t = 0.0952 cm/sec

X(cm)	N	n	K(cm/sec)	X/dh	Sh'x
0.25	13	27	2.57	0.17	72.07
0.42	11	25	2.38	0.29	66.75
0.66	9	23	2.19	0.44	61.41
1.33	7	21	2.00	0.93	56.07
2.24	5	19	1.81	1.57	50.73
4.15	3	17	1.62	2.90	45.39
7.47	1	15	1.43	3.13	40.05

$\frac{Sh'\left(\frac{x}{dh}=3.13\right)}{Sh_\infty}=1.46$

APPENDIX E (Contd.)

Duct 3:1, dh = 1.43 cm

Abrupt Entrance, Asymmetric Transfer

t = 8 min Θ = 22.5°C c/t = 0.0833 cm/sec

X(cm)	N	n	K(cm/sec)	X/dh	Sh'x
0.17	15	31	2.59	0.12	77.62
0.33	13	29	2.42	0.23	67.86
0.50	11	27	2.25	0.35	63.09
1.08	9	25	2.08	0.76	53.84
1.74	7	23	1.92	1.22	49.07
2.82	5	21	1.75	1.97	44.30
4.65	3	19	1.58	3.65	39.82
8.63	1	17	1.42	6.03	39.71

$\frac{Sh'\left(\frac{x}{dh} = 6.03\right)}{Sh_\infty} = 1.44$

$Sh_\infty = 0.023\ Re^{0.8}\ Sc^{0.33}$

Run 4: Re = 3700

t = 6 min Θ = 23.5°C c/t = 0.1031 cm/sec

X(cm)	N	n	K(cm/sec)	X/dh	Sh'x
0.21	9	15	1.55	0.15	43.36
0.66	7	13	1.34	0.46	37.58
2.08	5	11	1.13	1.45	31.80
4.57	3	9	0.93	3.20	26.02
11.21	1	7	0.72	7.84	20.24

$\frac{Sh'\left(\frac{x}{dh} = 7.84\right)}{Sh_\infty} = 0.85$

t = 9 min Θ = 23.5°C c/t = 0.0690 cm/sec

X(cm)	N	n	K(cm/sec)	X/dh	Sh'x
0.42	9	19	1.31	0.29	36.76
1.16	7	17	1.17	0.81	32.89
2.24	5	15	1.04	1.57	29.02
3.82	3	13	0.90	2.67	25.15
10.54	1	11	0.76	7.37	21.28

$\frac{Sh'\left(\frac{x}{dh} = 7.37\right)}{Sh_\infty} = 0.90$

APPENDIX E (Contd.)

Duct 3:1, dh = 1.43 cm

Abrupt Entrance, Asymmetric Transfer

t = 10 min Θ = 23.5°C c/t = 0.0621 cm/sec

X(cm)	N	n	K(cm/sec)	X/dh	Sh'x
0.37	13	27	1.68	0.26	50.94
0.58	11	25	1.55	0.41	47.00
1.08	9	23	1.43	0.76	43.36
1.91	7	21	1.30	1.34	39.42
3.15	5	19	1.18	2.21	35.78
5.06	3	17	1.06	3.54	32.14
7.89	1	15	0.93	5.52	26.12

$\frac{Sh'\left(\frac{x}{dh}=5.52\right)}{Sh_\infty}=1.10$

K = C n/t $Sh_\infty = 0.023\ Re^{0.8}\ Sc^{0.33}$

Run 5: Re = 2590

t = 8 min Θ = 23.5°C c/t = 0.0776 cm/sec

X(cm)	N	n	K(cm/sec)	X/dh	Sh'x
0.29	9	17	1.32	0.20	36.99
0.75	7	15	1.16	0.52	32.64
1.91	5	13	1.01	1.34	28.29
4.57	3	11	0.85	3.20	23.93
11.21	1	9	0.70	7.84	19.58

$\frac{Sh'\left(\frac{x}{dh}=7.84\right)}{Sh_\infty}=1.10$

t = 9 min Θ = 23.5°C c/t = 0.0690 cm/sec

X(cm)	N	n	K(cm/sec)	X/dh	Sh'x
0.17	13	21	1.45	0.12	40.63
0.37	11	19	1.31	0.26	36.76
0.75	9	17	1.17	0.52	32.89
1.66	7	15	1.04	1.16	29.02
3.57	5	13	0.90	2.50	25.15
8.30	3	11	0.76	5.80	21.28
11.37	1	9	0.62	7.95	17.41

$\frac{Sh'\left(\frac{x}{dh}=7.95\right)}{Sh_\infty}=0.98$

APPENDIX E (Contd.)

Duct 3:1, dh = 1.43 cm

Abrupt Entrance, Asymmetric Transfer

t = 10 min Θ = 23.5°C c/t = 0.0696 cm/sec

X(cm)	N	n	K(cm/sec)	X/dh	Sh'x
0.17	13	23	1.43	0.12	43.36
0.37	11	21	1.30	0.26	39.42
0.75	9	19	1.16	0.52	35.17
1.66	7	17	1.04	1.16	31.53
3.57	5	15	0.92	2.50	27.89
8.30	3	13	0.79	5.80	23.95
11.37	1	11	0.77	7.95	21.47

$\frac{Sh'\left(\frac{x}{dh} = 7.95\right)}{Sh_\infty} = 1.21$

K = C n/t $Sh_\infty = 0.023\ Re^{0.8}\ Sc^{0.33}$

Run 6: Re = 1760

t = 8 min Θ = 23.7°C c/t = 0.0765 cm/sec

X(cm)	N	n	K(cm/sec)	X/dh	Sh'x
0.66	5	9	0.69	0.46	19.31
1.49	3	7	0.54	1.04	15.02
6.64	1	5	0.38	4.64	10.74

$\frac{Sh'\left(\frac{x}{dh} = 4.64\right)}{Sh_\infty} = 0.82$

t = 9 min Θ = 23.7°C c/t = 0.0680 cm/sec

X(cm)	N	n	K(cm/sec)	X/dh	Sh'x
0.42	9	13	0.88	0.29	24.79
0.83	7	11	0.75	0.58	20.97
2.57	5	9	0.61	1.80	17.16
5.98	3	7	0.48	4.18	13.35
12.28	1	5	0.34	8.59	9.53

$\frac{Sh'\left(\frac{x}{dh} = 8.59\right)}{Sh_\infty} = 0.73$

APPENDIX E (Contd.)

Duct 3:1, dh = 1.43 cm

Abrupt Entrance, Asymmetric Transfer

t = 10 min Θ = 23.7°C c/t = 0.0612 cm/sec

X(cm)	N	n	K(cm/sec)	X/dh	Sh'x
0.33	9	15	0.90	0.23	27.29
0.75	7	13	0.78	0.52	23.65
2.00	5	11	0.66	1.40	20.01
5.15	3	9	0.54	3.60	16.37
12.04	1	7	0.43	8.42	12.01

$\frac{Sh'\left(\frac{x}{dh}=8.42\right)}{Sh_\infty}=0.92$

K = C n/t $Sh_\infty = 0.023\ Re^{0.8}\ Sc^{0.33}$

Run 7: Re = 528

t = 9 min Θ = 24°C c/t = 0.0598 cm/sec

X(cm)	N	n	K'(cm/sec)	X/dh	Sh'x
0.25	5	7	0.45	0.17	12.56
1.41	3	5	0.32	0.99	8.97
8.72	1	3	0.19	6.10	5.38

t = 10 min Θ = 24°C c/t = 0.0598 cm/sec

X(cm)	N	n	K'(cm/sec)	X/dh	Sh'x
0.25	7	9	0.54	0.17	15.09
0.75	5	7	0.42	0.52	11.74
2.91	3	5	0.30	2.03	8.38
9.66	1	3	0.18	6.76	5.03

t = 11 min Θ = 24°C c/t = 0.0543 cm/sec

X(cm)	N	n	K'(cm/sec)	X/dh	Sh'x
0.25	7	9	0.49	0.17	13.70
0.83	5	7	0.38	0.58	10.66
2.49	3	5	0.27	1.74	7.61
8.72	1	3	0.16	6.10	4.57

APPENDIX E (Contd.)

Duct 3:1, dh = 1.43 cm

Abrupt Entrance, Symmetric Transfer

Run 1: Re = 4610

t = 5 min Θ = 20.7°C c/t = 0.1540 cm/sec

X(cm)	N	n	K'(cm/sec)	X/dh	S'hx
0.42	7	19	2.93	0.29	82.05
1.33	5	17	2.62	0.93	73.41
4.98	3	15	2.31	3.48	64.77
9.96	1	13	2.00	6.97	56.14

$\frac{Sh'\left(\frac{x}{dh}=6.97\right)}{Sh''_\infty}=1.66$

t = 6 min Θ = 20.7°C c/t = 0.1253 cm/sec

X(cm)	N	n	K'(cm/sec)	X/dh	Sh'x
0.42	7	23	2.88	0.29	80.81
1.41	5	21	2.63	0.99	73.78
4.57	3	19	2.38	3.20	66.75
10.79	1	17	2.13	7.55	59.73

$\frac{Sh'\left(\frac{x}{dh}=7.55\right)}{Sh''_\infty}=1.76$

t = 7 min Θ = 20.7°C c/t = 0.1074 cm/sec

X(cm)	N	n	K'(cm/sec)	X/dh	Sh'x
0.25	7	27	2.90	0.17	81.31
0.83	5	25	2.69	0.58	75.29
2.08	3	23	2.47	1.45	69.26
4.57	1	21	2.26	3.20	63.24

$\frac{Sh'\left(\frac{x}{dh}=3.20\right)}{Sh''_\infty}=1.87$

t = 8 min Θ = 20.7°C c/t = 0.0940 cm/sec

X(cm)	N	n	K'(cm/sec)	X/dh	Sh'x
0.33	7	31	2.91	0.23	81.60
0.83	5	29	2.73	0.58	76.55
1.49	3	27	2.54	1.04	71.22
3.57	1	25	2.35	2.50	65.89

$\frac{Sh'\left(\frac{x}{dh}=2.50\right)}{Sh''_\infty}=1.95$

$Sh''_\infty = 1.2\ Sh_\infty$

$Sh_\infty = 0.023\ Re^{0.8}\ Sc^{0.33}$

APPENDIX E (Contd.)

Duct 3:1, dh = 1.43 cm

Abrupt Entrance, Symmetric Transfer

Run 2: Re = 4420

t = 6 min Θ = 22.8°C c/t = 0.1092 cm/sec

X(cm)	N	n	K'(cm/sec)	X/dh	Sh'x
0.33	7	25	2.73	0.23	76.55
1.63	5	23	2.51	1.14	70.43
7.06	3	21	2.29	4.94	64.30
12.45	1	19	2.07	8.71	58.18

$\frac{Sh'\left(\frac{x}{dh}=8.71\right)}{Sh''_\infty}=1.78$

t = 7 min Θ = 22.8°C c/t = 0.0936 cm/sec

X(cm)	N	n	K'(cm/sec)	X/dh	Sh'x
0.50	7	29	2.71	0.35	76.11
1.16	5	27	2.53	0.81	70.86
2.66	3	25	2.34	1.86	65.61
8.30	1	23	2.15	5.80	60.36

$\frac{Sh'\left(\frac{x}{dh}=5.80\right)}{Sh''_\infty}=1.84$

t = 8 min Θ = 22.8°C c/t = 0.0819 cm/sec

X(cm)	N	n	K'(cm/sec)	X/dh	Sh'x
0.25	11	35	2.87	0.17	80.38
0.58	9	33	2.70	0.41	75.78
1.25	5	31	2.54	0.87	71.19
2.49	5	29	2.38	1.74	66.60
4.98	3	27	2.21	3.48	62.00
10.79	1	25	2.05	7.55	57.41

$\frac{Sh'\left(\frac{x}{dh}=7.55\right)}{Sh''_\infty}=1.75$

$Sh''_\infty = 1.2\ Sh_\infty$

$Sh_\infty = 0.023\ Re^{0.8}\ Sc^{0.33}$

APPENDIX E (Contd.)

Duct 3:1, dh = 1.43 cm

Abrupt Entrance, Symmetric Transfer

Run 3: Re = 3830

t = 6 min Θ = 23°C c/t = 0.1075 cm/sec

X(cm)	N	n	K'(cm/sec)	X/dh	Sh'x
0.25	13	27	2.90	0.17	81.39
0.50	11	25	2.69	0.35	75.36
1.00	9	23	2.47	0.79	69.33
1.83	7	21	2.26	1.28	63.30
2.99	5	19	2.04	2.09	57.26
5.81	3	17	1.83	4.06	51.24
11.21	1	15	1.61	7.84	45.21

$\frac{Sh'}{Sh''_\infty}\left(\frac{x}{dh} = 7.84\right) = 1.55$

t = 7 min Θ = 23°C c/t = 0.0922 cm/sec

X(cm)	N	n	K'(cm/sec)	X/dh	Sh'x
0.20	11	31	2.86	0.14	80.14
0.42	9	29	2.67	0.29	74.97
0.91	7	27	2.49	0.64	69.80
1.60	5	25	2.31	1.12	64.63
2.82	3	23	2.12	1.97	59.46
6.64	1	21	1.94	4.64	54.29

$\frac{Sh'}{Sh''_\infty}\left(\frac{x}{dh} = 4.64\right) = 1.86$

APPENDIX E (Contd.)

Duct 3:1, dh = 1.43 cm

Abrupt Entrance, Symmetric Transfer

t = 9 min Θ = 23°C c/t = 0.0717 cm/sec

X(cm)	N	n	K'(cm/sec)	X/dh	Sh'x
0.12	17	41	2.94	0.08	82.44
0.25	15	39	2.80	0.17	78.51
0.50	13	37	2.65	0.35	74.31
0.83	11	35	2.51	0.58	70.38
1.33	9	33	2.37	0.93	66.45
2.16	7	31	2.23	1.51	62.53
3.49	5	29	2.08	2.44	58.32
6.06	3	27	1.94	4.24	54.28
11.62	1	25	1.79	8.13	50.26

$Sh'' \infty = 1.2\ Sh\infty$

$Sh\infty = 0.023\ Re^{0.8}\ Sc^{0.33}$

Run 4: Re = 3240

t = 6 min Θ = 22.3°C c/t = 0.1134 cm/sec

X(cm)	N	n	K'(cm/sec)	X/dh	Sh'x
0.25	9	21	2.38	0.17	66.77
0.90	7	19	2.15	0.63	60.41
2.49	5	17	1.93	1.74	54.06
9.55	3	15	1.70	6.68	47.70
13.86	1	13	1.47	9.69	41.34

APPENDIX E (Contd.)

Duct 3:1, dh = 1.43 cm

Abrupt Entrance, Symmetric Transfer

t = 8 min $\Theta = 22.3^{o}C$ c/t = 0.0850 cm/sec

X(cm)	N	n	K'(cm/sec)	X/dh	Sh'x
0.25	11	29	2.47	0.17	69.12
0.50	9	27	2.30	0.35	64.35
1.08	7	25	2.13	0.76	59.59
2.08	5	23	1.96	1.45	54.82
4.98	3	21	1.79	3.48	50.05
12.87	1	19	1.62	9.00	45.28

$\frac{Sh'\left(\frac{x}{dh} = 9.00\right)}{Sh''_{\infty}} = 1.71$

t = 9 min $\Theta = 22.3^{o}C$ c/t = 0.0717 cm/sec

X(cm)	N	n	K'(cm/sec)	X/dh	Sh'x
0.17	13	33	2.49	0.12	69.82
0.50	11	31	2.34	0.35	65.61
1.08	9	29	2.19	0.76	61.41
1.58	7	27	2.04	1.11	57.20
2.74	5	25	1.84	1.92	53.00
4.98	3	21	1.51	3.48	42.22
10.38	1	19	1.36	7.26	38.20

$\frac{Sh'\left(\frac{x}{dh} = 7.26\right)}{Sh''_{\infty}} = 1.49$

$Sh''_{\infty} = 1.2\ Sh_{\infty}$

$Sh_{\infty} = 0.023\ Re^{0.8}\ Sc^{0.33}$

Run 5: Re = 538

t = 9 min $\Theta = 23.5^{o}C$ c/t = 0.0690 cm/sec

X(cm)	N	n	K'(cm/sec)	X/dh	Sh'x
0.58	3	11	0.76	0.41	21.28
3.90	1	9	0.62	2.73	17.41

APPENDIX E (Contd.)

Duct 3:1, dh = 1.43 cm

Abrupt Entrance, Symmetric Transfer

t = 10 min Θ = 23.5°C c/t = 0.0621 cm/sec

X(cm)	N	n	K'(cm/sec)	X/dh	Sh'x
0.83	3	11	0.68	0.58	19.15
0.42	1	9	0.56	0.29	15.67

t = 11 min Θ = 23.5°C c/t = 0.0565 cm/sec

X(cm)	N	n	K'(cm/sec)	X/dh	Sh'x
0.58	5	13	0.78	0.41	21.87
2.57	3	11	0.66	1.80	18.51
8.72	1	9	0.54	6.10	15.14

APPENDIX E (Contd.)

Duct 2:1, dh = 1.27 cm

Calming Section, Asymmetric Transfer

Run 1: Re = 5812

t = 5 min $\Theta = 21.3^{o}C$ c/t = 0.147 cm/sec

X(cm)	N	n	K'(cm/sec)	X/dh	Sh'x	Nudp	Sh'x/Nudp
0.33	9	17	2.50	0.26	62.23	58.29	1.07
1.08	7	15	2.21	0.85	54.90	50.57	1.09
2.75	5	13	1.91	2.17	47.58	45.19	1.05
6.14	3	11	1.62	4.83	40.26	41.05	0.98
12.45	1	9	1.32	9.80	32.94	37.71	0.87

Sh' x/dh = 9.80/Sh∞ = 0.97

t = 6 min $\Theta = 21.3^{o}C$ c/t = 0.1225 cm/sec

X(cm)	N	n	K'(cm/sec)	X/dh	Sh'x	Nudp	Sh'x/Nudp
0.25	11	21	2.57	0.20	64.06	60.16	1.06
0.42	9	19	2.33	0.33	57.95	56.65	1.02
0.66	7	17	2.08	0.52	51.85	53.64	0.97
1.25	5	15	1.84	0.98	45.75	49.71	0.92
2.66	3	13	1.59	2.09	39.65	45.39	0.87
5.50	1	11	1.35	4.33	33.55	41.59	0.81

Sh' x/dh = 4.33/Sh∞ = 0.99

t = 7 min $\Theta = 21.3^{o}C$ c/t = 0.1050 cm/sec

X(cm)	N	n	K'(cm/sec)	X/dh	Sh'x	Nudp	Sh'x/Nudp
0.60	9	23	2.42	0.47	60.13	58.52	1.03
0.91	7	21	2.21	0.72	54.90	51.58	1.06
1.77	5	19	2.00	1.39	49.68	46.12	1.08
3.32	3	17	1.79	2.61	44.45	44.16	1.01
5.81	1	15	1.58	4.57	39.22	41.16	0.95

Sh' x/dh = 4.57/Sh∞ = 1.15

$Sh_{\infty} = 0.023\ Re^{0.8}\ Sc^{0.33}$

APPENDIX E (Contd.)

Duct 2:1, dh = 1.27 cm

Calming Section, Asymmetric Transfer

Run 2: Re = 3770

t = 7 min Θ = 22.3°C c/t = 0.0972 cm/sec

X(cm)	N	n	K'(cm/sec)	X/dh	Sh'x	Nudp	Sh'x/Nudp
0.33	5	19	1.85	0.26	45.99	41.23	1.12
0.83	3	17	1.65	0.65	44.14	36.91	1.20
4.57	1	15	1.46	3.60	36.30	34.49	1.05

Sh' x/dh = 3.60/Sh∞ = 1.51

t = 8 min Θ = 22.3°C c/t = 0.0841 cm/sec

X(cm)	N	n	K'(cm/sec)	X/dh	Sh'x	Nudp	Sh'x/Nudp
0.35	7	21	1.77	0.28	43.98	40.94	1.07
0.66	5	19	1.60	0.52	39.79	37.94	1.05
2.08	3	17	1.43	1.64	35.60	33.06	1.08
6.06	1	15	1.26	4.77	31.41	29.08	1.08

Sh' x/dh = 4.77/Sh∞ = 1.31

t = 10 min Θ = 22.3°C c/t = 0.0707 cm/sec

X(cm)	N	n	K'(cm/sec)	X/dh	Sh'x	Nudp	Sh'x/Nudp
0.17	11	29	2.05	0.13	51.05	44.55	1.15
0.35	9	27	1.91	0.28	47.53	41.04	1.16
0.62	7	25	1.77	0.49	44.01	38.23	1.15
1.15	5	23	1.63	0.91	40.49	35.43	1.14
2.82	3	21	1.48	2.22	36.97	31.92	1.16
7.22	1	19	1.34	5.69	33.45	28.41	1.18

Sh' x/dh = 5.69/Sh∞ = 1.39

Sh∞ 0.023 $Re^{0.8}$ $Sc^{0.33}$

APPENDIX E (Contd.)

Duct 2:1, dh = 1.27 cm

Calming Section, Asymmetric Transfer

Run 3: Re = 2355

t = 7 min $\Theta = 22.7^{o}C$ c/t = 0.0943 cm/sec

X(cm)	N	n	K'(cm/sec)	X/dh	Sh'x	Nudp	Sh'x/Nudp
0.17	7	17	1.60	0.13	39.92	30.64	1.30
0.42	5	15	1.41	0.33	35.22	27.49	1.28
1.41	3	13	1.23	1.11	30.52	23.77	1.28
5.56	1	11	1.04	4.38	25.83	20.16	1.28

Sh' x/dh = 4.38/Sh∞ = 1.56

t = 8 min $\Theta = 22.7^{o}C$ c/t = 0.0825 cm/sec

X(cm)	N	n	K'(cm/sec)	X/dh	Sh'x	Nudp	Sh'x/Nudp
0.12	7	17	1.40	0.09	34.92	31.95	1.09
0.33	5	15	1.24	0.26	30.81	28.30	1.09
1.00	3	13	1.07	0.79	26.71	24.77	1.08
3.74	1	11	0.91	2.94	22.60	21.15	1.07

Sh x/dh = 2.94/Sh∞ = 1.37

t = 10 min $\Theta = 22.7^{o}C$ c/t = 0.0660 cm/sec

X(cm)	N	n	K'(cm/sec)	X/dh	Sh'x	Nudp	Sh'x/Nudp
0.17	9	23	1.52	0.13	37.80	30.57	1.24
0.42	7	21	1.39	0.33	34.51	27.44	1.26
1.30	5	19	1.25	0.57	31.22	25.76	1.21
3.40	3	17	1.12	2.68	27.94	21.43	1.30
10.38	1	15	0.99	8.17	24.65	18.76	1.31

Sh' x/dh = 8.17/Sh∞ = 1.49

$Sh_{\infty} = 0.023\ Re^{0.8}\ Sc^{0.33}$

APPENDIX E (Contd.)

Duct 2:1, dh = 1.27 cm

Calming Section, Asymmetric Transfer

Run 4: Re = 707

t = 8 min $\Theta = 22.5^{o}C$ c/t = 0.0837 cm/sec

X(cm)	N	n	K'(cm/sec)	X/dh	Sh'x
0.33	5	9	0.75	0.26	18.76
1.25	3	7	0.59	0.98	14.59
7.14	1	5	0.42	5.62	10.42

t = 11 min $\Theta = 22.7^{o}C$ c/t = 0.060 cm/sec

X(cm)	N	n	K'(cm/sec)	X/dh	Sh'x
0.30	7	13	0.78	0.24	19.42
0.66	5	11	0.66	0.52	16.44
2.16	3	9	0.54	1.70	13.45
5.98	1	7	0.42	4.71	10.46

t = 12 min $\Theta = 22.7^{o}C$ c/t = 0.0550 cm/sec

X(cm)	N	n	K'(cm/sec)	X/dh	Sh'x
0.17	9	15	0.83	0.13	20.55
0.42	7	13	0.72	0.33	17.81
1.05	5	11	0.61	0.83	15.07
3.32	3	9	0.50	2.61	12.33
10.38	1	7	0.30	8.17	9.59

APPENDIX E (Contd.)

Duct 2:1, dh = 1.27 cm

Calming Section, Symmetric Transfer

Run 1: Re = 4710

t = 3 min $\Theta = 22.5^{o}C$ c/t = 0.223 cm/sec

X(cm)	N	n	K(cm/sec)	X/dh	Sh'x	Nu'dp	S'hx/Nu'dp
0.42	7	9	2.01	0.33	49.97	57.44	0.87
1.25	5	7	1.56	0.98	38.87	50.39	0.77
2.91	3	5	1.12	2.29	27.76	45.53	0.61
4.15	1	3	0.67	3.27	16.66	43.63	0.38

Sh' x/dh = 3.27/Sh''∞ = 0.47

t = 4 min $\Theta = 22.5^{o}C$ c/t = 0.167 cm/sec

X(cm)	N	n	K(cm/sec)	X/dh	Sh'x	Nu'dp	Shx/Nu'dp
0.33	7	13	2.17	0.26	54.06	59.13	0.91
0.58	5	11	1.84	0.46	45.74	53.26	0.83
1.25	3	9	1.50	0.98	37.42	50.30	0.74

Sh' x/dh = 0.98/Sh'∞ = 1.08

t = 5 min $\Theta = 22.5^{o}C$ c/t = 0.1339 cm/sec

X(cm)	N	n	K'(cm/sec)	X/dh	Sh'x	Nu'dp	Sh'x/Nu'dp
0.33	9	17	2.28	0.26	56.08	59.35	0.96
0.42	7	15	2.01	0.33	50.01	57.34	0.87
0.83	5	13	1.74	0.65	43.34	52.81	0.82
1.49	3	11	1.47	1.17	36.68	49.29	0.74
3.90	1	9	1.21	3.07	30.01	43.76	0.69

Sh' x/dh = 3.07/Sh''∞ = 0.87

Nud'p = 1.2 Nudp

$Nudp = Nud\ (Sc/Pr)^{0.33}$

$Nud = 0.03\ Re^{0.8}\ (x/dh)^{-0.12}$

Sh''∞ = 1.2 Sh∞

$Sh\infty = 0.023\ Re^{0.8}\ Sc^{0.33}$

APPENDIX E (Contd.)

Duct 2:1, dh = 1.27 cm

Calming Section, Symmetric Transfer

Run 2: Re = 3960

t = 6 min $\Theta = 20.8^{o}C$ c/t = 0.1273 cm/sec

X(cm)	N	n	K'(cm/sec)	X/dh	Sh'x	Nudp'	Sh'x/N'udp
0.50	9	15	1.91	0.39	47.55	54.82	0.87
0.91	7	13	1.65	0.72	41.21	50.96	0.81
1.95	5	11	1.40	1.54	34.87	46.51	0.75
3.74	3	9	1.15	2.94*	28.53	43.01	0.66
11.62	1	7	0.89	9.15	22.16	37.54	0.59

Sh' x/dh = 9.15/Sh''∞ = 0.74

t = 7 min $\Theta = 20.8^{o}C$ c/t = 0.1091 cm/sec

X(cm)	N	n	K'(cm/sec)	X/dh	Sh'x	N'udp	Sh'x/N'udp
0.33	11	17	1.85	0.26	46.16	57.56	0.80
0.83	9	15	1.64	0.65	40.75	51.53	0.79
1.33	7	13	1.42	1.05	35.32	48.69	0.73
2.20	5	11	1.20	1.73	29.88	45.84	0.65
3.57	3	9	0.98	2.81	24.45	43.25	0.57
7.47	1	7	0.76	5.88	19.02	39.58	0.61

Sh' x/dh = 5.88/Sh''∞ = 0.63

APPENDIX E (Contd.)

Duct 2:1, dh = 1.27 cm

Calming Section, Symmetric Transfer

t = 8 min $\Theta = 20.8^{o}C$ c/t = 0.0955 cm/sec

X(cm)	N	n	K'(cm/sec)	X/dh	Sh'x	Nud'p	Sh'x/N'udp
0.33	13	21	2.01	0.26	49.94	51.66	0.97
0.58	11	19	1.81	0.46	45.18	48.76	0.93
1.00	9	17	1.62	0.79	40.43	45.09	0.90
1.60	7	15	1.43	1.26	35.67	43.33	0.82
2.66	5	13	1.24	2.09	30.91	40.28	0.77
4.57	3	11	1.05	3.60	26.16	37.65	0.69
12.04	1	9	0.86	9.48	21.40	32.27	0.64

Sh'_{∞} x/dh = 9.48/Sh''_{∞} = 0.71

N'udp = 1.2 Nudp

$Nudp = Nud\ (Sc/Pr)^{0.33}$

$Nud = 0.03\ Re^{0.8}\ (x/dh)^{-0.12}$

$Sh''_{\infty} = 1.2\ Sh_{\infty}$

$Sh_{\infty} = 0.023\ Re^{0.8}\ Sc^{0.33}$

Run 3: Re = 1940

t = 6 min $\Theta = 23^{o}C$ c/t = 0.1075 cm/sec

X(cm)	N	n	K'(cm/sec)	X/dh	Sh'x	Nud'p	Sh'x/N'udp
0.33	9	13	1.40	0.26	34.80	29.08	1.20
1.25	7	11	1.18	0.98	29.44	24.79	1.19
2.91	5	9	0.97	2.29	24.09	22.40	1.08
6.33	3	7	0.75	4.98	18.74	20.40	0.92
12.45	1	5	0.54	9.80	13.38	18.81	0.71

Sh' x/dh = 9.80/Sh''_{∞} = 0.79

APPENDIX E (Contd.)

Duct 2:1, dh = 1.27 cm

Calming Section, Symmetric Transfer

t = 7 min $\Theta = 23^{o}C$ c/t = 0.0922 cm/sec

X(cm)	N	n	K'(cm/sec)	X/dh	Sh'x	N'udp	Sh'x/Nu'dp
0.33	7	15	1.38	0.26	34.44	29.07	1.18
1.25	5	13	1.20	0.99	29.85	24.78	1.20
3.32	3	11	1.01	2.62	25.25	22.04	1.15
12.45	1	9	0.83	9.84	20.66	18.80	1.10

Sh' x/dh = 9.48/Sh''$_{\infty}$ = 1.03

t = 8 min $\Theta = 23^{o}C$ c/t = 0.0806 cm/sec

X(cm)	N	n	K'(cm/sec)	X/dh	Sh'x	Nud'p	Sh'x/Nud'p
0.25	11	19	1.53	0.20	38.13	29.69	1.29
0.50	9	17	1.37	0.39	34.12	27.21	1.25
1.05	7	15	1.21	0.83	30.10	25.23	1.19
2.08	5	13	1.05	1.64	26.09	23.25	1.12
4.80	3	11	0.89	3.38	22.08	20.29	1.09
13.28	1	9	0.73	10.46	18.06	18.55	0.97

Sh' x/dh = 10.46/Sh''$_{\infty}$ = 1.06

N'udp = 1.2 Nudp

$Nudp = Nud\ (Sc/Pr)^{0.33}$

$Nud = 0.03\ Re^{0.8}\ (x/dh)^{-0.12}$

Sh''$_{\infty}$ = 1.2 Sh$_{\infty}$

$Sh_{\infty} = 0.023\ Re^{0.8}\ Sc^{0.33}$

APPENDIX E (Contd.)

Duct 2:1, dh = 1.27 cm

Calming Section, Symmetric Transfer

Run 4: Re = 706

t = 8 min $\Theta = 22.7^{o}C$ c/t = 0.0825

X(cm)	N	n	K'(cm/sec)	X/dh	Sh'x
0.42	5	9	0.74	0.33	18.49
1.25	3	7	0.58	0.98	14.38
6.39	1	5	0.41	5.03	10.27

t = 9 min $\Theta = 22.7^{o}C$ c/t = 0.0733

X(cm)	N	n	K'(cm/sec)	X/dh	Sh'x
0.42	7	11	0.81	0.33	20.08
1.17	5	9	0.66	0.92	16.43
3.24	3	7	0.51	2.55	12.78
9.96	1	5	0.37	7.84	9.13

t = 10 min $\Theta = 22.7^{o}C$ c/t = 0.0660

X(cm)	N	n	K'(cm/sec)	X/dh	Sh'x
0.33	9	13	0.86	0.26	21.41
0.58	7	11	0.73	0.46	18.21
1.63	5	9	0.60	1.28	14.83
3.98	3	7	0.46	3.13	11.53
10.96	1	5	0.33	8.63	8.24

APPENDIX E (Contd.)

Duct 3:1, dh = 1.43 cm

Calming Section, Asymmetric Transfer

Run 1: Re = 4706

t = 3 min $\Theta = 24^{o}C$ c/t = 0.1993

X(cm)	N	n	K(cm/sec)	X/dh	Sh'x	Nudp	Sh'x/Nudp
0.21	7	11	2.19	0.15	61.47	52.59	1.17
0.66	5	9	1.79	0.46	50.30	45.98	1.09
2.24	3	7	1.40	1.57	39.12	39.68	0.99
3.32	1	5	1.00	1.62	27.94	39.53	0.71

Sh' x/dh = 1.62/Sh∞ = 0.97

t = 5 min $\Theta = 24^{o}C$ c/t = 0.1196

X(cm)	N	n	K(cm/sec)	X/dh	Sh'x	Nudp	Sh'x/Nudp
0.17	9	19	2.27	0.12	63.72	54.02	1.18
0.50	7	17	2.03	0.35	57.01	47.51	1.20
1.66	5	15	1.79	1.16	50.30	41.15	1.22
3.32	3	13	1.55	2.32	43.60	37.86	1.15
9.96	1	11	1.32	6.97	36.89	33.18	1.11

Sh' x/dh = 6.97/Sh∞ = 1.28

t = 6 min $\Theta = 24^{o}C$ c/t = 0.0997

X(cm)	N	n	K(cm/sec)	X/dh	Sh'x	Nudp	Sh'x/Nudp
0.33	9	21	2.10	0.23	58.88	49.85	1.18
0.58	7	19	1.90	0.41	53.28	46.50	1.15
1.25	5	17	1.70	0.87	47.57	42.72	1.07
2.66	3	15	1.50	1.86	42.06	38.96	1.08
4.57	1	13	1.30	3.20	36.45	36.45	1.00

Sh' x/dh = 3.20/Sh∞ = 1.26

$Nudp = \dot{N}ud\ (Sc/Pr)^{0.33}$

$Nud = 0.03\ Re^{0.8}\ (X/dh)^{-0.12}$

$Sh\infty = 0.023\ Re^{0.8}\ Sc^{0.33}$

APPENDIX E (Contd.)

Duct 3:1, dh = 1.43 cm

Calming Section, Asymmetric Transfer

Run 2: Re = 3540

t = 7 min $\Theta = 22.4^{o}C$ c/t = 0.0965

X(cm)	N	n	K(cm/sec)	X/dh	Sh'x	Nudp	Shx/Nudp
0.42	7	15	1.45	0.29	40.66	38.70	1.05
1.33	5	13	1.25	0.93	35.18	33.65	1.05
4.57	3	11	1.06	3.20	29.76	29.01	1.03
13.70	1	9	0.87	9.32	24.43	25.52	0.96

Sh' x/dh = 9.32/Sh∞ = 1.07

t = 9 min $\Theta = 22.4^{o}C$ c/t = 0.0750

X(cm)	N	n	K(cm/sec)	X/dh	Sh'x	Nudp	Shx/Nudp
0.21	9	21	1.58	0.15	44.16	41.88	1.05
0.50	7	19	1.43	0.35	39.96	37.83	1.06
0.91	5	17	1.28	0.64	35.75	35.19	1.02
2.49	3	15	1.13	1.74	31.55	31.21	1.01
11.21	1	13	0.98	7.84	27.34	26.05	1.05

Sh' x/dh = 7.84/Sh∞ = 1.20

APPENDIX E (Contd.)

Duct 3:1, dh = 1.43 cm

Calming Section, Asymmetric Transfer

t = 10 min $\Theta = 22.4^{o}C$ c/t = 0.0676

X(cm)	N	n	K(cm/sec)	X/dh	Sh'x	Nudp	Sh'x/Nudp
0.08	13	25	1.69	0.06	47.39	46.75	1.01
0.25	11	23	1.55	0.17	43.46	41.26	1.05
0.50	9	21	1.42	0.35	39.82	37.84	1.05
1.08	7	19	1.28	0.76	35.89	34.47	1.04
2.32	5	17	1.15	1.62	32.35	31.48	1.03
6.23	3	15	1.01	4.36	28.32	27.95	1.01
9.13	1	13	0.88	6.38	24.64	26.70	0.92

Sh' x/dh = 6.38/Sh∞ = 1.08

$Nudp = Nud\ (Sc/Pr)^{0.33}$

$Nud = 0.03\ Re^{0.8}\ (X/dh)^{-0.12}$

$Sh\infty = 0.023\ Re^{0.8}\ Sc^{0.33}$

Run 3: Re = 2650

t = 6 min $\Theta = 22.4^{o}C$ c/t = 0.1093

X(cm)	N	n	K(cm/sec)	X/dh	Sh'x	Nudp	Sh'x/Nudp
0.12	9	13	1.42	0.08	39.84	35.82	1.11
0.50	7	11	1.20	0.35	33.71	30.01	1.12
1.08	5	9	0.98	0.76	27.58	27.34	1.01
3.32	3	7	0.77	2.32	21.45	23.92	0.90
12.45	1	5	0.55	8.71	15.32	20.41	0.75

Sh' x/dh = 8.71/Sh∞ = 0.84

APPENDIX E (Contd.)

Duct 3:1, dh = 1.43 cm

Calming Section, Asymmetric Transfer

t = 8 min $\Theta = 22.5^{o}C$ c/t = 0.0837

X(cm)	N	n	K(cm/sec)	X/dh	Sh'x	Nudp	Sh'x/Nudp
0.25	9	15	1.26	0.17	35.20	32.73	1.08
0.65	7	13	1.09	0.45	30.51	29.44	1.04
1.66	5	11	0.92	1.16	25.82	25.99	0.99
5.40	3	9	0.75	3.78	21.12	22.56	0.94
13.20	1	7	0.59	9.23	16.43	20.26	0.81

Sh' x/dh = 9.23/Sh∞ =

t = 9 min $\Theta = 22.5^{o}C$ c/t = 0.0744

X(cm)	N	n	K(cm/sec)	X/dh	Sh'x	Nudp	Sh'x/Nudp
0.25	11	17	1.27	0.17	35.61	32.81	1.09
0.54	9	15	1.12	0.38	31.41	29.63	1.06
1.16	7	13	0.97	0.81	27.20	27.25	1.00
2.75	5	11	0.82	1.92	22.98	24.34	0.99
8.72	3	9	0.67	6.18	18.79	21.17	0.88
11.62	1	7	0.52	8.13	14.60	20.58	0.71

Sh' x/dh = 8.71/Sh∞ = 0.80

$Nudp = Nud\ (Sc/Pr)^{0.33}$

$Nud = 0.03\ Re^{0.8}\ (X/dh)^{-0.12}$

$Sh\infty = 0.023\ Re^{0.8}\ Sc^{0.33}$

APPENDIX E (Contd.)

Duct 3:1, dh = 1.43 cm

Calming Section, Asymmetric Transfer

Run 4: Re = 528

t = 9 min $\Theta = 24^{o}C$ c/t = 0.0664 cm/sec

X(cm)	N	n	K'(cm/sec)	X/dh	Sh'x
0.33	5	9	0.60	6.29	16.76
1.00	3	7	0.46	4.90	13.03
9.96	1	5	0.33	3.50	9.31

t = 10 min $\Theta = 24^{o}C$ c/t = 0.0598 cm/sec

X(cm)	N	n	K'(cm/sec)	X/dh	Sh'x
0.42	7	11	0.66	0.29	18.44
1.16	5	9	0.54	0.81	15.09
4.07	3	7	0.42	2.85	11.74
11.62	1	5	0.30	8.13	8.30

t = 11 min $\Theta = 24^{o}C$ c/t = 0.0543 cm/sec

X(cm)	N	n	K'(cm/sec)	X/dh	Sh'x
0.25	7	11	0.58	0.17	16.26
0.66	5	9	0.48	0.46	13.46
2.41	3	7	0.37	1.69	10.37
11.62	1	5	0.27	3.50	7.57

APPENDIX E (Contd.)

Duct 3:1, dh = 1.43 cm

Calming Section, Symmetric Transfer

Run 1: Re = 4410

t = 6 min $\Theta = 23.5^{o}C$ c/t = 0.1035 cm/sec

X(cm)	N	n	K'(cm/sec)	X/dh	Sh'x	N'udp	Sh'x/Nu'dp
0.17	9	23	2.38	0.12	66.75	61.61	1.08
0.42	7	21	2.17	0.29	60.94	55.28	1.10
1.16	5	19	1.97	0.81	55.14	48.93	1.13
3.82	3	17	1.76	2.67	49.34	42.41	1.16
9.55	1	15	1.55	6.68	45.43	37.99	1.20

Sh' x/dh = 6.68/Sh''∞ = 1.39

t = 7 min $\Theta = 23.5^{o}C$ c/t = 0.0887 cm/sec

X(cm)	N	n	K'(cm/sec)	X/dh	Sh'x	N'udp	Sh'x/Nu'dp
0.17	9	27	2.39	0.12	67.14	61.61	1.09
0.42	7	25	2.22	0.29	62.18	55.28	1.12
0.91	5	23	2.04	0.64	57.20	50.38	1.14
2.16	3	21	1.86	1.51	52.23	45.41	1.15
8.30	1	19	1.69	5.80	47.26	38.64	1.22

Sh' x/dh = 5.80/Sh''∞ = 1.44

t = 10 min $\Theta = 23.5^{o}C$ c/t = 0.0621

X(cm)	N	n	K'(cm/sec)	X/dh	Sh'x	N'udp	Sh'x/Nu'dp
0.25	11	37	2.30	0.18	64.49	58.69	1.10
0.42	9	35	2.17	0.29	60.85	55.35	1.10
0.66	7	33	2.05	0.46	57.48	52.49	1.10
1.91	5	31	1.93	1.34	54.12	46.29	1.17
4.15	3	29	1.80	2.90	50.47	41.99	1.20
10.79	1	27	1.68	7.55	47.11	37.22	1.27

Sh' x/dh = 7.55/Sh''∞ = 1.44

APPENDIX E (Contd.)

Duct 3:1, dh = 1.43 cm

Calming Section, Symmetric Transfer

$N'udp = 1.2\ Nudp$

$Nudp = Nud(Sc/Pr)^{0.33}$

$Nud = 0.03\ Re^{0.8}\ (X/dh)^{-0.12}$

$Sh''\infty = 1.2\ Sh\infty$

$Sh\infty = 0.023\ Re^{0.8}\ Sc^{0.33}$

Run 2: Re = 3730

t = 5 min $\Theta = 22.5^{o}C$ c/t = 0.1339

X(cm)	N	n	K'(cm/sec)	X/dh	Sh'x	Nu'dp	Sh'x/Nud'p
0.50	7	15	2.01	0.35	56.32	47.34	1.19
2.16	5	13	1.74	1.51	48.81	39.72	1.23
5.15	3	11	1.47	3.60	41.30	35.79	1.15
9.96	1	9	1.21	6.97	33.79	33.06	1.02

Sh' x/dh = 6.97/Sh'∞ = 1.18

t = 7 min $\Theta = 22.5^{o}C$ c/t = 0.0956 cm/sec

X(cm)	N	n	K'(cm/sec)	X/dh	Sh'x	Nu'dp	Sh'x/Nud'p
0.17	7	23	2.20	0.12	61.65	53.85	1.14
0.42	5	21	2.01	0.29	56.29	48.34	1.16
1.25	3	19	1.82	0.87	50.93	42.41	1.20
4.15	1	17	1.63	2.90	45.57	36.73	1.24

Sh x/dh = 2.90/Sh'∞ = 1.59

APPENDIX E (Contd.)

Duct 3:1, dh = 1.43 cm

Calming Section, Symmetric Transfer

t = 10 min Θ = 22.7°C c/t = 0.066 cm/sec

X(cm)	N	n	K'(cm/sec)	X/dh	Sh'x	N'udp	Sh'x/N'udp
0.08	11	35	2.31	0.06	64.77	58.43	1.11
0.25	9	33	2.18	0.18	61.13	51.33	1.19
0.50	7	31	2.05	0.35	57.48	47.16	1.22
1.00	5	29	1.91	0.70	53.56	43.40	1.23
2.16	3	27	1.78	1.51	49.91	39.65	1.26
6.13	1	25	1.65	4.36	42.26	35.06	1.21

Sh x/dh = 4.36/Sh'$_\infty$ = 1.48

N'udp = 1.2 Nudp

Nudp = Nud(Sc/Pr)$^{0.33}$

Nud = 0.03 Re$^{0.8}$ (x/dh)$^{-0.12}$

Sh'$_\infty$ = 1.2 Sh$_\infty$

Sh$_\infty$ = 0.023 Re$^{0.8}$ Sc$^{0.33}$

Run 3: Re = 3240

t = 5 min Θ = 22.7°C c/t = 0.0734 cm/sec

X(cm)	N	n	K'(cm/sec)	X/dh	Sh'x	N'udp	Sh'x/Nu'dp
0.33	5	15	1.98	0.23	55.52	44.46	1.25
0.83	3	13	1.72	0.58	48.11	39.81	1.21
3.74	1	11	1.45	2.62	40.71	33.22	1.23

Sh' x/dh = 2.62/Sh''$_\infty$ = 1.59

APPENDIX E (Contd.)

Duct 3:1, dh = 1.43 cm

Calming Section, Symmetric Transfer

t = 9 min $\Theta = 22.7^{o}C$ c/t = 0.0734 cm/sec

X(cm)	N	n	K'(cm/sec)	X/dh	Sh'x	Nu'dp	Sh'x/Nu'dp
0.21	9	27	1.98	0.15	55.57	46.94	1.18
0.54	7	25	1.84	0.38	51.45	41.91	1.23
1.16	5	23	1.69	0.81	47.32	38.24	1.24
2.49	3	21	1.54	1.74	43.22	34.89	1.24
6.31	1	19	1.39	4.41	39.10	31.20	1.25

Sh' x/dh = 4.41/Sh''∞ = 1.53

t = 10 min $\Theta = 22.7^{o}C$ c/t = 0.0660 cm/sec

X(cm)	N	n	K'(cm/sec)	X/dh	Sh'x	Nu'dp	Sh'x/Nu'dp
0.17	11	31	2.05	0.12	57.48	48.10	1.20
0.33	9	29	1.91	0.23	53.56	44.37	1.21
0.75	7	27	1.78	0.53	49.91	40.27	1.24
1.41	5	25	1.65	0.99	46.27	37.29	1.24
3.57	3	23	1.52	2.50	42.62	33.56	1.27
9.96	1	21	1.39	6.97	38.97	29.53	1.32

Sh' x/dh = 6.97/Sh''∞ = 1.52

Nu'dp = 1.2 Nudp

$Nudp = Nud\ (Sc/Pr)^{0.33}$

$Nud = 0.03\ Re^{0.8}\ (X/dh)^{-0.12}$

Sh''∞ = 1.2 Sh∞

$Sh\infty = 0.023\ Re^{0.8}\ Sc^{0.33}$

APPENDIX E (Contd.)

Duct 3:1, dh = 1.43 cm

Calming Section, Symmetric Transfer

Run 4: Re = 2360

t = 7 min $\Theta = 21.5^{o}C$ c/t = 0.1034 cm/sec

X(cm)	N	n	K'(cm/sec)	X/dh	Sh'x	Nu'dp	Sh'x/Nu'dp
0.42	3	9	0.93	0.29	26.08	33.52	0.78
2.91	1	7	0.72	2.03	20.30	26.57	0.76

Sh' x/dh =

t = 8 min $\Theta = 21.5^{o}C$ c/t = 0.0905 cm/sec

X(cm)	N	n	K'(cm/sec)	X/dh	Sh'x	Nu'dp	Sh'x/Nu'dp
0.25	5	11	1.00	0.17	27.91	35.67	0.78
1.00	3	9	0.87	0.70	22.84	30.21	0.76
4.57	1	7					

Sh x/dh =

t = 9 min $\Theta = 21.5^{o}C$ c/t = 0.0804 cm/sec

X(cm)	N	n	K'(cm/sec)	X/dh	Sh'x	Nu'dp	Sh'x/Nu'dp
0.17	7	13	1.05	0.12	29.45	31.11	0.95
0.58	5	11	0.89	0.41	24.68	26.77	0.92
2.49	3	9	0.72	1.74	20.18	22.67	0.89
9.96	1	7	0.56	6.97	15.70	17.85	0.88

Sh' x/dh = 6.97/Sh''$_{\infty}$ = 0.79

N'udp = 1.2 Nudp

$Nudp = Nud\ (Sc/Pr)^{0.33}$

$Nud = 0.03\ Re^{0.8}\ (X/dh)^{-0.12}$

$Sh''_{\infty} = 1.2\ Sh_{\infty}$

$Sh_{\infty} = 0.023\ Re^{0.8}\ Sc^{0.33}$

APPENDIX E (Contd.)

Duct 3:1, dh = 1.43 cm

Calming Section, Symmetric Transfer

Run 5: Re = 528

t = 9 min $\Theta = 24.3^{o}C$ c/t = 0.065 cm/sec

X(cm)	N	n	K'(cm/sec)	X/dh	Sh'x
0.42	5	5	0.33	0.29	9.11
1.25	3	3	0.20	0.87	5.47
4.15	1	1	0.07	2.90	1.82

t = 10 min $\Theta = 24.3^{o}C$ c/t = 0.058 cm/sec

X(cm)	N	n	K'(cm/sec)	X/dh
0.25	5	5	0.29	0.17
1.25	3	3	0.17	0.87
4.57	1	1	0.06	3.20

t = 12 min $\Theta = 24.3^{o}C$ c/t = 0.049 cm/sec

X(cm)	N	n	K'(cm/sec)	X/dh	Sh'x
0.66	5	5	0.24	0.46	6.83
2.49	3	3	0.15	1.74	4.10
11.21	1	1	0.05	7.84	1.37

APPENDIX F

Calculation of Correction Factor F in the equation Shx = F Sh'x

Considering Figure F1:

$$Qdc = P\,\dot{m}\,dx \text{ (mass balance)} \tag{F1}$$

where: Q = Volume flow rate, C = Concentration, $\dot{m}$ = mass flux, dx = differential length of channel and P = perimeter of the duct.

$$\dot{m} = K(C_s - C) \tag{F2}$$

K being the mass transfer coefficient on the assumption that the concentration C of the swelling agent in the air is negligible.

$$\dot{m} = K' C_s \tag{F3}$$

then:

$$Qdc = P\,dx\,K'\,C_s \tag{F4}$$

From (F2) and (F3), we have:

$$K = \frac{K'C_s}{C_s - C} \tag{F5}$$

Now, from (F4):

$$\Delta C_{12} = \int_1^2 dc = \frac{PC_s}{Q} \int_1^2 K'\,dx \tag{F6}$$

Since:

$$C_s - C/x = 2 = C_s - \int_0^2 dc \simeq C_s - \int_1^2 dc \tag{F7}$$

(because x_1 can be taken as close as we wish to x = 0), we have from (F6) and (F7) that:

$$C_s - \int_1^2 dc = C_s - \frac{PC_s}{Q} \int_1^2 K'\,dx \tag{F8}$$

or

$$C_s - C = C_s \left(1 - \frac{P}{Q} A_2\right) \tag{F9}$$

Fig. F1 : True and Apparent Mass Transfer Coefficient K and K^{I} in a Rectangular Duct with Streamwise Concentration Variation.

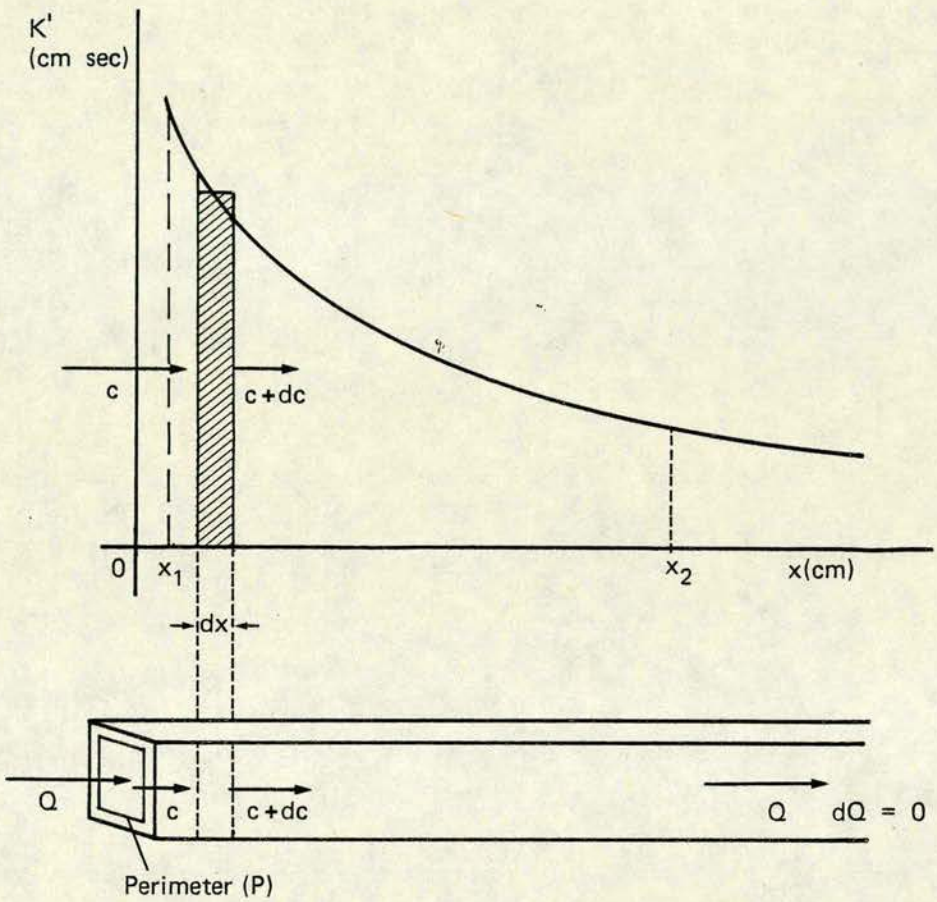

Since $\int_1^2 K'\,dx$ is the area under the curve K' vs x from x_1 to x_2 (again taking x_1 sufficiently close to x = 0 so that $C_1 \simeq 0$).

Substituting e.q. (F9) into e.q. (F5), we get:

$$K = K'/(1 - \frac{PA_2}{Q}) \tag{F10}$$

For the Sherwood Number we have:

$$Shx = \frac{Kdh}{D} \tag{F11}$$

From (F10) we get for the Sherwood number:

$$Shx = \frac{K'dh}{D}/(1 - \frac{PA_2}{Q}) \tag{F12}$$

The area under the curve Sh'x vs x/dh is given by $A^o = \int \frac{k'dh}{D}\, d\,(\frac{d}{dh})$

or $A^o = \int \frac{K'dx}{D}$ but we know that:

$$\int K'dx = A_2 \;\therefore\; A^o = A_2/D \tag{F13}$$

Substituting A_2 in (F12) we have:

$$Shx = \frac{K'dh}{D}/(1 - \frac{PA^oD}{Q}) \tag{F14}$$

The Reynolds number is given by: $Re = \frac{dhU}{\nu}$ and dh = 4(Flow Area)/P, so that: $Re = \frac{4\,(\text{Flow Area})u}{P\nu}$, but (Flow Area) (Velocity) = Q

therefore $Re = 4Q/P\nu$ and from here:

$$Q = \frac{Re\ P\nu}{4} \tag{F15}$$

Substituting (F15) into (F14)

$$Shx = \frac{K'dh}{D}/(1 - \frac{PA^oD}{RePv/4}) \tag{F16}$$

Noticing that Sh'x = K'dh/D and that the Schmidt number, Sc = ν/D, we finally have:

$$Shx = Sh'x/(1 - \frac{4A^o}{ReSc}) \qquad (F17)$$

Calling: $(1 - \frac{4A^o}{ReSc}) = F$, the final equation is:

$$Shx = F\ Sh'x \qquad (F18)$$

This equation gives the corrected Sherwood number (Shx) as a function of the factor (F) and the uncorrected Sherwood number (Sh'x).

APPENDIX G

Corrected Data for Sherwood Number (Shx) and Mass Transfer Coefficient (K)

Duct 2:1, dh = 1.27 cm

Abrupt Entrance, Asymmetric Transfer

Corrected Data

Run 1: Re = 5815 $\Theta = 22^{o}C$ t = 8 min

X/dh	Sh'x	Area		Shx	Shx/dh = 6.87/Sh∞
0.20	78.40			78.40	1.57
0.33	74.15			74.15	
0.72	69.93			69.93	
1.24	65.69			65.69	
1.70	61.45			61.45	
2.29	57.21	161.17	1.04	59.50	
3.40	52.97	214.98	1.05	55.62	
6.87	48.74	365.65	1.09	53.13	

Run 2: Re = 5103 $\Theta = 22.7^{o}C$ t = 9 min

X/dh	Sh'x	Area	F	Shx	Shx/dh = 4.57/Sh∞
0.33	63.99			63.99	1.46
0.52	60.26			60.26	
0.91	56.52			56.52	
1.57	53.08			53.08	
2.22	49.30			49.30	
3.01	45.57	156.93	1.04	47.39	
4.57	42.08	221	1.06	44.60	

APPENDIX G (Contd.)

Duct 2:1, dh = 1.27 cm

Abrupt Entrance, Asymmetric Transfer

Run 3: Re = 3380 $\Theta = 22.5^{o}C$ t = 9 min

X/dh	Sh'x	Area	F	Shx	Shx/dh = 7.65/Sh∞
0.13	57.52			57.52	1.60
0.26	53.78			53.78	
0.46	50.05			50.05	
0.82	46.31			46.31	
1.37	42.58			42.50	
2.22	38.84	111.36	1.05	40.78	
4.12	35.11	164.83	1.07	37.57	
7.65	31.37	279.97	1.12	35.13	

Run 4: Re = 2120 $\Theta = 22.7^{o}C$ t = 10 min

X/dh	Sh'x	Area	F	Shx	Shx/dh = 7.84/Sh∞
0.17	41.09			41.09	1.91
0.33	37.85			37.85	
0.75	34.61			34.61	
1.64	31.37			31.37	
3.79	28.14	125.07	1.09	30.67	
7.84	24.65	227.97	1.17	28.84	

APPENDIX G (Contd.)

Duct 2:1, dh = 1.27 cm

Abrupt Entrance, Asymmetric Transfer

Run 5: Re = 704 $\Theta = 24^{o}C$ t = 12 min

X/dh	Sh'x	Area	F	Shx
0.13	33.37			33.37
0.52	31.13	15.80	1.03	32.06
1.64	28.64	46.25	1.10	31.40
3.92	26.15	114.05	1.28	33.47

Area = area under the curve at specified x/dh

$Shx = Sh'x\ F$

$F = 1/(1 - \frac{4A}{ReSc})$

$Sh_{\infty} = 0.023^{0.8}\ Sc^{0.33}$

APPENDIX G (Contd.)

Duct 2:1, dh = 1.27 cm

Abrupt Entrance, Symmetric Transfer

Run 1: Re = 6625 Θ = 23.7°C t = 10 min

X/dh	Sh'x	Area	F	Shx	Shx/dh = 4.15/Sh∞
0.33	80.77			80.77	1.32
0.43	77.72			77.72	
0.65	74.67			74.67	
0.91	71.62			71.62	
1.17	68.57	73.63	1.02	69.94	
1.57	65.53	107.01	1.02	66.98	
2.44	62.48	169.74	1.04	64.98	
3.78	59.43	228.86	1.05	62.40	
5.83	56.38	340.71	1.07	60.33	
9.15	53.23	528.64	1.12	59.62	

Run 2: Re = 5480 Θ = 23.7°C t = 10 min

X/dh	Sh'x	Area	F	Shx	Shx/dh = 8.17/Sh∞
0.13	77.72			77.72	1.45
0.33	74.67			74.67	
0.52	71.62			71.62	
0.72	68.57			68.57	
0.99	65.53			65.53	
1.25	62.48	76.95	1.02	63.73	
1.75	59.43	79.65	1.02	60.62	
2.61	56.38	160.23	1.04	58.64	
4.06	53.34	241.79	1.06	56.54	
8.17	50.29	445.51	1.12	56.32	

APPENDIX G (Contd.)

Duct 2:1, dh = 1.27 cm

Abrupt Entrance, Symmetric Transfer

Run 3: Re = 3840 $\Theta = 21.7^{o}C$ t = 10 min

X/dh	Sh'x	Area	F	Shx	Shx/dh = 6.14/Sh'∞
0.20	51.54			51.54	0.99
0.52	47.81			47.81	
0.79	44.32			44.32	
1.08	40.84			40.84	
1.54	37.35			37.35	
2.29	33.86	81.68	1.03	34.88	
3.60	30.38	129.43	1.05	31.98	
6.14	26.89	199.88	1.07	28.77	

Run 4: Re = 2360 $\Theta = 22.5^{o}C$ t = 10 min

X/dh	Sh'x	Area	F	Shx	Shx/dh = 2.49/Sh'∞
0.13	44.82			44.82	1.66
0.33	41.58			41.58	
0.79	38.35			38.35	
1.11	34.86	45.00	1.02	35.56	
1.96	31.62	64.13	1.04	32.88	

APPENDIX G (Contd.)

Duct 2:1, dh = 1.27 cm

Abrupt Entrance, Symmetric Transfer

Run 5: Re = 707 $\Theta = 23^{o}C$ t = 10 min

X/dh	Sh'x	Area	F	Shx
0.26	27.30			27.30
0.52	24.09			24.09
1.83	20.88	35.23	1.07	22.34
7.19	17.67	96.17	1.22	21.56

Area = area under the curve at specified x/dh

Shx = Sh'x F

$Sh'_{\infty} = 1.2\ Sh_{\infty}$

$Sh_{\infty} = 0.023\ Re^{0.8}\ Sc^{0.33}$

APPENDIX G (Contd.)

Duct 3:1, dh = 1.43 cm

Abrupt Entrance, Asymmetric Transfer

Run 1: Re = 5710 $\Theta = 22.8^{o}C$ t = 8 min

X/dh	Sh'x	Area	F	Shx	Shx/dh = 7.55/Sh∞
0.15	89.17			89.17	1.76
0.32	84.68			84.68	
0.50	79.91			79.91	
0.73	75.43			75.43	
1.08	70.94			70.94	
1.86	66.18			66.18	
2.73	61.69	178.55	1.04	64.16	
4.24	57.20	266.85	1.06	60.63	
7.55	52.44	453.23	1.12	58.73	

Run 2: Re = 5120 $\Theta = 22.7^{o}C$ t = 8 min

X/dh	Sh'x	Area	F	Shx	Shx/dh = 4.27/Sh∞
0.19	76.55			76.55	1.68
0.26	72.06			72.06	
0.61	67.30			67.30	
1.04	62.53			62.53	
1.74	57.76			57.76	
2.67	53.28	151.36	1.04	55.41	
4.27	48.51	277.59	1.06	51.42	

APPENDIX G (Contd.)

Duct 3:1, dh = 1.43 cm

Abrupt Entrance, Asymmetric Transfer

Run 3: Re = 4470 Θ = 23.5°C t = 8 min

X/dh	Sh'x	Area	F	Shx	Shx/dh = 3.65/Sh∞
0.12	72.62			77.62	1.51
0.23	67.86			67.86	
0.35	63.09			63.09	
0.76	53.84			53.84	
1.22	49.07			49.07	
1.97	44.30			44.30	
3.65	39.82	166.94	1.05	41.81	

Run 4: Re = 3700 Θ = 23.5°C t = 10 min

X/dh	Sh'x	Area	F	Shx	Shx/dh = 3.54/Sh∞
0.26	50.94			50.94	1.43
0.41	47.00			47.00	
0.76	43.36			43.36	
1.34	39.42			39.42	
2.21	35.78			35.78	
3.54	32.14	131.94	1.05	33.75	

Run 5: Re = 2590 Θ = 23.5°C t = 10 min

X/dh	Sh'x	Area	F	Shx	Shx/dh = 5.80/Sh∞
0.12	43.36			43.36	1.48
0.26	39.42			39.42	
0.52	35.17			35.17	
1.16	31.53			31.53	
2.50	27.89	75.12	1.04	29.01	
5.80	23.95	168.13	1.10	26.35	

APPENDIX G (Contd.)

Duct 3:1, dh = 1.43 cm

Abrupt Entrance, Asymmetric Transfer

Run 6: Re = 1760 $\Theta = 23.7^{o}C$ t = 10 min

X/dh	Sh'x	Area	F	Shx	Shx/dh = 3.60/Sh ∞
0.23	27.29			27.29	1.32
0.52	23.65			23.65	
1.40	20.01			20.01	
3.60	16.37	68.21	1.05	17.19	

Run 7: Re = 528 $\Theta = 24^{o}C$ t = 11 min

X/dh	Sh'x	Area	F	Shx
0.17	13.70			13.70
0.58	10.66			10.66
1.74	7.61	19.17	1.05	8.80
6.10	4.57	43.22	1.12	5.63

Area = area under the curve at the given x/dh

$$F = 1/1 - \frac{4A}{ReSc}$$

$$Sh_{\infty} = 0.023\ Re^{0.8}\ Sc^{0.33}$$

APPENDIX G (Contd.)

Duct 3:1, dh = 1.43 cm

Abrupt Entrance, Symmetric Transfer

Run 1: Re = 4610 Θ = 21°C t = 8 min

X/dh	Sh'x	Area	F	Shx	Shx/dh = 6.97/Sh'∞
0.23	81.60			81.80	2.04
0.58	76.55			76.55	
1.04	71.22	74.96	1.02	72.64	
2.50	65.89	159.3	1.05	69.08	

Run 2: Re = 4420 Θ = 22.8°C t = 8 min

X/dh	Sh'x	Area	F	Shx	Shx/dh = 2.50/Sh'∞
0.17	80.38			80.38	2.05
0.41	75.78			75.78	
0.87	71.19			71.19	
1.74	66.60	144.44	1.04	69.26	
3.48	42.00	235.48	1.08	66.96	

Run 3: Re = 3830 Θ = 23°C t = 9 min

X/dh	Sh'x	Area	F	Shx	Shx/dh = 2.44/Sh'∞
0.08	82.44			82.44	2.14
0.17	78.51			78.51	
0.35	74.31			74.31	
0.38	70.38			70.38	
0.93	66.45			66.45	
1.51	62.53	106.67	1.04	65.03	
2.47	58.32	166.38	1.07	62.40	

APPENDIX G (Contd.)

Duct 3:1, dh = 1.43 cm

Abrupt Entrance, Symmetric Transfer

Run 4: Re = 3240 Θ = 22.3°C t = 9 min

X/dh	Sh'x	Area	F	Shx	Shx/dh = 1.92/Sh'∞
0.12	69.82			69.82	2.03
0.35	65.61			65.61	
0.76	61.41			61.41	
1.11	57.20	51.83	1.02	58.34	
1.92	53.00	116.75	1.05	55.65	

Run 5: Re = 2538 Θ = 23.3°C t = 10 min

X/dh	Sh'x	Area	F	Shx	Shx/dh = 7.55/Sh'∞
0.29	33.23			33.23	0.86
0.58	30.34			30.34	
1.45	27.45			27.45	
2.90	24.56	73.61	1.04	25.54	
7.55	21.67	187.88	1.10	23.84	

Run 6: Re = 528 Θ = 23.5°C t = 9 min

X/dh	Sh'x	Area	F	Shx	Shx/dh = 6.10/Sh'∞
0.41	21.87			21.87	
1.80	18.51	26.22	1.07	19.81	
6.10	15.14	93.22	1.30	19.68	

Area = area under the curve to the given x/dh

$F = 1/[1 - {}^{4A}/ReSc)]$

Shx = Sh'x F

APPENDIX G (Contd.)

Duct 2:1, dh = 1.27 cm

Calming Section, Asymmetric Section

Run 1: Re = 5812 Θ = 21.3°C t = 7 min

X/dh	Sh'x	Area	F	Shx	Nudp	Shx/Nudp
0.26	60.13			60.13	58.52	1.028
0.72	54.90			54.90	51.58	1.064
1.39	49.68			49.68	46.12	1.077
2.61	44.45			44.45	44.16	1.007
4.57	39.22	209.34	1.05	41.18	41.16	1.000

Shx/dh = 4.57/Sh∞ = 1.21

Run 2: Re = 3770 Θ = 22.3°C t = 10 min

X/dh	Sh'x	Area	F	Shx	Nudp	Shx/Nudp
0.13	51.05			51.05	44.55	1.146
0.28	47.53			47.53	41.04	1.158
0.49	44.01			44.01	38.23	1.151
0.91	40.49	44.82	1.02	41.30	35.43	1.166
2.22	36.97	101.32	1.04	38.45	31.92	1.205
5.69	33.45	201.24	1.08	36.13	28.41	1.272

Shx/dh = 5.69/Sh∞ = 1.51

Run 3: Re = 2355 Θ = 22.7°C t = 10 min

X/dh	Sh'x	Area	F	Shx	Nudp	Shx/Nudp
0.13	37.80			37.80	30.57	1.237
0.33	34.51			34.51	27.44	1.258
0.57	31.22	31.14	1.02	31.84	25.76	1.236
2.68	27.94	78.55	1.04	29.06	21.43	1.356
8.17	24.65	219.31	1.14	28.10	18.76	1.498

Shx/dh = 8.17/Sh∞ = 1.71

APPENDIX G (Contd.)

Duct 2:1, dh = 1.27 cm

Calming Section, Asymmetric Section

Run 4: Re = 707 Θ = 22.7°C t = 12 min

X/dh	Sh'x	Area	F	Shx
0.13	20.55			20.55
0.33	17.81			17.81
0.83	15.07			15.07
2.61	12.33	35.13	1.07	13.19
8.17	9.59	82.52	1.19	1.41

Area = area under curve at specified X/dh

$Shx = Sh'x\ F$

$F = 1/(1 - \frac{4A}{ReSc})$

$Nudp = Nud\ (Sc/Pr)^{0.33}$

$Nud = 0.03\ Re^{0.8}\ (X/dh)^{-0.12}$

$Sh_\infty\ 0.023\ Re^{0.8}\ Sc^{0.33}$

APPENDIX G (Contd.)

Duct 2:1, dh = 1.27 cm

Calming Section, Symmetric Transfer

Run 1: Re = 4710 $\Theta = 22.5^{o}C$ t = 5 min

X/dh	Sh'x	Area	F	Shx	Nud'p	Shx/Nud'p
0.26	56.68			56.68	59.35	1.52
0.33	50.01			50.01	57.34	1.45
0.65	43.34			43.34	52.81	1.45
1.17	36.68	43.58	1.01	37.05	49.29	1.42
3.07	30.01	108.91	1.03	30.91	43.76	1.45

Shx/dh = 3.07/Sh'∞ = 0.90

Run 2: Re = 3960 $\Theta = 20.8^{o}C$ t = 8 min

X/dh	Sh'x	Area	F	Shx	Nud'p	Shx/Nud'p
0.26	49.94			49.94	51.66	0.97
0.46	45.18			45.18	48.76	0.93
0.79	40.43			40.43	45.09	0.90
1.26	35.67			35.67	43.33	0.82
2.09	30.91			30.91	40.28	0.77
3.60	26.16	116.28	1.04	27.21	37.65	0.72
9.48	21.40	250.56	1.09	23.33	32.27	0.72

Shx/dh = 9.48/Sh'∞ = 0.78

APPENDIX G (Contd.)

Duct 2:1, dh = 1.27 cm

Calming Section, Symmetric Transfer

Run 3: Re = 1940 $\Theta = 23^{o}C$ t = 10 min

X/dh	Sh'x	Area	F	Shx	Nud'p	Shx/Nud'p
0.20	38.13			38.13	29.69	1.29
0.39	34.12			34.12	27.21	1.25
0.83	30.10			30.10	25.23	1.19
1.64	26.09	47.04	1.03	26.87	23.25	1.12
3.38	22.08	53.18	1.04	22.96	20.29	1.13
10.46	18.06	221.03	1.18	21.31	18.55	1.15

Shx/dh = 10.46/Sh'∞ = 1.26

Run 4: Re = 706 $\Theta = 22.7^{o}C$ t = 10 min

X/dh	Sh'x	Area	F	Shx
0.26	21.41			21.41
0.46	18.12			18.12
1.28	14.83			14.83
3.13	11.53			11.53
8.63	8.24	84.92	1.19	9.81

Area = area under the curve at given X/dh

Shx = Sh'x F

$$F = 1/(1 - \frac{4A}{ReSc})$$

$$Nu'dp = 1.2\ Nudp\ (Sc/Pr)^{0.33}$$

$$Nudp = 0.03\ Re^{0.8}\ (x/dh)^{-0.12}$$

Sh'∞ 1.2 Sh∞

$$Sh\infty = 0.023\ Re^{0.8}\ Sc^{0.33}$$

APPENDIX G (Contd.)

Duct 3:1, dh = 1.43 cm

Calming Section, Asymmetric Transfer

Run 1: Re = 4706 $\Theta = 24^{o}C$ t = 6 min

X/dh	Sh'x	Area	F	Shx	Nudp	Shx/Nudp
0.23	58.88			58.88	49.85	1.18
0.41	53.28			53.28	46.50	1.15
0.87	47.57			45.57	42.73	1.07
1.86	42.06			42.06	38.96	1.08
3.20	36.45	130.42	1.04	37.91	36.45	1.04

Shx/dh = 3.20/Sh∞ = 1.32

Run 2: Re = 3540 $\Theta = 22.4^{o}C$ t = 10 min

X/dh	Sh'x	Area	F	Shx	Nudp	Shx/Nudp
0.06	47.39			43.39	46.75	1.01
0.17	43.39			43.46	41.26	1.05
0.35	39.82			39.82	37.84	1.05
0.76	35.89			35.89	34.47	1.04
1.62	32.35			33.32	31.48	1.06
4.36	28.32	157.18	1.06	30.02	27.95	1.07

Shx/dh = 4.36/Sh∞ = 1.32

Run 3: Re = 2650 $\Theta = 22.5^{o}C$ t = 9 min

X/dh	Sh'x	Area	F	Shx	Nudp	Shx/Nudp
0.17	35.61			35.61	32.81	1.09
0.38	31.41			31.41	29.63	1.06
0.81	27.20			27.20	27.25	1.00
1.92	22.98			22.98	24.34	0.99
6.10	18.79	132.84	1.07	20.11	21.17	0.95

Shx/dh = 6.10/Sh∞ = 1.11

APPENDIX G (Contd.)

Duct 3:1, dh = 1.43 cm

Calming Section, Asymmetric Transfer

Run 4: Re = 528 $\Theta = 24^{o}C$ t = 11 min

X/dh	Sh'x	Area	F	Shx
0.17	16.26			16.26
0.46	13.46			13.46
1.69	10.37	19.14	1.05	10.89
3.50	7.57	36.50	1.10	8.33

Area = area under the curve

Shx = Sh'x F

$F = 1/(1 - \frac{4A}{ReSc})$

$Nudp = Nud\ (Sc/Pr)^{0.33}$

$Nud = 0.03\ Re^{0.8}\ (X/dh)^{-0.12}$

$Sh_{\infty} = 0.023\ Re^{0.8}\ Sc^{0.33}$

APPENDIX G (Contd.)

Duct 3:1, dh = 1.43 cm

Calming Section, Symmetric Transfer

Run 1: Re = 4410 $\Theta = 23.5^{o}C$ t = 10 min

X/dh	Sh'x	Area	F	Shx	Nud'p	Shx/Nud'p
0.18	64.49			64.49	58.69	1.10
0.29	60.85			60.85	55.35	1.10
0.46	57.48			57.48	52.49	1.10
1.34	54.12			54.12	46.29	1.17
2.90	50.47	162.05	1.05	52.99	41.99	1.26
7.55	47.11	376.97	1.13	53.22	37.22	1.43

Shx/dh = 7.55/Sh'∞ = 1.63

Run 2: Re = 3730 $\Theta = 22.5^{o}C$ t = 10 min

X/dh	Sh'x	Area	F	Shx	Nud'p	Shx/Nud'p
0.06	64.77			64.77	58.43	1.11
0.18	61.13			61.13	51.33	1.19
0.35	57.48			57.48	47.16	1.22
0.70	53.56			53.56	43.40	1.23
1.51	49.91			49.91	39.65	1.26
4.36	42.26	210.46	1.08	45.64	35.06	1.30

Shx/dh = 4.36/Sh'∞ = 1.60

APPENDIX G (Contd.)

Duct 3:1, dh = 1.43 cm

Calming Section, Symmetric Transfer

Run 3: Re = 3240 $\Theta = 22.7^{o}C$ t = 10 min

X/dh	Shx	Area	F	Shx	Nud'p	Shx/Nud'p
0.12	57.48				48.10	1.20
0.23	53.56				44.37	1.21
0.53	49.91				40.27	1.24
0.99	46.27				37.29	1.24
2.50	42.62	115.53	1.05	44.75	33.56	1.33
6.97	39.97	286.72	1.13	44.04	29.53	1.49

$Shx/dh = 6.97/Sh_{\infty} = 1.57$

Run 4: Re = 2360 $\Theta = 21.5^{o}C$ t = 9 min

X/dh	Sh'x	Area	F	Shx	Nud'p	Shx/Nud'p
0.12	29.45			29.45	31.11	0.95
0.41	24.68			24.68	26.77	0.92
1.74	20.19			20.19	22.67	0.89
6.97	15.70	127.05	1.08	16.96	17.88	0.95

$Shx/dh = 6.97/Sh'_{\infty} = 0.86$

APPENDIX G (Contd.)

Duct 3:1, dh = 1.43 cm

Calming Section, Symmetric Transfer

Run 5: Re = 528

X/dh	Sh'x	Area	F	Shx
0.46	6.83			6.83
1.74	4.10			4.10
7.84	1.37	15.41	1.04	1.42

Area = area under curve

$Shx = Sh'x\ F$

$F = 1/(1 - \frac{4A}{ReSc})$

$Nud'p = 1.2\ Nud\ (Sc/Pr)^{0.33}$

$Nud = 0.03\ Re^{0.8}\ (X/dh)^{-0.12}$

$Sh'_{\infty} = 1.2\ Sh_{\infty}$

$Sh_{\infty} = 0.023\ Re^{0.8}\ Sc^{0.33}$

APPENDIX H

Data for the Consolidated Log-Log Plot of Shx/Re^{X} vs x/dh

Duct 3:1, dh = 1.43 cm

Calming Section, Asymmetric Transfer

Run 1 Re = 4700 $\Theta = 24^{o}C$ t = 6 min

X/dh	Shx	$Shx/Re^{0.83}$
0.23	58.88	0.053
0.41	53.28	0.048
0.87	47.57	0.043
1.86	42.06	0.038
3.20	37.91	0.034

Run 2 Re = 3540 $\Theta = 22.4^{o}C$ t = 10 min

X/dh	Shx	$Shx/Re^{0.83}$
0.06	47.39	0.054
0.17	43.46	0.049
0.35	39.82	0.045
0.76	35.89	0.041
1.62	33.32	0.038
4.36	30.02	0.034

Run 3 Re = 2650 $\Theta = 22.5^{o}C$ t = 9 min

X/dh	Shx	$Shx/Re^{0.83}$
0.17	35.61	0.051
0.38	31.41	0.045
0.81	27.20	0.039
2.03	22.98	0.033
6.18	20.11	0.029

APPENDIX H (Contd.)

Duct 3:1, dh = 1.43 cm

Calming Section, Asymmetric Transfer

Run 1 Re = 4410 Θ = 23.5°C t = 10 min

X/dh	Shx	$Shx/Re^{0.83}$
0.18	64.49	0.061
0.29	60.85	0.057
0.46	57.48	0.054
1.34	54.12	0.051
2.90	52.99	0.050
7.55	53.22	0.050

Run 2 Re = 3730 Θ = 22.5°C t = 10 min

X/dh	Shx	$Shx/Re^{0.83}$
0.66	64.77	0.070
0.18	61.13	0.066
0.35	57.48	0.062
0.70	53.56	0.058
1.51	49.91	0.054
4.36	45.54	0.049

APPENDIX H (Contd.)

Duct 3:1, dh = 1.43 cm

Calming Section, Asymmetric Transfer

Run 3 Re = 3240 $\Theta = 22.7^{o}C$ t = 10 min

X/dh	Shx	$Shx/Re^{0.83}$
0.12	57.48	0.070
0.23	53.56	0.065
0.53	49.91	0.061
0.99	46.27	0.056
2.50	44.75	0.055
6.97	44.04	0.054

Run 4 Re = 2360 $\Theta = 21.5^{o}C$ t = 9 min

X/dh	Shx	$Shx/Re^{0.83}$
0.12	29.45	0.047
0.41	24.68	0.039
1.74	20.19	0.032
6.97	16.96	0.027

APPENDIX H (Contd.)

Duct 2:1, dh = 1.27 cm

Calming Section, Asymmetric Transfer

Run 1 Re = 5812 Θ = 21.3°C t = 7 min

X/dh	Shx	$Shx/Re^{0.6}$
0.26	60.13	0.332
0.72	54.90	0.303
1.39	49.68	0.274
2.61	44.45	0.245
4.57	41.18	0.227

Run 2 Re = 3370 Θ = 22.3°C t = 10 min

X/dh	Shx	$Shx/Re^{0.6}$
0.13	51.05	0.365
0.28	47.53	0.340
0.49	44.01	0.315
0.91	41.30	0.295
2.22	38.45	0.275
5.69	36.13	0.258

Run 3 Re = 2355 Θ = 22.7°C t = 10 min

X/dh	Shx	$Shx/Re^{0.6}$
0.13	37.80	0.358
0.33	34.51	0.327
0.57	31.84	0.302
2.68	29.06	0.275
8.17	28.10	0.266

APPENDIX H (Contd.)

Duct 2:1, dh = 1.27 cm

Calming Section, Symmetric Transfer

Run 1 Re = 4710 Θ = 25.5°C t = 5 min

X/dh	Shx	$Shx/Re^{0.6}$
0.26	56.68	0.355
0.33	50.01	0.313
0.65	43.24	0.271
1.17	37.05	0.232
3.07	30.9	0.193

Run 2 Re = 3960 Θ = 20.8°C t = 8 min

X/dh	Shx	$Shx/Re^{0.6}$
0.26	49.94	0.347
0.46	45.18	0.314
0.79	40.43	0.281
1.26	35.67	0.248
2.09	30.91	0.215
3.60	27.21	0.189
9.48	23.33	0.169

Run 3 Re = 1940 Θ = 23°C t = 10 min

X/dh	Shx	$Shx/Re^{0.6}$
0.20	38.13	0.406
0.39	34.12	0.363
0.83	30.10	0.321
1.64	26.87	0.286
3.38	22.96	0.245
10.46	21.33	0.227

APPENDIX I

Derivation of the equation 5.1.2

Legkiy and Makarov (1971) gave in their paper the following equation: $Nux = 0.029\ Rex^{0.8}\ (X/d)^{0.08}$ (5.1.1) valid at $Rex > 25 \times 10^3$, for fully developed flow in rectangular ducts. In that equation X is the total heated length of the duct and Nux is an average Nusselt number in consequence. We are interested in having an expression for the local Nusselt number at a given X_1.

The relationship between the local Nusselt number and the average one is:

$$Nux_1 = x_1\left(\frac{dNux}{dx}\right)_X \qquad (I1)$$

because: $Nux = \int_0^{x_1=x} Nux_1\, dx / \int_0^{x_1=x} x_1\, dx_1$

5.1.1 can be written, being $Rex = xu/\nu$, as:

$$Nux = 0.029\ \left(\frac{u}{\nu}\right)^{0.8}\ \left(\frac{1}{d}\right)^{0.08}\ X^{0.8}\ X^{0.08} \qquad (I2)$$

$$Nux = 0.029\ \left(\frac{u}{\nu}\right)^{0.8}\ \left(\frac{1}{d}\right)^{0.08}\ X^{0.88} \qquad (I3)$$

Taking the derivative of

$$\left(\frac{dNux}{dx}\right)_X = 0.0236\left(\frac{u}{\nu}\right)^{0.8}\ \left(\frac{1}{d}\right)^{0.08}\ X^{-0.12} \qquad (I4)$$

From I.1 we have

$$Nux_1 = 0.0236\left(\frac{u}{\nu}\right)^{0.8}\ \left(\frac{1}{d}\right)^{0.08}\ X_1\ X^{-0.12} \qquad (I5)$$

$$Nux_1 = 0.0236\left(\frac{u}{\nu}\right)^{0.8}\ \left(\frac{1}{d}\right)^{0.08}\ X_1^{0.88} \qquad (I6)$$

Noticing that: $X_1^{0.88}$ is equal to: $X_1^{0.8}\ X_1^{0.08}$

we can write I6 as:

$$Nux_1 = 0.036 Rex_1^{0.8} \left(\frac{x_1}{d}\right)^{0.08} \qquad (I7)$$

Now:

$$Nud = \frac{Nux_1}{x_1/d} \qquad (I8)$$

so that:

$$\frac{Nux_1}{x_1/d} = 0.036 \frac{Rex_1^{0.8}}{(x_1/d)^{0.8}} \frac{x_1/d)^{0.08}}{(x_1/d)^{0.2}} \qquad (I9)$$

making: $(x_1/d) = (x_1/d)^{0.8} (x_1/d)^{0.2}$

Therefore:

$$Nud = 0.036 Red^{0.8} \left(\frac{x_1}{d}\right)^{-0.12} \qquad (I10)$$

APPENDIX J

Laminar Flow

Comparison between the Corrected Sherwood Number (Shx) and the Nusselt Number obtained by the relation proposed by Sellers et al (1956)

Duct 3:1 rh = 0.36 cm

Calming Section Asymmetric Transfer

Re = 528 Pe = Re Sc = 1578.72

Shx/rh = 0.88/Nu = 0.52

Calming Section Symmetric Transfer

Shx/rh = 1.88/1.2 Nu = 0.10 ; Re = 528 Pe = 1578.72

Duct 2:1 rh = 0.32 cm

Calming Section Asymmetric Transfer

Shx/rh = 1.0/Nu = 0.59 ; Re = 707, Pe = 211393

Calming Section Symmetric Transfer

Re = 706 Pe = 2110.94

Shx/rh = 1.50/1.2 Nu = 0.65

$$Nu = 1.357\left(\left(\frac{x/r_w}{Pe}\right)\right)^{-0.33}$$

Comparison between the Corrected Sherwood Number and the Nusselt Number obtained by the expression given by Knudsen & Katz (1958)

Duct 3:1 dh = 1.43 cm

Abrupt Entrance Asymmetric Transfer

Re = 528 Pe = 1578.72

Shx/dh = 4.5/(Num/1.2) = 0.44

Abrupt Entrance Symmetric Transfer

Re = 538 Pe = 1608.62

Shx/dh = 2/Num = 1.03

Duct 2:1 dh = 1.27 cm

Abrupt Entrance Asymmetric Transfer

Re = 704 Pe = 2104.96

Shx/dh = 3/Num/1.2 = 2.03

Abrupt Entrance Symmetric Transfer

Re = 707 Pe = 2113.93

Shx/dh = 3/Num = 1.09

$$Num = \frac{0.664(G'z)^{0.5}}{Pr^{0.17}} \left[1 + 6.27 \left(\frac{Pr}{G'z}\right)^{0.44} \right]^{0.5}$$

$$G'z = \frac{Pe}{X/dh}$$

APPENDIX K

Derivation of the Equation $K' = \frac{cn}{t}$

In an element of polymer film of unit area undergoing recession r in time t, the volume of swelling agent removed is:

$$Vs = 1.r \tag{K1}$$

Mass of swelling agent removed in unit time per unit area:

$$r\,\rho s/t \tag{K2}$$

This mass flux is equal also too:

$$\dot{m}s = k\,(C_s - C_b) \tag{K3}$$

where k is the mass transfer coefficient, C_s is the concentration of the swelling agent at the surface and C_b its concentration in the bulk of stream. If the concentration C_b is negligible then:

$$\dot{m}s = k'\,C_s \tag{K4}$$

Since

$$k' = \frac{r\rho_s}{tC_s} \tag{K5}$$

If the vapour of the swelling agent having a saturated vapour pressure P_s, obeys the perfect gas law, and the molecular weight of the swelling agent is M, we have:

$$k' = \frac{r\,\rho_s}{t\,M\,P_s}\,RT \tag{K6}$$

putting:

$$C \equiv \frac{r\,\rho_s\,RT}{M\,P_s} \tag{K7}$$

it follows that:

$$k' = \frac{cn}{t} \tag{K8}$$

where $c = \frac{C}{n}$

Nomenclature

A	Area	cm^2
C	Experimental Constant	cm
C_s	Concentration of Swelling Agent	$gm./cm^3$
C_p	Specific Heat Capacity	$cal/gm\ ^oK$
D	Diffusion Coefficient	cm^2/sec
d	Pipe Diameter	cm
dh	Hydraulic Diameter	cm
fapp	Apparent Friction Factor	
f	Friction Factor	
g	Acceleration Due to Gravity	cm/sec^2
h	Heat Transfer Coefficient	$cal/cm^2\ ^oK$ sec
H	**Length Of Wetted-wall Column**	**cm**
K	Convective Mass Transfer Coefficient	cm/sec
K'	Uncorrected Convective Mass	cm/sec
K_L	Liquid-Side Mass Transfer Coefficient	cm/sec
K	Thermal Conductivity	$cal/cm^2\ ^oK$
Lhy	Hydrodynamical Entrance Length	cm
M	Molecular Weight of Swelling Agent	gm/gmo l
m	Mass	gm
$\dot{m}$	Mass Flux	gm/cm^2 sec
N	Nominal Fringe Order	
n	Absolute Fringe Order	
$\overline{n}$	Absolute Odd Fringe Order	
P_{BM}	Logarithmic Average Pressure	atm
P_s	Vapour Pressure of Swelling Agent	mm Hg
Q	Volume Flow Rate	cm^3/sec
R	Universal Gas Constant	$mm\ Hg\ cm^3/^oK$ gmo l
r	Surface Recession	cm
r_ω	Pipe Radius	cm

r_h	Hydraulic Radius	cm
T	Absolute Temperature	^oK
t	Fluid Stream Run Time	sec
u	Bulk Velocity of Air Stream	cm/sec
V_s	Volume of Swelling Agent	cm^3
x	Streamwise Distance from Commencement of Test Section	cm
Z	Length of Contact (Wetted Columns)	cm

Dimensionless Quantities

C_A^*	Dimensionless Concentration	=	$\frac{C_A - C_{A1}}{\Delta C_A}$
G'_Z	$\equiv$ Pe (dh/x)		
N_u	Nusselt Number	=	$\frac{hd}{K}$
N_{um}	Mean Nusselt Number	=	$\frac{hd}{K}$
P_e	Peclet Number	=	Re Sc
P_r	Prandtl Number	=	$\frac{C_p \mu}{K}$
Re	Reynolds Number	=	$\frac{du}{v}$
Re_x	Local Reynolds Number	=	$\frac{xu}{v}$
S_c	Schmidt Number	=	$\frac{v}{D}$
S_h	Sherwood Number	=	$\frac{Kd}{D}$
Sh_x	Local Sherwood Number	=	$\frac{Kdh}{D}$
Sh_∞	Fully Developed Sherwood Number	=	$\frac{Kdh}{D}$
t^*	Dimensionless time	=	$\frac{tu}{d}$
∇^*	Dimensionless nabla	=	$d\nabla$

T^*	Dimensionless Temperature	=	$\frac{T - T_1}{\Delta T}$
X^+	Axial Co-ordinate for the Hydrodynamic Entrance	=	$\frac{x}{Re\ dh}$

Greek Symbols

Γ	Liquid-rate	gm/cm.min
λ	Wavelength of Laser Light	cm
μ	Viscosity	gm/cm sec
μ_a, μ_p, μ_{px}, μ_g	Index of Refraction of Air, Polymer, Perspex and Glass respectively	
ν	Kinematic Viscosity	cm^2/sec
ν_1, ν_2	Difference between Absolute Order Fringe (n) and the next Absolute Odd Order Fringe ($\bar{n}$)	
ρ_s	Density of Swollen Agent	gm/cm^3

Bibliography

B

Beek, W.J. and Muttzall, K.M.K. 1975, Transport Phenomena, John Wiley & Sons N.Y.

Blagius, H. 1908, Z. Math. U. Phys. Sci. 1.

Brundrett, E. and Baines, W.D. 1964, J. Fluids Mech. 19, 375-394.

Brundrett, E. and Burroughs, P.R. 1967, Int. J. Heat Mass Transfer 10, 1133-42.

Butters, J.N. and Leendertz, J.A. 1969, J. of Phys. E 2, 116.

C

Carlson, G.A. and Hornbeck, R.W. 1973, J. Appl. Mech. 40.

Chen, R.Y. 1973, J. Fluids Eng. 95, 153-158.

Chiang, S.H. and Toor, H.L. 1959, 5, 165.

Chilton, T.H. and Colburn, A.P. 1934, Ind. Eng. Chem. 26, 1183.

Christian, W.J. Ch. and Kezios, S.P. 1959, A.I. Ch.E. J, 5, 61.

Clark, S.H. and Kays, W.M. 1953, Trans. ASME, 75, 859.

Coulson, J.M. and Richardson, J.F. 1964, Chemical Engineering Vol. I, 2nd Edition, Pergammon Press, London.

Curr, R.M., Sharma D. and Tatchel, D.G. 1972, Comput. Methods Appl. Mech. Eng. 1, 143-158.

D

Deissler, R.G. 1950, NACA TN 2138.

Deissler, R.G. 1953, NACA TN 3016.

Deissler, R.G. 1955, NACA Report 1210.

Deissler, R.G. and Taylor, M.F. 1956, Heat Transfer Conference (AEC), N.Y.

Deissler, R.G. and Taylor, M.F. 1959, NASA TR No. 12-31

Dittus, F.W. and Boelter, L.M.K. 1930, Univ. of California (Berkeley) Publs. Eng. 2:443.

Duffy, D.E. 1970, J. of Phys. E. 3, 561.

Drexel, R.E. and McAdams, W.H. 1945, (Feb.) NACA, WR-W-108.

F

Friedmann, M., Gillss, J. and Liron, N. 1968, Appli. Sci. Res. 19, 426-438.

G

Gessner, F.B. and Jones, J.B. 1965, J. Fluid Mech. 23, (4), 689-713.

Gessner, F.B. 1973, J. Fluid Mech. 58, 1-25.

Gilliland, E.R. and Sherwood, T.K. 1934, Ind. Eng. Chem. 26, 516.

Grosse-Wilde, H. and Uhlenbusch, J. 1978, Int. J. Heat Mass Transfer, 21, 677.

H

Harnett, J.P. and Eckert, E.R.G. 1957, Trans. ASME, 13, 247.

Harnett, J.P., Koh, J.C.Y. and McComas, S.T. 1962, Trans. ASME J. Heat Transfer, 82.

Higbie, R. 1935, Trans. Am. Inst. Chem. Eng. 31, 365.

Holmes, D.B. and Vermeulen, J.R. 1968, Chem. Eng. Sci. 23, 717.

I

Ibragimov, M.H., Petrishchev, V.S. and Sabelev, G.I. 1971, Int. J. Heat Mass Transfer 14, 1033-1037.

K

Kapur, D.N., 1973, Ph.D. Thesis, Chem. Eng. Dept., Univ. of Edinburgh.

Kapur, D.N. and Macleod, N. 1974, Int. J. Heat Mass Transfer, 17, 1151.

Kapur, D.N. and Macleod N. 1976, I & EC Product Res. Dev 15, 50.

Knudsen, J.G. and Katz, D.L.V. 1958, Fluid Dynamics and Heat Transfer, McGraw-Hill N.Y.

L

Langhaar, H.L. 1942, Trans. ASME, 64, A-55.

Larson, R.I. and Yerazumis S. 1973, Int. J. Heat Mass Transfer 16, 1-121.

Latzko, H. 1921, Zeitschr. f. angew. Math. u. Mech. 1, 227-280.

Launder, B.E. and Ying, W.M. 1972, J. Fluid Mech. 54, 289-295.

Launder, B.E. and Ying, W.M. 1973, Proc. Instn. Mech. Engrs. 187, 455-461.

Legkiy, V.M. and Makarov, A.S. 1971, Heat Transfer, Soviet Research, 3, 1-9.

Leutheusser, H.J. 1961, Ph.D. Thesis, Dept. Mech. Eng. Univ. of Toronto.

Linton, W.H. and Sherwood, T.K. 1950, Chem. Eng. Prog. 46, 258.

Lyczkowsky, R.W., Solbrig, C.W. and Gidaspow, D. 1969, Inst. Gas Thechnol. Tech. Inf. Cent. File 3229, 3424S, Chicago.

M

Macleod, N. and Todd, B. 1973, Int. J. Heat Mass Transfer 16, 485.

Maslen, S.H. 1958, Quart. Appl. Math. 16, 173.

Masliyah, J.H. and Nguyen, T.T. 1977, Can. J. Chem. Eng. 55, 156.

Masliyah, J.H. and Nguyen, T.T. 1979, Int. J. Heat Mass Transfer 22, 273.

McAdams, W.H. 1954, Heat Transmission, 3rd Edition, McGraw-Hill, N.Y.

Miles, J.B. and Shis, J.S. 1967, Mech. Eng. Dept., Univ. of Missouri, Columbia (unpublished paper).

Moissis, R. 1957, Master's Thesis, M.I.T.

Montgomery, S.R. and Wibulswas, P. 1966, Proc. Int. Heat Transfer Conference 3rd, AIChE 1, 104-112.

Muchnik, G.F., Solomonov, S.D. and Gordon, A.R. 1973, J. Eng. Phys. 25, 1268.

N

Nikuradse, J. 1926, Thesis, Gottingen.

Nikuradse, J. 1930, Ing. Arch. 1, 306-332.

Nikuradse, J. 1932, Ver. deutsch. Ing. Forschungsheft No. 356.

O

Oman, R.A. 1959, Ph.D. Thesis, M.I.T.

P

Persen, L.N. 1972, Introduction to Boundary Layer Theory, Tapir-Forlag.

Prandtl, L. 1926, Verh. 2nd. Int. Kong. fur Tech. Mech. Zurich, 62-75.

R

Raimondi, P. and Toor, H.L. 1959, AICh.E. J. 5, 165.

Rothfus, R.R., Kermode, R.I. and Hackworth, J.H. 1964, Chem. Eng. 71, 178.

S

Schiller, L. and Kirsten, H. 1929, Z. tech. Phys. 10 : 268.

Scriven, L.E. and Pigford, R.L. 1958, AICh.E. J. 4, 439.

Sellars, J.R., Tribus, M. and Klein, J.S. 1956, Trans. ASME, 78 : 441.

Shah, R.K. and London, A.L. 1971, TR No. 75, Dept. Mech. Eng. Standford Univ. Calif.

Shah, R.K. and London, A.L. 1978, Advances in Heat Transfer, Laminar Flow Forced Convection in Ducts, Supplement 1, Academic Press, N.Y.

Spalding, D.B. 1961, J. Appl. Mech. 28, Ser. E.

T

Toor, H.L. and Marchello, J.M. 1958, AICh.E. J. 4, 97.

V

Vivian, J.E. and Peaceman, D.W. 1956, AICh.E. J. 2, 437.

W

Wiginton, C.L. and Dalton, C. 1970, J. Appl. Mech. 37, 854.

Whitman, W.G. 1923, Chem. and Met. Eng. 29, 147.